LABEL-FREE IMMUNOSENSOR

FOR TOXIN DETECTION IN FOOD MATRIX

By

CHANGHOON CHAI

A Dissertation submitted to the

Graduate School-New Brunswick

Rutgers, The State University of New Jersey

in partial fulfillment of the requirements

for the degree of

Doctor of Philosophy

Graduate Program in Department of Food Science

written under the direction of

Professor Paul Takhistov

and approved by

_____

_____

_____

_____

New Brunswick, New Jersey

October 2008

ABSTRACT OF THE DISSERTATION

Label-free Immunosensor for Toxin Detection in Food Matrix

By CHANGHOON CHAI

Dissertation Director:

Professor Paul Takhistov

A method for the detection of biological toxins in foods has to be sensitive, rapid, and field-applicable since toxin detection is on the front line of food safety and food protection against bioterrorism. In this thesis a sensitive, rapid, and label-free electrochemical impedance spectroscopy (EIS) immunosensor was developed and its performance in real foods was demonstrated.

To improve the sensitive of EIS immunosensor, nanoporous aluminum was applied as the substrate of EIS immunosensor. Well ordered nanoporous aluminum having ~30nm in pore diameter was obtained by anodizing food grade aluminum in 0.3M oxalic acid at 40V. EIS immunosensor for the detection of staphylococcal enterotoxin B (SEB) or ricin was developed by immobilizing anti-SEB or ricin on nanoporous aluminum using 3-aminopropyltriethoxysilane (APTES). Particularly efficient immobilization of antibody (Ab) was attained by silanization of aluminum in 2% APTES for 4hrs.

A time-resolved EIS of immunosensor was performed to investigate the effect of immunoreaction on impedimetric signal outputs. Immunoreaction between immobilized

Ab and its target toxin resulted in gradual changes in the spectra of impedimetric signal outputs. The change by immunoreaction was significant especially in real part of impedance (Z') at the frequency region from 10kHz to 100kHz. The specific changes of Z' to immunoreaction also could be observed at pH 3.0 and pH 5.0. Using developed EIS immunosensor, it was possible to detect the presence of 10pg/ml of SEB in 15min without amplification of signal output such as labeling step. Moreover EIS immunosensor was applicable to real foods even to acidic foods.

Acknowledgement

There are lots of people I would like to thank for their encouragement to make me accomplish my long journey.

Foremost I would like to thank god for watching me and my beautiful wife, and giving us a healthy baby.

I would like to express sincere gratitude to my advisor, Professor Paul Takhistov, Ph.D. His infinite curiosity and integral view on research always inspired me. Moreover I am grateful for his patience.

I am deeply grateful to my committee, Professor Kit L. Yam, Ph.D., Professor Qingrong Huang, Ph.D. and Professor Stanley M. Dunn, Ph.D. for their kind advices to understand insight view of my research.

I would like also thank to all the rest of the academic and support staff of Food Science Department of Rutgers.

I am grateful to Eungchil Lee, and Heeyoon Moon for their hearty consideration on her daughter and me and also thank Hoshin and Hyejin, and Yongshin, Hyunjung and their future son.

I feel a deep sense of gratitude for my mother who taught me that only diligence and frankness can give a success. I could accomplish this because of her mantra that she showed and taught me. I also would like to thank my sister, Jungyoung, her husband, Jeaeun, and their daughter, Kyungmi, and my brother, Changsun, his wife, Jungmin, and their daughter, Minjin.

Table of Contents

Lists of tables

List of figures

Chapter 1. General introduction

1.1.   Introduction

Developing a sensitive and rapid method or device for identification of

bioterrorism toxins in foods is one of the major challenges in biosensor development.

Especially its importance is being increased in recent years as the threat of bioterrorism.

Bioterrorism toxins are easy to manufacture, and release via foods in addition nanolevel

intake can break out their virulence [15], making bioterrorism difficult to prevent. Hence the

practical front line of bio-defense may be to detect and discard contaminated foods as

quickly as possible [45]. To achieve this, the detection method for bioterrorism toxins has to

be sensitive to detect the presence of bioterrorism toxins in nanolevel, rapid to complete the

detection, simple to make anyone do the detection, and inexpensive to distribute widely.

Immunosensors have been the subject of increasing interest during the past decade

because of their sensitivity, specificity, rapidity, and simplicity. The traditional

immunosensors include methods such as ELISA (enzyme-linked immunosorbent assay),

RIA (radioimmunoassay), and electrophoretic immunoassay. However most of traditional

immunosensors involve complicate steps, thus they are tedious and time consuming [49].

Hence many studies currently are focused on the development of rapid and simple

immunosensors. Electrochemical impedance spectroscopy (EIS) immunosensor especially

may be the one that is able to overcome the disadvantages of traditional immunosensors in

regard that EIS immunosensor is able to separate immunoreaction occurring at the

liquid-surface interface directly without additional steps such as labeling, furthermore EIS

immunosensor is more amenable for miniaturization and economization. However the sensitivity is remained as a major problem for EIS immunosensor [30].

Nanomaterials as platform of immunosensor have been investigated to improve the sensitivity. It has been reported that the use of nanostructured materials as platforms of immunosensors allows for higher sensitivity, more reliability, faster analysis, and smaller size of devices also it seems to be promising that the use of nanomaterials can improve the sensitivity of EIS immunosensors. Nanomaterials, studied to improve the sensitivity of immunosensors, include nanoparticles, nanowires, nanotubes, and nanoporous materials. However their high raw material and manufacturing cost hinder the development of cost efficient and field-applicable immunosensor. Hence search for new and inexpensive nanomaterials which are applicable to immunosensor is of considerable interest.

To develop a sensitive, rapid, and inexpensive EIS immunosensor for the detection of bioterrorism toxins, food grade aluminum was fabricated into nanoporous structure and used as a substrate of EIS immunosensor in this thesis. For better sensitivity, a method to immobilize (incorporate) antibody intimately on nanoporous aluminum surface was developed, and the effect of the dimension of nanoporous structure on the sensitivity of EIS immunosensor and the electrochemical regime of EIS analysis for the detection of bioterrorism toxins were studied. Finally the performance of developed EIS immunosensor for the detection of bioterrorism toxins is presented.

1.2.   Bioterrorism toxins

Biodefense has become more important in the battle against terrorists acts. Bioterrorism toxins include viruses, pathogens, and toxins causing death or serious damage in health. Human exposure to biological toxins may occur through inhalation, skin exposure or ingestion of contaminated foods or water. The most potent pathway for outbreaks will be ingestion of foods and water. The World Health Organization (WHO) has warned the seriousness of bioterrorism through contaminated foods [50]. The Centers for Disease Control and Prevention (CDC) classified biological toxins into three categories (A, B, and C), depending on how easily they can be spread and the severity of illness or death they cause (Table 1.1) [5]. Category A toxins includes the highest priority toxins posing a risk to the public and national security and having a serious potential for large-scale dissemination. Category B toxins are the second highest priority being moderately easy to disseminate and having moderate morbidity rates. Category C toxins are third highest priority and include pathogens that have potential for high morbidity or mortality [5].

Category B toxins are regarded as the most potent bioterrorism toxins due to the ease of production. They are available from naturally occurring sources. Source itself can be used as a bioterrorism toxin, or simple treatment such as simple incubation of resources can produce high toxicity. Consequently category B toxins can be produced at home and spread out easily to the public. Most of all category B toxins can cause severe illness or death by the intake of small amount, for example, staphylococcal enterotoxin B (SEB) can paralyze an adult by the intake of 100ng [15]. In World War I and II category B toxins including glanders, ricin, staphylococcal enterotoxin B, and typhus have been used as

Category	A	B	C
Biological toxins	Anthrax (*Bacillus anthracis*)	Staphylococcal enterotoxin B	Emerging infectious diseases such as Nipah virus and hantavirus
	Botulism (*Clostridium botulinum* toxin)	Ricin toxin from *Ricinus communis* (castor beans)	
	Plague (*Yersinia pestis*)	Brucellosis (*Brucella* species)	
	Smallpox (variola major)	Epsilon toxin of *Clostridium perfringens*	
	Tularemia (*Francisella tularensis*)	Food safety threats (e.g. *Salmonella* species, *Escherichia coli* O157:H7, *Shigella*)	
	Viral hemorrhagic fevers (filoviruses and arenaviruses)	Glanders (*Burkholderia mallei*)	
		Melioidosis (*Burkholderia pseudomallei*)	
		Psittacosis (*Chlamydia psittaci*)	
		Q fever (*Coxiella burnetii*)	
		Typhus fever (*Rickettsia prowazekii*)	
		Viral encephalitis (alphaviruses)	
		Water safety threats (e.g. *Vibrio cholerae, Cryptosporidium parvum*)	

Table 1.1 Classification of biological toxins into category A, B, and C [5]

biological weapons [4] particularly ricin has been used for assassination. The threat of bioterrorism has been prolonged to the present even in United States. In 2003 London police arrested terrorists due to bioterrorism plots using ricin and ricin powder has been found in the mail at the White House in Washington D.C.[20].

1.3.   Immunosensors

Immunosensor, a type of biosensors, is by definition a compact analytical device, incorporating immunological recognition elements either intimately connected to or integrated within signal transducers [47]. In addition to two major components of immunosensors (immunological recognition elements and signal transducers), substrates to mediate immunological recognitions to signal transducers can be included as a part of immunosensor (Figure 1.1).

Immunological recognition elements may include antibody (Ab), antigen (Ag), and their fragments, and exist as immobilized forms usually on substrates. Signal transducers monitor physicochemical changes resulted from immunoreaction between immunological recognition elements and target molecules, and convert to analytical signals. On the basis of highly sensitive and specific immunoreaction, immunosensors provide a sensitive and selective method for the detection of target molecules. Thus, immunosensors have been attracted considerable interest in the research fields of human health care, veterinary health care, bioprocess control, food safety control, and biodefense [24].
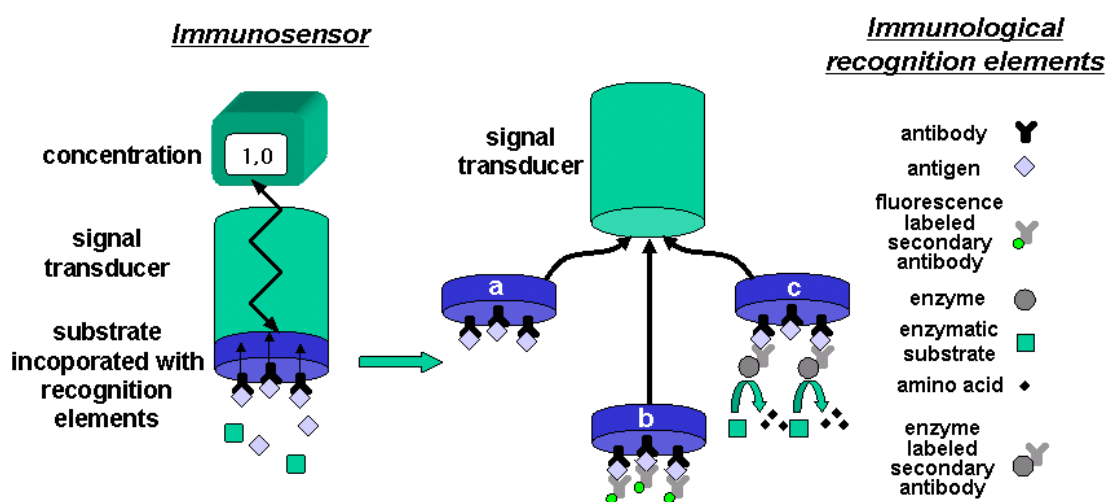
Figure 1.1. Schematic representations of immunosensors. a: direct immunosensor, b: indirect immunosensor using fluorescence, c: indirect immunosensor using enzyme [29].

Figure 1.1 shows schematic configurations of immunosensors and their schematic detection process. Immunosensors can be classified to direct (Figure 1.1. a) and indirect (Figure 1.1. b and c) methods upon the detection process or the sort of signal transducers. As the concern of simplicity and speed of immunosensors, direct immunosensors are favored rather than indirect immunosensors. A large number of immunosensors have been developed based on optical signal transducers such as ELISA or RIA. These traditional optical immunosensors are well established, moreover commercially available. However they are usually time-consuming and tedious since sample pretreatments or labeling steps (Figure 1.1. b, c) are necessary. Hence a lot of efforts have been put into the development of a rapid, simple, and sensitive immunosensor with real-time monitoring. Recently, with progress of chemistry, physics, and electrochemistry, sensitive and rapid immunosensors have been reported. Especially nanolevel detection within minutes has been achieved by immunosensors based on highly advanced signal transducers such as surface plasmon resonance (SPR) [40], evanescent wave [43], and quartz crystal microbalance (QCM) [32]. Despite of their high sensitivity and rapidity, their expensive instrumentations or complicate manipulations are probably drawbacks as signal transducers of immunosensors for the detection of bioterrorism toxins. On the other hand, electrochemical techniques as signal transducers have some advantages over optic based transducers in regard that they are more amenable for miniaturization and economization. Electrochemical techniques used for biosensors include amperometry, potentiometry, and electrochemical impedance spectroscopy (EIS). Amperometry and potentiometry have been extensively studied and most frequently used for biosensors. They are simple and inexpensive so biosensors based on amperometry or potentiometry are commercially available [11, 19]. However they are not

suitable for the detection of electrochemically non-active substances including

bioterrorism toxins. Recently EIS is of considerable interest as an electrochemical signal

transducer of immunosensors because EIS is able to monitor the behavior of

electrochemically non-active substances near electrode. In this thesis, EIS is employed as a

signal transducer of immunosensor for the detection of bioterrorism toxins, and the

performance of toxin detection was investigated and discussed.

1.4. Antibody immobilization

In immunosensors, immunological recognition elements are usually presented as

immobilized forms on substrates. As the recognition of target molecule is the first step of

the detection, immobilized forms of immunological recognition elements may play

important roles to determine sensitivity, reliability, and reproducibility of immunosensors.

Immunological recognition elements should be immobilized intimately and stably without

damaging their specificity and reactivity in order to develop a sensitive and reliable

immunosensor [12, 24, 30]. The application of appropriate method for the immobilization can

achieve a good intimacy and minimize the drawbacks of immunoassay arising from the

blockage of binding sites of Ab [1, 30]. Furthermore the production cost of immunosensor will

be reduced by the appropriate immobilization method. As commercial Ab including

anti-SEB and anti-ricin were used as immunological recognition elements to develop

immunosensors in this thesis, the immobilization of intact Ab onto solid substrates were

studied and discussed.

Ab is a protein consisting of amino acids having side groups. These side groups have their own physical and chemical characteristics and are distributed over the entire surface of Ab. Using physical or chemical characteristics of side groups, Ab can be immobilized on solid surface nonspecifically or specifically [51]. Nonspecific immobilization may use physical interactions such as hydrophobic, dipolar, and/or electrostatic interactions, and are widely use to immobilize enzymes onto organic or inorganic surface because of cost effectiveness [3, 51]. However, in nonspecific immobilization, the blockage of binding sites of Ab frequently occurs and it may damage the specificity and sensitivity of immobilized Ab [24, 51]. Immobilization of Ab without the blockage of binding sites can be achieved by specific chemical immobilization usually employing covalent interaction. Moreover specific chemical immobilization can endow good reliability and reproducibility of immunosensors because Ab can be immobilized intimately through stable covalent bonding on the surface of substrate [39].

Thiols and polysiloxanes are widely used to modify the surface chemistry of inorganic materials and immobilize Ab on the surface [12, 51]. With or without the use of linkers, Ab can be covalently immobilized on chemically modified surface of substrates. Particularly sulfide groups, highly reactive to covalent interaction, are frequently included in Ab or can be engineered into Ab by site-directed mutagenesis, in addition sulfide groups reacts specifically with thiols thus diverse immobilization methods using thiols have been widely studied and introduced [51]. However it may be difficult to immobilize intact Ab using thiols without specific linkers such as protein A and G because sulfide groups in intact Ab are not exposed to the surface but buried into its structure. Polysiloxanes are polymers consisting of an inorganic silicon-oxygen backbone with organic side groups

attached to the silicon atoms, which are four coordinate. Because of its high potential to achieve good intimacy and stability, immobilization of Ab using polysiloxanes are widely applied in various fields of analytical studies such as chromatography [8], optical [21], mechanical [37], and electrochemical biosensors [34]. Polysiloxanes form self-assembled monolayers (SAMs) on metal oxide surface by silanol (-Si-O-) and siloxane (-Si-O-Si-) [41]. Polysiloxanes are applied to immobilize diverse organic substances because functional groups of SAMs can be chemically modified to form the active intermediate that can react with various organic substances [8, 12, 22, 28]. For Ab immobilization, glutaraldehyde is often used to modify the chemical reactivity of functional groups of polysiloxane SAMs. Generally, on the external surface, Ab has lysine having amine residue that is reactive to form covalent bonding as globular proteins do, thus Ab can be linked with functionalized SAMs by the addition of glutaraldehyde [12]. We focused on polysiloxane to search and develop an appropriate method for Ab immobilization on aluminum surface since aluminum was used as a substrate of immunosensors in this thesis.

1.5.   EIS immunosensor

Electrochemical impedance spectroscopy (EIS) is a sensitive and non-destructive technique, which can monitor the dynamics of bound or mobile charges in the interfacial regions of electrode [26, 33]. EIS is highly effective to characterize the physicochemical properties of the intermediate between liquid and solid although it can not lead the identification of the chemical bond [17].

EIS combines the analysis of both the resistive and capacitive properties of materials, based on the perturbation of a system at equilibrium by a small amplitude sinusoidal excitation signal. Usually, EIS is conducted at different frequency of current [2]. The big advantages of this technique are a) an experimental ability to make high precision measurement because the response may be indefinitely steady and can therefore be averaged over a long term, b) an ability to treat the response theoretically by linearized current-potential characteristics, c) measurement in a short time and over a wide frequency range[2], and d) independent characterization of resistive and capacitive properties of intermediate at liquid and solid interface by analyzing the phase shift and amplitude (or real and imaginary parts of impedance) of current [6, 36].

The advantage of EIS as a signal transducer of immunosensor is that EIS can monitor the target substance directly without labeling, thus it is expected that an direct analysis of immunosensor can be developed and industrialized based on EIS [48]. Impedance responds sensitively to the changes in the local geometry, the dielectricity, or the surface potential, driven by adsorption of certain substances or by changes in translational and rotational degree of chemical residues on solid surface [18, 46]. The adsorption of organic substance on electrode surfaces enhance the increase in capacitance [6] and the reduction in polarizability of solid surface results the increase in impedance [18]. Therefore the idea to use EIS as signal transducers for the direct detection of affinity interactions seems to be promising [7, 35].

The target analytes for impedimetric immunosensor may be Ab, Ag, and DNA. The associations of target analytes with their counterparts which can be Ab for Ag, Ag for Ab [9, 17, 38], or complimentary DNA for target DNA [16] influence the electrochemical properties of

immunosensor. The immunosensor to detect glycoprotein, which is associated with human mammary tumor, was presented [25]. The adsorption of glycoprotein on a gold electrode, where Ab for glycoprotein was immobilized, induced the increase in resistance while the dissociation of glycoprotein by urea induced the decrease in resistance. Therefore, it is certain that the association of organic material, which is not electrochemically active, hinders the electric current flow and induces the increase in resistance [25]. The Ab-Ag reaction is an equilibrium process and the impedimetric signal may be proportional to the level of Ab-Ag reaction. When the different concentration of human IgG was introduced on anti-human IgG immobilized immunosensor, the imaginary impedance domain in the Nyquist plot increased as the concentration of human IgG. The impedimetric signal showed a linear relationship with human IgG concentration at the range from 10-80ng/ml and even extremely low concentration (10pg/ml) could be measured [38]. DNA also could be detected with an impedimetric immunosensor. When complimentary DNA was introduced to DNA immunosensor, there was specific increase in impedance especially at 120Hz [18].

As referred above the method for the detection of bioterrorism toxins have to be as sensitive to detect them in nanolevel. However, frequently, the development of a sensitive and rapid EIS immunosensor has been problematic because of its low sensitivity arising from the difficulty to immobilize enough number of immunological recognition elements intimately. Furthermore current studies for impedimetric immunosensor stay in the model systems. Hence, in this thesis, to overcome current drawbacks of EIS immunosensors, nanofabrication, surface chemistry, and electrochemical behaviors of Ab-Ag reaction were studied and discussed.

1.5.1.　　EIS

Impedance is a general expression, which can be applied to any electrical entity impeding the flow of current. Unlike classic resistance, the concept of impedance includes frequency of electrical current. Impedance follows Ohm's law at a frequency of 0 Hz (1. 1). Thus impedance could be used to denote a resistance, a pure reactance, or as is most likely in the real world, a complex combination of both reactance and resistance.

$$R = \frac{E}{I} \tag{1. 1}$$

As impedance is the perturbation of electrical current under certain frequency, the current and potential can be expressed:

$$E(t,\omega) = E_0 \cos(t,\omega) , \ I(t,\omega) = I_0 \cos(t,\omega - \theta)$$

$$\dot{Z}(t,\omega) = \frac{E(t,\omega)}{I(t,\omega)} = \frac{E_0 \cos(t,\omega)}{I_0 \cos(t,\omega - \theta)} = Z_0 \frac{\cos(t,\omega)}{\cos(t,\omega - \theta)} \tag{1. 2}$$

where $\omega = 2\pi f$, ω = the radial frequency, $E(t)$ = the potential at time t, E_0 = the amplitude of the signal, $I(t)$ = the current at t, I_0 = the amplitude of the signal, θ = shifted phase, $\dot{Z}$ = the impedance. Using Eulers relationship:

$$e^{j\theta} = \cos\theta + j\sin\theta \tag{1. 3}$$

the potential and current response may be expressed as:

$$E(t) = E_0 e^{j\omega t}, \ I(t) = I_0 e^{(j\omega t - j\theta)}$$

Therefore, the impedance is then represented and simplified as:

$$\dot{Z}(t,\omega) = \frac{E_0 \cos(t,\omega)}{I_0 \cos(t,\omega)} = Z_0 e^{j\omega t} = Z_0(\cos\theta + j\sin\theta) = Z'(t,\theta) + jZ'' \tag{1. 4}$$
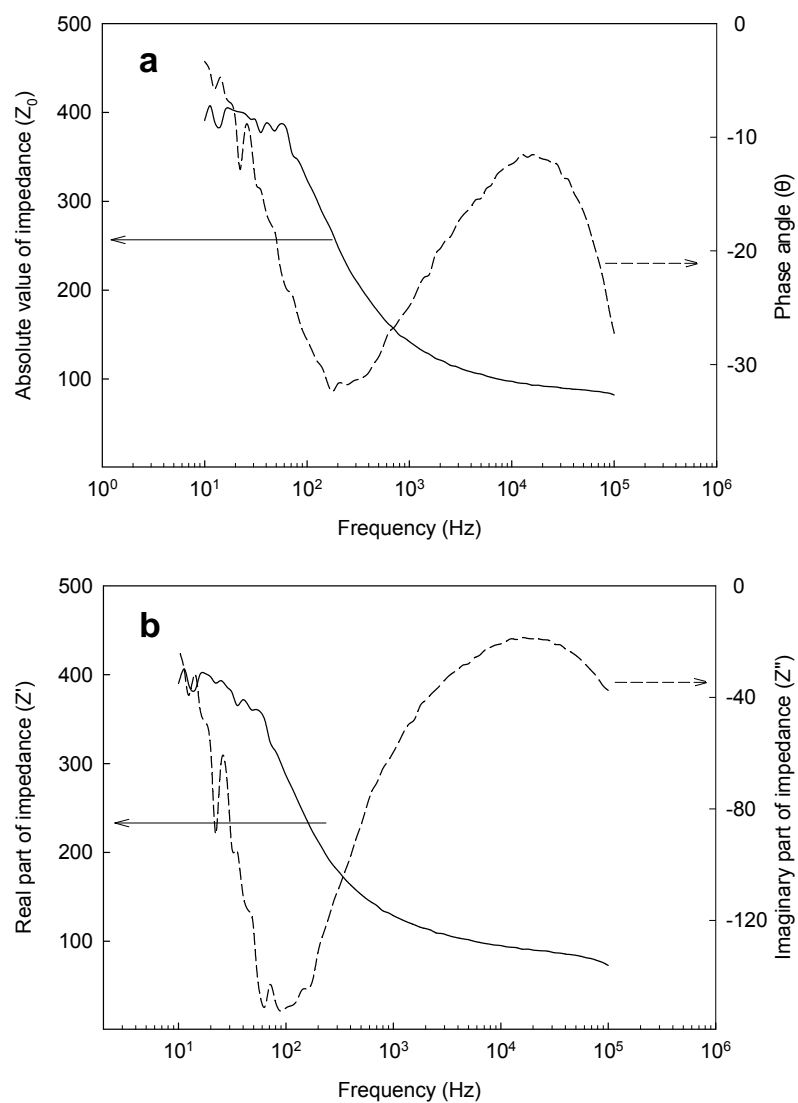
Figure 1.2. Typical spectra of a) absolute value of impedance (Z_0) and phase angle (θ),

and b) real part of impedance (Z'), and imaginary part of impedance (Z'').

where Z_0 = a quantity of impedance, θ = phase angle, Z' = real part of impedance, and Z'' = imaginary part of impedance.

As discussed previously EIS allows collecting over a wide range of frequency even over a long term of analysis. Figure 1.2 shows typical bode plots of Z_0 and θ or Z' and Z''. Z_0 from immunosensor. The characteristics of impedance of immunosensor at certain time can be elucidated by interpreting θ. The increase of θ indicates the increase of inductive characteristics and the decrease of θ indicates the increase of capacitive characteristics. Additionally, as θ is dependent on Z' and Z'' (1. 5), it can be assumed that Z' represents inductive characteristics and Z'' capacitive characteristics. Consequently the presentation of impedimetric signal outputs by Z' and Z'' enables to present each characteristic.

$$\tan\theta = \frac{Z''}{Z'} \qquad (1.5)$$

Bode plots of are great means to understand the impedimetric characteristics of immunosensor. However the intuitive differences in impedimetric signal outputs from each EIS immunosensor make it difficult to distinguish the effect of immunoreaction on impedimetric signal outputs or to compare impedimetric signal outputs from different EIS immunosensor. Hence normalized values of impedimetric signal outputs (1. 6) were used in this thesis to distinguish the effect of immunoreaction on impedimetric signal outputs and to compare impedimetric signal outputs from different EIS immunosensor.

$$Z_{norm} = \frac{Z_t}{Z_{initial}} \qquad (1.6)$$

1.5.2.   Mode of EIS analysis

Measuring mode of EIS of immunosensor can be designed based on the combination of immunosensor and auxiliary electrodes (counter electrode and/or reference electrode). Impedance of immunosensor can be analyzed under two different modes of EIS as illustrated in Figure 1.3, where WE, CE, RE are acronyms for working (i.e. immunosensor), counter and reference electrodes, respectively. Three-electrodes mode (Figure 1.3.a) is widely used in electroanalytical chemistry since the polarization of WE enforced between WE and RE make it possible to exclude the background effect on impedance. However, three-electrode mode is rarely used as a signal transducer of immunosensor, despite its great potential for the development of highly sensitive and reliable immunosensors. In two-electrode mode of EIS (Figure 1.3. b), WE and CE are arranged in symmetry and the impedance including the bulk properties of sample solution and the physicochemical reactions on WE can be obtained. Although two-electrode mode of EIS has a drawback that it is inevitable to inclusion of the background effects, the simplicity in its structure make it amenable for the miniaturization.

1.6.   Nanomaterials for immunosensors

Nanotechnology may be referred as a field of an applied science and technology whose subjects are on the control of materials in nanoscale (usually 1-100nm) and the study of physicochemical phenomena from nanomaterials. The dimension of nanomaterials is commonly comparable with the critical length or width of physicochemical phenomena, and this makes nanomaterials have unique properties that are
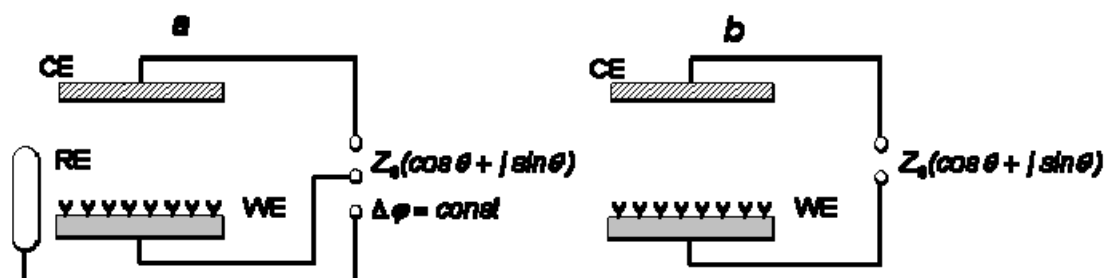
Figure 1.3. Schematic representation of modes of EIS analysis a) three-electrode mode and

b) two-electrode mode.

different from those of the bulk-materials [27] furthermore gives new opportunity to use such nanomaterials in novel applications and devices [42]. Because of their unique characteristics that are applicable to diverse scientific areas, nanomaterials is of great interest to physicists, chemists, biologists, electrical, and mechanical engineers, and computer scientists [14].

Of particular interests to immunosensor engineers are the facts that 1) nanomaterials have high surface areas than do planar materials, and 2) its dimensional scale is comparable to the critical size or length of immunological recognition elements of immunosensor. As the size or length of immunological recognition elements is mostly in between 1nm to 100nm, nanoarrays of immunological recognition elements are possibly fabricated using nanomaterials. In addition, nanomaterials provide more surface area to incorporate or immobilize immunological recognition elements on their surface than do planar materials hence large number of immunological recognition elements on the surface of immunosensor can be attained by the use of nanomaterials. Moreover the number of immunological recognition elements on the surface of immunosensor may play an important role to determine the critical attributes of immunosensor such as sensitivity, reliability, and speed since the detection of target molecule by immunosensor is initiated from the formation of complexes between immunological recognition elements and their counterparts. Therefore by the use of nanomaterials as substrates of immunosensors can improve sensitivity, reliability, and speed.

Nanotubes (e.g. carbon nanotubes) [44], nanowires (e.g. silicon nanowires) [10], nanoparticles (e.g. cadmium-selenide nanocrystals, gold nanocolloid) [13, 23], and nanoporous materials (e.g. nanoporous silicon) [31] have been studied as substrates of immunosensors, and those studies showed picolevel detections in several minutes.

However it is complicate and expensive to produce such nanomaterials. Despite of their high potential to improve sensitivity and speed of immunosensor, their high raw material costs and manufacturing costs may hinder the further development of inexpensive immunosensors for field-applications. Hence search and/or development of a new nanomaterial that is able to endow cost-efficiency to immunosensor were major interest in this study. We used anodic nanoporous aluminum as a substrate of immunosensor because nanoporous aluminum substrate is cheap and easy to develop. Its applicability to impedimetric immunosensor was studied and its insights as a substrate of immunosensor were discussed.

1.7.   Objectives

Main objective of this thesis is to develop sensitive, rapid, and direct immunosensors that are more amenable for economization and miniaturization in order for the detection of bioterrorism toxins. EIS, capable of direct detection and more amenable for miniaturization, was used as a signal transducer of immunosensor. However it was necessary for search and/or development of new processing methods to improve the sensitivity of EIS immunosensor since frequently the development of a sensitive and rapid EIS immunosensor has been problematic because of its low sensitivity. For this, the systematic studies including nanofabrication, surface modification, and electrochemical analysis have been carried out together with search for a new nanomaterial that is more cost efficient than other nanomaterials.

Chapter 1 *"General introduction"* is to address the review of literature and to introduce general features, manufacturing processes of immunosensors, and application of nanomaterials to immunosensors.

Chapter 2 *"Development of nanoporous aluminum by anodization"* is to produce nanoporous aluminum to be used as the substrate of EIS immunosensor. Food grade aluminum (FGA) was used to develop a cost-efficient nanoporous material. Porous structure on FGA was controlled electrochemically and/or chemically then the surface morphology was investigated by visualization of the surface using surface probe microscopy (SPM).

Chapter 3 *"Development of a practical method for Ab immobilization on aluminum surface"* is to develop a practical method to immobilize Ab on aluminum surface. Since the use of aluminum as the substrate of immunosensor has not been reported, it was necessary to develop a method of Ab immobilization onto aluminum surface in order for the development of EIS immunosensor. To mediate Ab with aluminum surface, APTES, frequently used for the surface modification of oxide layer was used. By contact angle measurement and fluorescence studies, the appropriate concentration of APTES and time of silanization for Ab immobilization on aluminum surface were determined.

Chapter 4 *"Homogenous distribution of antibody on nanoporous surface for the application of immunosensor"* is to investigate the effect of pore diameter on Ab immobilization. Nanoporous aluminum was applied to EIS immunosensor in order to improve the sensitivity by increasing the number of immobilized Ab on the substrate of immunosensor. However the dimension of nanoporous structure on anodized aluminum should be considered since nanoporous aluminum to increase the number of immobilized

Ab should be comparable to the dimension of Ab. The effect of pore diameter on the number of immobilized Ab was investigated by visualizing surface morphology of immunosensor based on nanoporous structure and by fluorescence studies

Chapter 5 *"Label-free toxin detection by means of time-resolved electrochemical impedance spectroscopy"* is to evaluate the appropriation of modes of EIS analysis and to demonstrate the performance of developed EIS immunosensor. EIS immunosensor can be analyzed using two different modes of EIS. The appropriation of each mode of EIS was evaluated by comparing the sensitivity of EIS immunosensor. Moreover the limit of detection and time of detection were discussed.

Chapter 6 *"Applicability of EIS immunosensor to foods including acidic foods"* is to investigate the applicability of EIS immunosensor to real foods especially to acidic foods. The effect of adsorption of acids or ions on EIS immunosensor on impedimetric signal outputs was studied by a time-resolved EIS and the feasibility of EIS immunosensor in real foods was discussed.

1.8.   References

1. Arnold, M. A.; Rechnitz, G. A., Optimization of a tissue-based membrane electrode for guanine. Analytical Chemistry 1982, Vol. 54, 777-782.

2. Bard, A. J.; Faulkner, L. R., Electrochemical Methods: Fundamentals and Applications. 2nd ed.; John Wiley & Sons: Singapore, 2001; 368.

3. Barker, S. A., Immobilization of the biological component of biosensors. In; Turner, A. P. F.; Karube, I.; Wilson, G. S. (Ed.); Biosensors: Fundamentals and Applications, Oxford University Press: New York, USA, 1987; 770.

4. Bellamy, R. J.; Freedman, A. R., Bioterrorism. QJM 2001, Vol. 94, 227-234.

5. CDC, Bioterrorism agents /
    diseases. http://www.bt.cdc.gov/bioterrorism/overview.asp (December 15 2007),

6. Cheng, T. J.; Lin, T. M.; Chang, H. C., Physical adsorption of protamine for heparin
    assay using a quartz crystal microbalance and electrochemical impedance
    spectroscopy. Analytica Chimica Acta 2002, Vol. 462, 261-273.

7. Chiang, K.-L.; Krull, U. J.; Nikolelis, D. P., Ellipsometric determination of the
    structure of surface-stabilized bilayer lipid membranes on silver metal. Analytica
    Chimica Acta 1997, Vol. 357, 73-77.

8. Collins, K. E.; Bottoli, C. B. G.; Vigna, C. R. M.; Bachmann, S.; Albert, K.; Collins,
    C. H., Self-immobilization of poly(methyloctylsiloxane) on high-performance
    liquid chromatographic silica. Journal of Chromatography A 2004, Vol. 1029,
    43-48.

9. Cui, X.; Pei, R.; Wang, Z.; Yang, F.; Ma, Y.; Dong, S.; Yang, X., Layer-by-layer
    assembly of multilayer films composed of avidin and biotin-labeled antibody for
    immunosensing. Biosensors and Bioelectronics 2003, Vol. 18, 59-67.

10. Cui, Y.; Wei, Q.; Park, H.; Lieber, C. M., Nanowire nanosensors for highly sensitive
    and selective detection of biological and chemical species. Science 2001, Vol. 293,
    1289-1292.

11. D'Orazio, P., Biosensors in clinical chemistry. Clinica Chimica Acta 2003, Vol. 334,
    41-69.

12. Dubrowski, A., Adsorption - from theory to practice. Advances in Colloid and
    Interface Science 2001, Vol. 93, 135-224.

13. Englebienne, P., Use of colloidal gold surface plasmon resonance peak shift to infer
    affinity constants from the interactions between protein antigens and antibodies
    specific for single or multiple epitopes. The Analyst 1998, Vol. 123, 1599-1603.

14. European-Commission,
Nanotechnology. http://ec.europa.eu/research/leaflets/nanotechnology/index_en.ht
ml (September 24 2007),

15. Evenson, M. L.; Ward Hinds, M.; Bernstein, R. S.; Bergdoll, M. S., Estimation of
human dose of staphylococcal enterotoxin A from a large outbreak of
staphylococcal food poisoning involving chocolate milk. International Journal of
Food Microbiology 1988, Vol. 7, 311-316.

16. Farace, G.; Lillie, G.; Hianik, T.; Payne, P.; Vadgama, P., Reagentless biosensing
using electrochemical impedance spectroscopy. Bioelectrochemistry 2002, Vol. 55,
1-3.

17. Gabrielli, C., Electrochemical impedance spectroscopy: principles, instrumentation,
and applications. In; Rubinstein, I. (Ed.); Physical Electrochemistry, Principles,
Methods, and Applications, Marcel-Dekker: New York, USA, 1995; 243-292.

18. Gheorghe, M.; Guiseppi-Elie, A., Electrical frequency dependent characterization
of DNA hybridization. Biosensors and Bioelectronics 2003, Vol. 19, 95-102.

19. Ghindilis, A. L.; Atanasov, P.; Wilkins, M.; Wilkins, E., Immunosensors:
electrochemical sensing and other engineering approaches. Biosensors and
Bioelectronics 1998, Vol. 13, 113-131.

20. Gibson, J.; Drociuk, D.; Fabian, T.; Brundage, S.; Ard, L.; Fitzpatrick, N.;
Moorhead, W.; Schwartz, M.; Kilbourne, E.; Schier, J.; M. Patel; Belson, M.; Rubin,
C.; Osterloh, J.; Deitchman, S.; Kiefer, M.; Meyer, R., Investigation of a
ricin-containing envelope at a postal facility —South Carolina, 2003. Morbidity and
Mortality Weekly Report 2003, Vol. 52, 1129-1131.

21. Grant, S. A.; Pierce, M. E.; Lichlyter, D. J.; Grant, D. A., Effects of immobilization
on a FRET immunosensor for the detection of myocardial infarction. Analytical and
Bioanalytical Chemistry 2005, Vol. 381, 1012-1018.

22. Halliwell, C. M.; Cass, A. E., A factorial analysis of silanization conditions for the immobilization of oligonucleotides on glass surfaces. Analytical Chemistry 2001, Vol. 73, 2476-2483.

23. Han, M.; Gao, X.; Su, J. Z.; Nie, S., Quantum-dot-tagged microbeads for multiplexed optical coding of biomolecules. Nature Biotechnology 2001, Vol. 19, 631-635.

24. Ho, M. Y. K.; Rechmitz, G. A., An introduction to biosensors. In; Nakamura, R. M.; Kasahara, Y.; Rechnitz, G. A. (Ed.); Immunochemical Assays and Biosensor Technology for the 1990s, Americal Society for Microbiology: Washington, D.C., USA, 1992; 275-290.

25. Jie, M.; Ming, C. Y.; Jing, D.; Cheng, L. S.; Huai na, L.; Jun, F.; Xiang, C. Y., An electrochemical impedance immunoanalytical method for detecting immunological interaction of human mammary tumor associated glycoprotein and its monoclonal antibody. Electrochemistry Communications 1999, Vol. 1, 425-428.

26. Jonscher, A. K., Dielectric Relaxation in Solids. Chelsea Dielectrics Press: London, England, 1983; 380.

27. Kodama, K.; Iikubo, S.; Taguchi, T.; Shamoto, S., Finite size effects of nanoparticles on the atomic pair distribution functions. Acta Crystallographica Section A 2006, Vol. 62, 444-453.

28. Kumar, A.; Larsson, O.; Parodi, D.; Liang, Z., Silanized nucleic acids: a general platform for DNA immobilization. Nucleic Acids Research 2000, Vol. 28, E71-e71.

29. Leca-Bouvier, B.; Blumatrice, L. J., Biosensors for protein detection: a review. Analytical Letters 2005, Vol. 38, 1491-1517.

30. Lillie, G.; Payneb, P.; Vadgamac, P., Electrochemical impedance spectroscopy as a platform for reagentless bioaffinity sensing. Sensors and Actuators B 2001, Vol. B78, 249-256.

31. Lin, J. N.; Herron, J.; Andrade, J. D.; Brizgys, M., Characterization of immobilized antibodies on silica surfaces. IEEE Transactions on Biomedical Engineering 1988, Vol. 35, 466-471.

32. Liss, M.; Petersen, B.; Wolf, H.; Prohaska, E., An aptamer-based quartz crystal protein biosensor. Analytical Chemistry 2002, Vol. 74, 4488-4495.

33. Macdonald, J. R., Impedance Spectroscopy-Emphasizing Solid Materials and Systems. Wiley-Interscience: New York, USA, 1987; 346.

34. Mantzila, A. G.; Prodromidis, M. I., Performance of impedimetric biosensors based on anodically formed Ti/TiO_2 electrodes. Electroanalysis 2005, Vol. 17, 1878-1885.

35. Nikolelis, D. P.; Krull, U. J., Bilayer lipid membranes for electrochemical sensing. Electroanalysis 1993, Vol. 5, 539-545.

36. Norlin, A.; Pan, J.; Leygraf, C., Investigation of interfacial capacitance of Pt, Ti and TiN coated electrodes by electrochemical impedance spectroscopy. Biomolecular Engineering 2002, Vol. 19, 67-71.

37. Okahata, Y.; Ebara, Y.; Sato, T., Quantitative detection of protein binding to the membrane surface using a quartz-crystal microbalance. In; Lvov, Y.; Mèohwald, H. (Ed.); Protein Architecture: Interfacing Molecular Assemblies and Immobilization Biotechnology, Marcel-Dekker: New York, USA, 2000; 55-74.

38. Ouerghi, O.; Touhami, A.; Jaffrezic-Renault, N.; Martelet, C.; Ouada, H. B.; Cosnier, S., Impedimetric immunosensor using avidin-biotin for antibody immobilization. Bioelectrochemistry 2002, Vol. 56, 131-133.

39. Patel, N.; Davies, M. C.; Hartshorne, M.; Heaton, R. J.; Roberts, C. J.; Tendler, S. J. B.; Williams, P. M., Immobilization of protein molecules onto homogeneous and mixed carboxylate-terminated self-assembled monolayers. Langmuir 1997, Vol. 13, 6485-6490.

40. Pei, R.; Yang, X.; Wang, E., Enhanced surface plasmon resonance immunosensing using a streptavidin-biotinylated protein complex. The Analyst 2001, Vol. 126, 4-6.

41. Plueddemann, E. P., Silane Coupling Agents. 2nd ed.; Plenum Press: New York, USA, 1991; 253.

42. Sigma-Aldrich, Nanomaterials: tutorial on nanotechnology, nanotools and nanostructured materials. http://www.sigmaaldrich.com/Area_of_Interest/Chemistry/Materials_Science/Nanomaterials/Tutorial.html (September 24 2007),

43. Spiridonova, V. A.; Kopylov, A. M., DNA aptamers as radically new recognition elements for biosensors. Biochemistry 2002, Vol. 67, 706-709.

44. Star, A.; Gabriel, J. C. P.; Bradley, K.; Gruner, G., Electronic detection of specific protein binding using nanotube FET devices. Nano Letters 2003, Vol. 3, 459-463.

45. Sullivan, B. M., Bioterrorism detection: the smoke and the canary. Technology Review Journal 2003, Vol. 11, 135-141.

46. Sutherland, R. M.; Dahne, C.; Place, J. F.; Ringrose, A. S., Optical detection of antibody-antigen reactions at a glass-liquid interface. Clinical Chemistry 1984, Vol. 30, 1533-1538.

47. Turner, A. P. F.; Karube, I.; Wilson, G. S., Biosensors: Fundamentals and Applications. Oxford University Press: New York, USA, 1987; 770.

48. Vagin, M. Y.; Karyakina, E. E.; Hianik, T.; Karyakin, A. A., Electrochemical transducers based on surfactant bilayers for the direct detection of affinity interactions. Biosensors and Bioelectronics 2003, Vol. 18, 1031-1037.

49. Veetil, J. V.; Ye, K., Development of immunosensors using carbon nanotubes. Biotechnology Progress 2007, Vol. 23, 517-531.

50. WHO, WHO (World Health Organization) publishes guidance to minimize terrorist threats to food. Central European Journal of Public Health 2003, Vol. 11, 62.

51. Yang, S.; Perex-Luna, V. H.; Lopez, G. P., Two-dimensional pattering of proteins. In; Lvov, Y.; Mèohwald, H. (Ed.); Protein Architecture: Interfacing Molecular Assemblies and Immobilization Biotechnology, Marcel-Dekker: New York, USA, 2000; 356-389.

Chapter 2. Development of nanoporous aluminum by anodization

2.1.   Introduction

Sensitivity and speed are regarded most importantly for immunosensor that is one of most practical methods for bio-defense against bioterrorism since these they may determine the efficiency of bio-defense. However the development of EIS immunosensor for the detection of bioterrorism toxins has been problematic due to its low sensitivity despite of its advantageous features such as non-destructive and direct analysis without labeling [2, 19], and amenability for miniaturization [1].

Recently, to improve sensitivity of immunosensors, nanomaterials have been investigated as substrates of immunosensors, and it has been reported that the use of nanomaterials can improve sensitivity, speed, and reliability of immunosensors [14]. Nanomaterials that can be used for immunosensor may include nanoparticles (e.g. gold nanocolloids) [31], nanowires (e.g. silicon nanowires) [4], nanotubes (e.g. carbon nanotubes) [27], and nanoporous materials (e.g. nanoporous silicon) [18]. Nanoporous materials may be more appropriate to use as substrates of electrochemical immunosensors because it may be easier to integrate nanoporous materials within electrochemical signal transducers compared to other nanomaterials.

Among diverse porous inorganic materials, porous silicon is most widely used for immunosensor because of its unique optical and electrical properties enhanced from quantum confinement effects [3, 5]. Porous silicon can be produced by electrochemically, and

the pore diameter can be controlled easily from nanoscale to microscale by adjusting the parameters of electrochemical fabrication [6, 11]. Especially silicon oxide layer, that can allow Ab immobilization on the surface of porous silicon by deposition of coupling reagents such as polysiloxane, is formed on the surface of porous silicon by oxidization during electrochemical fabrication [8, 20]. Consequently porous silicon is regarded as a versatile substrate of immunosensor with optical or electrochemical detection. However electrochemical fabrication of porous silicon is tedious and need extreme caution since it is inevitable to use flammable or explosive reagents such as piranha solution and hydrofluoric acid. Moreover high raw material cost of porous silicon can also be an obstacle for economization of immunosensor. In addition it is very difficult to cut silicon to desired shapes. Hence, in this study, search and development of a new nanoporous material that is more cost effective were of interest in order to develop a sensitive and rapid EIS immunosensor.

Porous aluminum oxide layer is one of the most attractive inorganic materials to use as a substrate of electrochemical immunosensor since it is very feasible to control the surface morphology and modify the surface chemistry. Regularly arrayed porous structure on the surface of aluminum can be obtained by aluminum anodization under appropriate condition, and even the pore diameter can be controlled easily from a few nanometers to several hundred nanometers by adjusting the applied voltage [9, 13, 24]. In addition further control of the pore diameter without any change of pore density is possible by a simple chemical process, known as pore widening process that widens the pore diameter by dissolving aluminum oxide in the pore wall in an acidic solution. Pore widening is a chemical reaction that is dependent on the reaction time and temperature, so the pore

diameter can be controlled precisely to desired scale by adjusting reaction time or temperature [12, 17]. Consequently anodization is a very feasible method to obtain nanoporous aluminum oxide layer with desired scale. Also it is more cost effective than lithographic methods since anodization is conducted in generic chemicals by applying low voltage (less than 100V). Most of all, theoretically, aluminum oxide is applicable to Ab immobilization using polysiloxanes. In the angle of device engineering, aluminum is more flexible to develop a device with a desired shape than silicon because aluminum is easy to cut to desired shapes. Therefore it has been proposed to use nanoporous anodic aluminum in order to develop a sensitive and rapid EIS immunosensor [28] however EIS immunosensor based on porous aluminum substrate has not been reported. In this study, Food Grade Aluminum (FGA) that is cheap and commonly used for food packaging was used to endow amenability of economization on EIS immunosensor and fabricated to nanoporous structure. The pore diameter was controlled by adjusting the applied voltage of anodization and/or pore widening. FGA were anodized at different the applied voltage (10, 20, 30, 40, or 50V) then anodized aluminum at 30 and 40V were subjected to pore widening for further control of the pore diameter. 5%wt/v phosphoric acid was used for pore widening and different temperature (10, 15, 20, or 25°C) was applied in order to control the pore diameter. The surface morphology, especially pore diameter, of nanoporous aluminum oxide layer was investigated using surface scanning microscopy (SPM). In this chapter, fabrication of nanoporous aluminum oxide layers into different pore diameters is described and discussed, and the effects of pore diameter on Ab immobilization are described and discussed in chapter 3 and chapter 4.

2.1.1.   Methodological background

Aluminum anodization is a well established electrochemical process commonly

employed in the metal finishing industry to passivate and protect aluminum from corrosion

and abrasion[10]. Anodization forms aluminum oxide layer on the surface of aluminum in

electrolytes by supplying DC voltage. The surface morphology can be controlled by

electrolyte and anodization conditions such as the applied voltage and temperature [15, 24, 25].

If electrolyte that cannot dissolve the oxide is used for aluminum anodization, oxide layer

may grow only as long as the resistance of oxide layer hinders current to flow. The

resultant oxide layer is very thin and nonporous. If electrolyte that can dissolve oxide

slightly is used, porous aluminum oxide layer may be formed on the surface of aluminum.

Sulfuric, chromic, phosphoric, and oxalic acid are widely used in certain applications to

manufacture porous aluminum oxide layer on the surface of aluminum. Porous fabrication

of aluminum surface is widely used to improve adhesion of coloring pigments or to color

the surface by deposition of other metals into pores [10].

The formation of porous aluminum oxide layer by anodization follows a sequence

of several stages that can be divided to three stages; 1) a thin and nonporous aluminum

oxide layer formation, 2) pore initiation, and steady pore growth [29]. As this reaction

involves electric field enhanced chemical dissolution of oxide at oxide/electrolyte interface

and metal dissolution into oxide at metal/oxide interface (Figure 2.1), 3) electric field is a

key parameter to control the speed of anodization and pore diameter [29]. Pore diameter is

controllable from a few nanometers to several hundred nanometers by adjusting electric
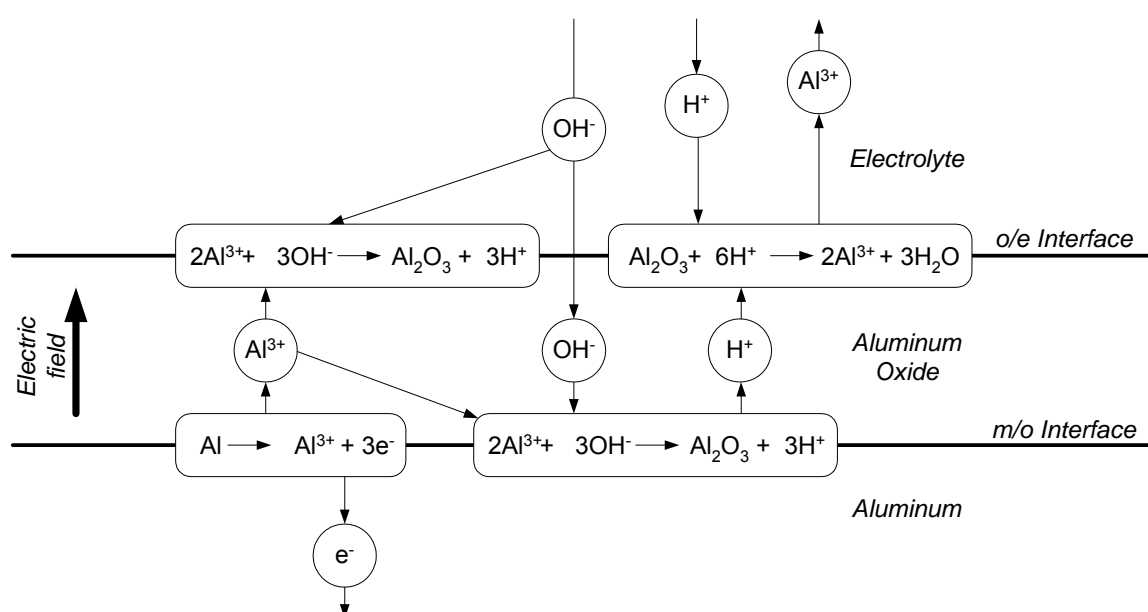
Figure 2.1. Schematic diagram of the electrochemical reactions and ionic paths involved during anodization of aluminum [29].

field. Moreover it is easy and very feasible to control pore diameter because of a linear dependence of pore diameter on the applied voltage [24, 25]. In the metal finishing industry, 15 ~ 21V is commonly applied to enhance porous aluminum oxide layer, and pore diameter is 10 ~ 150nm upon the electrolyte and the applied voltage [9]. Due to its feasibility, and well arrayed and controllable structure of nanoporous aluminum oxide layer, the interest in use of porous anodic aluminum oxide layer to synthesize nanomaterials such as nanowires is rapidly growing [28]. Porous anodic aluminum oxide layer is frequently used as a template to synthesize nanowires and nanoarray [21, 26, 30].

2.2. Materials and methods

2.2.1. Materials

Oxalic acid, anhydrous 98% and phosphoric acid, 85% solutions in water were purchased from Acros Organics (NJ, USA). Ethanol, HPLC grade and acetone, HPLC grade were purchased from Fisher Scientific (Fair Lawn, NJ, USA). Perchloric acid, 60% and 2-butoxyethanol were purchased from Alfa Aesar (Ward Hill, MA, USA) and J. T. Baker (Phillipsburg, NJ, USA). Electropolishing solution was prepared by mixing 70.0vol.% of ethanol, 13.8vol.% of distilled water (DI water), 10.0vol.% of 2-butoxyethanol, and 6.2vol.% of perchloric acid. Commercial grade aluminum (alloy 1100, thickness 0.25 mm), polycarbonate, and stainless steel 316 were purchased from McMaster-Carr (Dayton, NJ, USA). A custom-designed electrochemical chamber was used to anodize aluminum. Its body was made of polycarbonate. To avoid the

accumulation of air bubble during aluminum anodization, stainless steel mesh was used as cathode and stainless steel having 12.8cm in its diameter was embedded to support aluminum to be anodized. An internal compartment of the chamber is conically-shaped. The distance between cathode and anode was 5cm.

2.2.2. Methods

Anodization. Alloy 1100 was cut into 12.8cm in diameter and heated at 500°C to anneal the aluminum discs after cleaning the surface with acetone. To get smooth surface, aluminum discs were polished electrochemically in the electropolishing solution (70% ethanol, 15.6% water, 15% 2-butoxyethanol, and 4.4% perchloric acid) for 40 seconds with vigorous stirring at 42V, supplied by PC-controlled DC power supply (model number 1787A, BK Precision Corp.,Yorba Linda, CA, USA). Electropolished aluminum substrates were used to anodize aluminum. Aluminum anodization was performed in 0.3M oxalic acid at 10, 20, 30, 40, or 50V by PC-controlled DC power supplier. During the anodization, temperature was maintained at 5°C by Isotemp refrigerated circulator (model number 3016, Fisher Scientific, Pittsburgh, PA, USA). After vigorous rinsing with DI water, anodized aluminum at 30 and 40 V were immersed into 5wt% phosphoric acid for 1hr at different temperature (10, 15, 20, and 25°C). Nanoporous aluminum discs were washed with SDI water and dried in nitrogen atmosphere. To prevent accidental surface contamination, anodized aluminum discs were heated at 150°C for 30 min and stored in sterilized condition.

Morphological analysis of nanoporous aluminum. Morphological changes of aluminum were analyzed by Scanning Probe Microscope (SPM) Q-Scope 350 (Quesant

Inst. Corp., Agoura Hills, CA, USA) in tapping mode with NSC-16 cantilevers. A specialized software package, SPIP 3.3 (NanoScience, Phoenix, AZ, USA) was used for image processing and analysis of nanoscale patterns on aluminum surface.

2.3.   Results and discussion

Alloy 1100, food grade aluminum (FGA), commonly used for food packaging, is usually finished mechanically thus its surface is rough as seen in Figure 2.2. a. Since the surface morphology of aluminum before anodization affects the surface morphology of anodized aluminum, FGA was polished electrochemically to synchronize the surface area and surface geometry of each FGA disc. Especially, for substrates of immunosensor, the synchronization may be very critical for the reliability and reproducibility of immunosensor because the difference in the surface area or geometry between substrates can affect the number of immobilized Ab as well as signal outputs from immunosensor. To synchronize the surface of aluminum, FGA was electropolished in electropolishing solution at 42V for 20sec and the temperature was maintained at 5°C. Electropolishing changed the rough surface of FGA to planar surface (Figure 2.2). Then electropolished FGA was subjected to anodization or used to develop planar immunosensor (Planar immunosensor will be described and discussed in chapter 3 and chapter 4.).

Electropolished FGA was anodized in 0.3M oxalic acid solution, and the temperature and reaction time for aluminum anodization were restricted to 5°C and 20sec in order to limit the parameters affecting the surface morphology, especially the pore diameter. To control the pore diameter, the applied voltage for aluminum anodization was varied to 10, 20, 30, 40, and 50V. Figure 2.3 shows the surface morphology of anodized
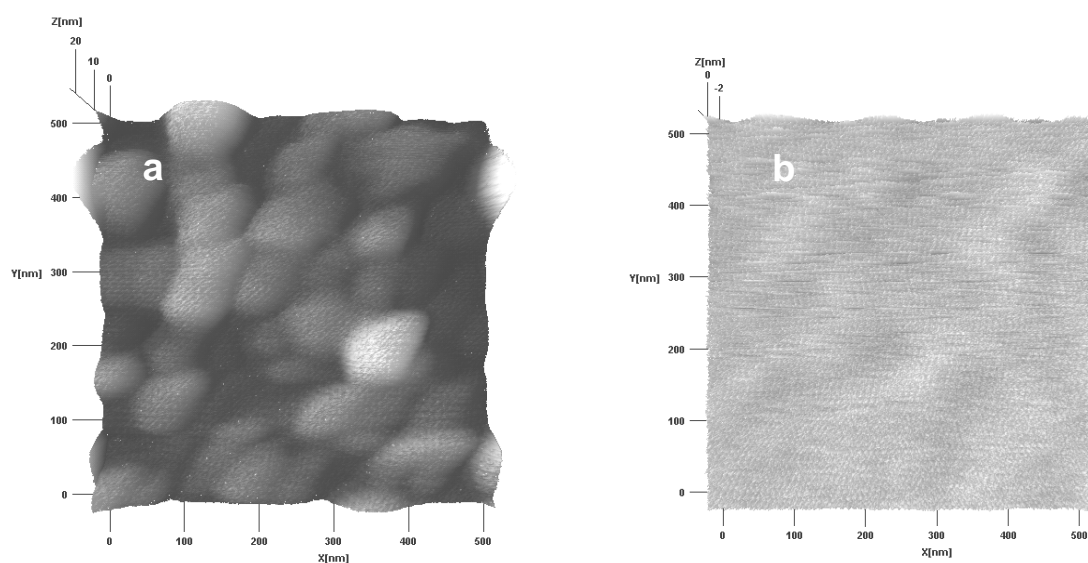
Figure 2.2. Surface morphology of food grade aluminum; alloy 1100 a) before and b) after electropolishing at 42V for 40sec. Images obtained from SPM analysis were processed using SPIP software v.3.3.
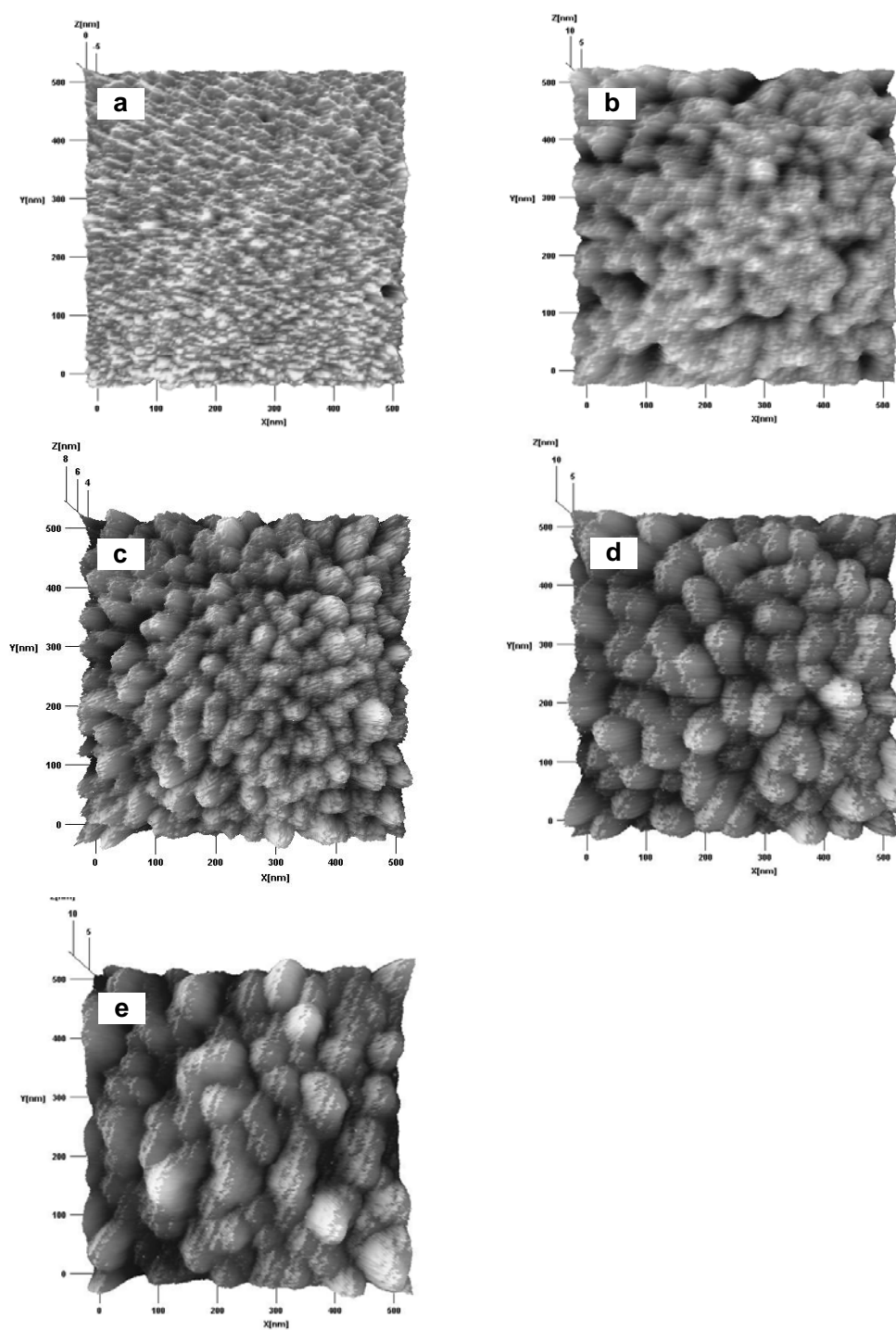
Figure 2.3. Surface morphology of anodized FGA at (a) 10V; (b) 20V; (c) 30V; (d) 40V, (e) 50V in 0.3% oxalic acid. Images obtained from SPM analysis were processed using SPIP software v.3.3.

FGA at different applied voltage. The surface of aluminum oxide layer was turned to porous structure by anodization and the porous structure became more significant as the increase of the applied voltage. As seen from SPM images, by the increase of the applied voltage for aluminum anodization, the pore diameter is increased. Although, from SPM images of anodized FGA, it is difficult to find highly ordered hexagonal arrays of nanopores that are frequently observed on the surface of anodized aluminum when laboratory grade aluminum (LGA) is anodized at an appropriate condition [7], the surface morphology of anodized FGA shows relatively well ordered porous structure (Figure 2.3). However the surface of anodized FGA at 50V is not regularly arrayed and shows differences in grain height or pore depth. Since it has been reported that highly well ordered porous structure can be observed from the surface of anodized LGA at 50V or even higher than 50V [23], the irregular structure on anodized FGA at 50V may be due to the impurity of aluminum content of FGA. Because of its irregular surface structure, anodization of FGA at 50V was put out of scope to develop nanoporous aluminum in order to improve the sensitivity of EIS immunosensor.

SPIP software was used to analyze the pore diameter. A specific option, named pore analysis, in SPIP software allowed to get the average value of the pore diameter on anodized aluminum by analyzing SPM images and they are presented in Table 2.1 and

Table 2.2. The pore diameter at 10, 20, 30, and 40V is 11.3, 14.9, 23.4, and 29.9nm in the pore diameter respectively (Table 2.1). As observed in other studies, the pore diameter from anodized FGA increases proportionally to the applied voltage [24, 25] moreover the pore diameter from anodized FGA at each voltage is well corresponding to that obtained from LGA [24]. Therefore we concluded that aluminum anodization conducted in this study was

Voltage for anodization (V)	The diameter of nanopore ± Standard deviation (nm)
10	11.3 ± 3.59
20	14.9 ± 7.11
30	23.4 ± 9.35
40	29.9 ± 0.92

Table 2.1. Average pore diameter on nanoporous FGA enhanced by anodization at 10, 20, 30, and 40V in 0.3M oxalic acid.

Treatment		The pore diameter± SD (nm)
Anodization voltage (V)	Temperature (^{o}C)	
30	Before pore widening	23.4 ± 9.35
	10	24.6 ± 10.4
	15	25.1 ± 11.9
	20	24.9 ± 7.65
	25	25.7 ± 9.02
40	Before pore widening	29.9 ± 0.92
	10	35 ± 13.5
	15	37.7 ± 13.3
	20	35 ±15.6
	25	38.7 ± 13

Table 2.2. Average pore diameter of anodized FGA after pore widening in 5%wt/v

phosphoric acid at the different temperature for 1hr.

valid and particularly the surface morphology from anodized FGA can be comparable to that from anodized LGA.

As referred in introduction, this study is to develop nanoporous aluminum as substrate of EIS immunosensor. Hence the pore diameter fabricated FGA had to be compared to the size of Ab. Ab is around 12nm in diameter, 12nm in height, and 3nm in thickness [16, 22]. Therefore one can easily note that aluminum anodization at 10 or 20V that results 11.3 or 14.9nm in the pore diameter cannot give adequate diameter for Ab immobilization into nanopores. It can be assumed that 23.4 or 29.9nm in the pore diameter fabricated by the anodization at 30 or 40V will give more appropriate surface morphology to nanoporous aluminum as substrate of EIS immunosensor however appropriate diameter to lead more efficient Ab immobilization can be between 23.4 and 29.9nm or bigger than 29.9nm. Hence anodized aluminum was subjected to pore widening for the further control of the pore diameter. The control of the pore diameter through pore widening was carried out by adjusting temperature because the acid dissolution of aluminum oxide is a chemical reaction depending on the temperature [17]. Anodized aluminum at 30 or 40V was put into 5%wt/v phosphoric acid for 1hr at different temperature (10, 15, 20, and 25°C). Up to 15°C, the pore diameter was increased proportionally to the applied temperature of pore widening step however, at relatively high temperature (20°C<), the change of the pore diameter was not proportional to the applied temperature. The oxide dissolution in phosphoric acid at relatively high temperature might be excessive hence non-proportional increase in the pore diameter at relatively high temperature might be caused by the excessive dissolution of either the wall of nanopore or the upper surface of oxide layer.

However the pore widening step enabled to control the pore diameter in a few nanometers by simple adjustment of temperature in a limited condition (<15 $^{\circ}$C).

2.4.   Conclusion

FGA, having less purity in aluminum content than LGA, has been hardly investigated as academic purposes such as nanopattering or development of nanoporous substrates. In this study, we fabricated the surface of FGA into nanoporous structure in order to investigate the potential of FGA as a nanoporous substrate of EIS immunosensor. Relatively well ordered nanoporous aluminum oxide layer could be obtained by anodization of FGA. The pore diameter could be controlled easily by adjusting the applied voltage of anodization, and the pore diameter could be controlled further by pore widening. Particularly the pore diameter of anodized FGA is predictable since the surface morphology of porous aluminum oxide obtained from anodization of FGA from 10 to 40V is comparable to that from anodization of LGA at same applied voltage. Therefore it can be concluded that anodized FGA from 10 to 40V can be applied to nanopatterning or development of nanoporous substrates.

2.5.   References

1. Bakker, E., Electrochemical sensors. Analytical Chemistry 2004, Vol. 76, 3285-3298.

2. Bard, A. J.; Faulkner, L. R., Electrochemical Methods: Fundamentals and Applications. 2nd ed.; John Wiley & Sons: Singapore, 2001; 368.

3. Canham, L. T., Silicon quantum wire array fabrication by electrochemical and chemical dissolution of wafers. Applied Physics Letters 1990, Vol. 57, 1046-1048.

4. Cui, Y.; Wei, Q.; Park, H.; Lieber, C. M., Nanowire nanosensors for highly sensitive and selective detection of biological and chemical species. Science 2001, Vol. 293, 1289-1292.

5. Cullis, A. G.; Canham, L. T.; Calcott, P. D. J., The structural and luminescence properties of porous silicon. Journal of Applied Physics 1997, Vol. 82, 909-965.

6. De Stefano, L.; Rendina, I.; Moretti, L.; Tundo, S.; Rossi, A. M., Smart optical sensors for chemical substances based on porous silicon technology. Applied Optics 2004, Vol. 43, 167-172.

7. Deng, P. Y.; Bai, X. D.; Chen, X. W.; Feng, Q. L., Anodic oxidization of aluminum at high current densities and mechanism of film formation. Journal of The Electrochemical Society 2004, Vol. 151, B284-B289.

8. Dubrowski, A., Adsorption - from theory to practice. Advances in Colloid and Interface Science 2001, Vol. 93, 135-224.

9. Edwards, J., Coating and surface treatment systems for metals: a comprehensive guide to selection. ASM International: Materials Park, Ohio, USA, 1997; 470.

10. Grubbs, C. A., Anodizing of aluminum. Metal Finishing 2002, Vol. 100, 463-478.

11. Herino, R.; Bomchil, G.; Barla, K.; Bertrand, C.; Ginoux, J. L., Porosity and pore size distributions of porous silicon layers. Journal of The Electrochemical Society 1987, Vol. 134, 1994-2000.

12. Hwang, S. K.; Jeong, S. H.; Hwang, H. Y.; Lee, O. J.; Lee, K. H., Fabrication of highly ordered pore array in anodic aluminum oxide. Korean Journal of Chemical Engineering 2002, Vol. 19, 467-473.

13. Jessensky, O.; Muller, F.; Gosele, U., Self-organized formation of hexagonal pore structures in anodic alumina. Journal of The Electrochemical Society 1998, Vol. 145, 3735-3740.

14. Jianrong, C.; Yuqing, M.; Nongyue, H.; Xiaohua, W.; Sijiao, L., Nanotechnology and biosensors. Biotechnology Advances 2004, Vol. 22, 505-518.

15. Johansson, A.; Lu, J.; Carlsson, J. O.; Boman, M., Deposition of palladium nanoparticles on the pore walls of anodic alumina using sequential electroless deposition. Journal of Applied Physics 2004, Vol. 96, 5189-5194.

16. Kienberger, F.; Mueller, H.; Pastushenko, V.; Hinterdorfer, P., Following single antibody binding to purple membranes in real time. EMBO Reports 2004, Vol. 5, 579-683.

17. Li, A. P.; Muller, F.; Birner, A.; Nielsch, K.; Gosele, U., Hexagonal pore arrays with a 50-420 nm interpore distance formed by self-organization in anodic alumina. Journal of Applied Physics 1998, Vol. 84, 6023-6026.

18. Lin, J. N.; Herron, J.; Andrade, J. D.; Brizgys, M., Characterization of immobilized antibodies on silica surfaces. IEEE Transactions on Biomedical Engineering 1988, Vol. 35, 466-471.

19. Macdonald, J. R., Impedance Spectroscopy-Emphasizing Solid Materials and Systems. Wiley-Interscience: New York, USA, 1987; 346.

20. Mery, E.; Alekseev, S. A.; Zaitsev, V. N.; Barbier, D., Covalent grafting of ion-exchanging groups on porous silicon for microsystem applications. Sensors and Actuators B: Chemical 2007, Vol. 126, 120-125.

21. Metzger, R. M.; Konovalov, V. V.; Ming, S.; Tao, X.; Zangari, G.; Bin, X.; Benakli, M.; Doyle, W. D., Magnetic nanowires in hexagonally ordered pores of alumina. Magnetics, IEEE Transactions on 2000, Vol. 36, 30-35.

22. Muppalla, S.; Brandon, L. D.; Jessica, L. C.; Allen, H. P., Opalescent appearance of an IgG1 antibody at high concentrations and its relationship to noncovalent association. Pharmaceutical Research 2004, Vol. 21, 1087.

23. Ohgai, T.; Gravier, L.; Hoffer, X.; Lindeberg, M.; Hjort, K.; Spohr, R.; Ansermet, J. P., Template synthesis and magnetoresistance property of Ni and Co single nanowires electrodeposited into nanopores with a wide range of aspect ratios. Journal of Physics D: Applied Physics 2003, Vol. 36, 3109-3114.

24. Ono, S.; Masuko, N., Evaluation of pore diameter of anodic porous films formed on aluminum. Surface and Coatings Technology 2003, Vol. 169-170, 139-142.

25. Parkhutik, V. P.; Shershulsky, V. I., Theoretical modelling of porous oxide growth on aluminium. Journal of Physics D: Applied Physics 1992, Vol. 25, 1258-1263.

26. Routkevitch, D.; Tager, A. A.; Haruyama, J.; Almawlawi, D.; Moskovits, M.; Xu, J. M., Nonlithographic nano-wire arrays: fabrication, physics, and device applications. IEEE Transactions on Electron Devices 1996, Vol. 43, 1646-1658.

27. Sotiropoulou, S.; Gavalas, V.; Vamvakaki, V.; Chaniotakis, N. A., Novel carbon materials in biosensor systems. Biosensors and Bioelectronics 2003, Vol. 18, 211-215.

28. Takhistov, P., Electrochemical synthesis and impedance characterization of nano-patterned biosensor substrate. Biosensors and Bioelectronics 2004, Vol. 19, 1445-1456.

29. Thamida, S. K.; Chang, H. C., Nanoscale pore formation dynamics during aluminum anodization. Chaos 2002, Vol. 12, 240-251.

30. Xiao, Z. L.; Han, C. Y.; Welp, U.; Wang, H. H.; Kwok, W. K.; Willing, G. A.; Hiller, J. M.; Cook, R. E.; Miller, D. J.; Crabtree et, a., Fabrication of alumina nanotubes and nanowires by etching porous alumina membranes. Nano Letters 2002, Vol. 2, 1293-1297.

31. Xu, X.; Liu, S.; Ju, H., A novel hydrogen peroxide sensor via the direct electrochemistry of horseradish peroxidase immobilized on colloidal gold modified screen-printed electrode. Sensors 2003, Vol. 3, 350-360.

Chapter 3.   Development of a practical method for Ab immobilization on aluminum surface

3.1.   Introduction

The development of a sensitive and rapid EIS immunosensor frequently encounters problems because of difficulties to immobilize enough number of Ab intimately and stably on the surface of EIS immunosensor [8]. Intimacy of immobilized Ab with signal transducer plays an important role for the sensitivity of immunosensor [6], and the stability of immobilized Ab may also determine the reliability and reproducibility of immunosensor. The intimacy and stability of immobilized Ab on immunosensor can be achieved when an appropriate method is applied for Ab immobilization [6]. Accordingly search and/or development of an appropriate method for Ab immobilization onto food grade aluminum were of interest in this chapter.

Polysiloxanes have been widely used to immobilize proteins on the surface of metal oxide [13]. Polysiloxanes can form self assembled monolayers (SAMs) on the surface of oxide layer by forming silanol bonding with oxide layer then proteins can be covalently bonded on SAMs of polysiloxanes by the addition of linkers such as glutaraldehyde. Because of covalent bonding, proteins that are immobilized on oxide layer by the use of polysiloxane are stable thus polysiloxanes are widely applied for protein immobilization in various fields of analytical studies such as chromatography [2], optical [5], mechanical [12], and electrochemical biosensors [10]. Among diverse polysiloxanes, 3-aminopropyltryethoxysilane (APTES) is most frequently used for protein

immobilization onto oxide layer because of its wide applicability from organic to inorganic materials [11]. Protein immobilization using APTES is simple and easy thus industrial protocol is even available [9, 15].

The surface chemistry of aluminum oxide may be very similar to that of silicon oxide thus it is assumed that proteins can be immobilized on aluminum oxide in a same manner of protein immobilization onto silicon oxide if APTES is used for protein immobilization. Besides the immobilization of various enzymes on aluminum oxide by the use of APTES has been reported [1, 4, 16]. Especially APTES form an extremely thin SAMs (approximately less than 6nm in thickness) on aluminum oxide layer [7, 11] therefore it is quite promising that good intimacy of Ab with signal transducers can be achieved if APTES is used for Ab immobilization for the development of immunosensor. However Ab immobilization on aluminum oxide layer for the development of immunosensor has not been reported therefore a method for Ab immobilization on the surface of aluminum has to be established.

The properties of SAMs of APTES depend on silanization time and APTES concentration [11, 13]. To investigate appropriate silanization time and APTES concentration to achieve the efficient Ab immobilization, planar aluminum was silanized at different APTES concentration (0, 0.1, 1, 2, 3, and 4% of APTES) for different silanization time (0, 1, 2, 4, 6, and 8hrs). The formation of SAMs of APTES on aluminum was investigated by measuring water contact angle on silanized aluminum at different conditions. The formation of SAMs of APTES can be estimated by contact angle however it doesn't reflect the reactivity and efficiency of formed SAMs of APTES on Ab immobilization. For this, fluorescent study was carried out. FITC conjugated Ab (FITC-Ab) was immobilized on

silanized aluminum at different conditions by addition of glutaraldehyde then the amount of immobilized Ab was quantified by fluorescence measurement from FITC-Ab immobilized immunosensors.

3.1.1. Methodological background

3-aminopropyltriethoxysilane (APTES, $C_9H_{23}NO_3Si$) comprising an amino group and three alkoxyl groups is the commonest silane coupling agent. Alkoxyl groups of APTES are highly reactive and readily hydrolyzed to silanol groups when they are exposed to a hydrated surface in addition the functionality of APTES can be controlled by the substitution of an amine group for certain application therefore APTES is widely used in the plastic industry, the glass-fiber industry, fabric treatments, and etc [13]. APTES has been produced by several chemical companies all over the world so industrial grade APTES is commercially available.

When APTES is applied to aluminum oxide, alkoxyl groups of APTES may be hydrolyzed to silanol groups with hydroxyl groups that exist spontaneously on the surface of aluminum oxide at ambient condition, and then SAMs of APTES may be formed on the surface (Figure 3.1. a). The formation of SAMs depends on silanization time and APTES concentration [3, 13], and for example the thickness of SAMs of APTES is varied from 5 to 10nm depending on APTES concentration and/or silanization time [11, 13]. Accordingly silanization time and APTES concentration are regarded as critical variables affecting the formation of SAMs of APTES on aluminum oxide.

In Ab immobilization on aluminum oxide using APTES, Ab can be immobilized covalently on silanized aluminum oxide by the addition of glutaraldehyde (Figure 3.1).
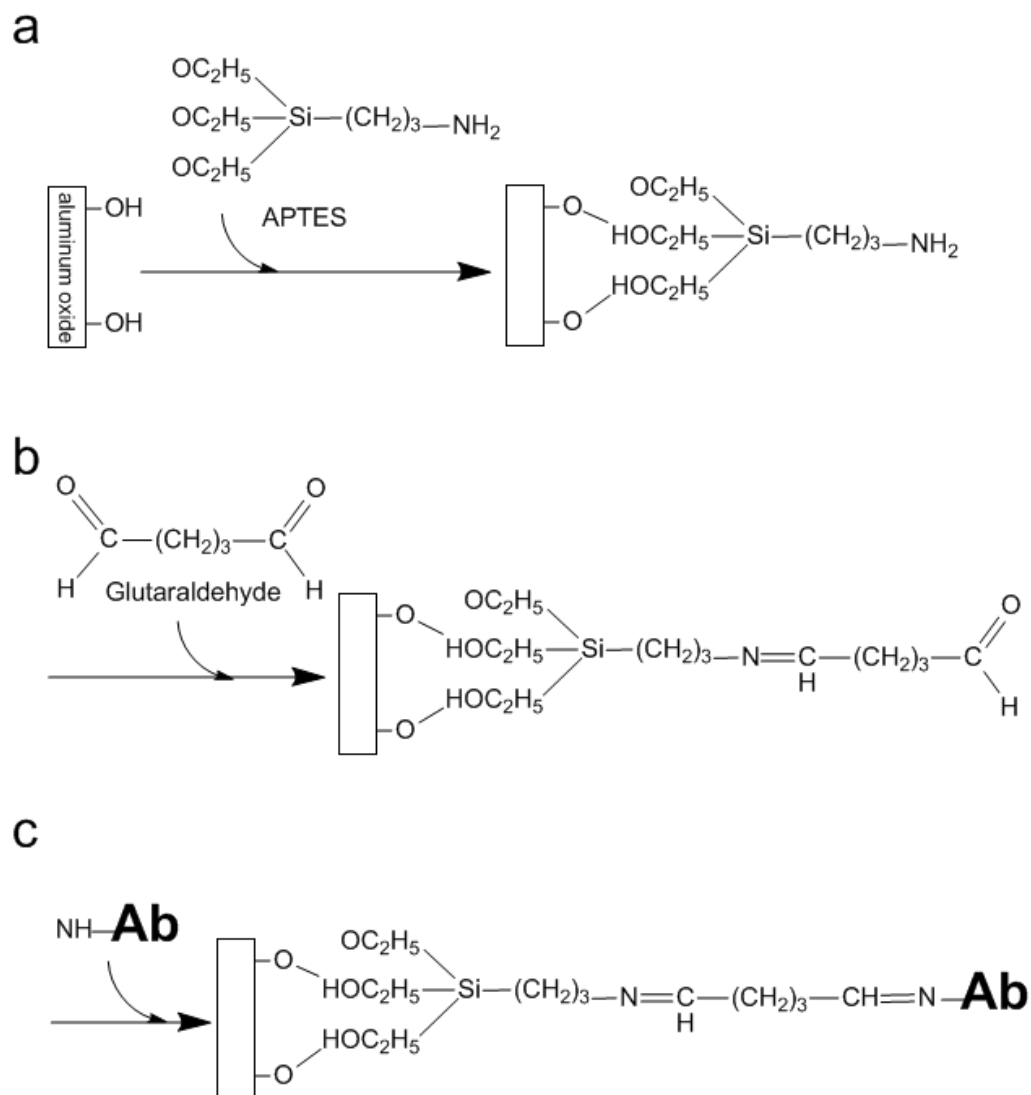
Figure 3.1. Schematic presentation of Ab immobilization using APTES. a) aluminum

silanization in APTES, b) surface activation of silanized aluminum by glutaraldehyde, and

c) covalent crosslinking of Ab onto aluminum via APTES and glutaraldehyde.

Thus it is quite certain that the surface properties of SAMs of APTES may affect Ab immobilization. To investigate the surface properties, contact angle measurement is frequently employed since the formation of SAMs change the surface energy. Although the structure or chemical properties of SAMs cannot be estimated from contact angle measurement, the coverage of SAMs over the surface of aluminum oxide can be estimated. Therefore the coverage and formation of SAMs of APTES on aluminum oxide was estimated by measuring contact angle in this study.

3.2.   Materials and methods

3.2.1.   Materials

Ethanol, HPLC grade and acetone, HPLC grade were purchased from Fisher Scientific (Fair Lawn, NJ, USA). 3-Aminopropyltriethoxysilane (APTES) 98% was purchased from Strem Chemicals (Newburyport, MA, USA). Glutaraldehyde 70% v/v (Grade I), and ethanolamine 98% were purchased from Sigma Aldrich (St. Louis, MO, USA).

3.2.2.   Methods

Aluminum silanization. Electropolished aluminums were silanized in 0, 0.1, 1, 2, 3, and 4% v/v solution of APTES in ethanol at 63°C. Aluminum silanized for at 0, 1, 2, 4, 6, and 8hrs were collected then an excess of APTES on aluminum surface was removed by ultra-sonication in SDI water, and dried in nitrogen.

Immobilization of anti-SEB. Silanized aluminum was activated in 2.5%
glutaraldehyde for 2hrs. Activated aluminum was placed into the solution containing
10μg/ml of anti-SEB for 1hr at 37°C and, further, for 12hrs at 4°C. Remaining vacant sites
on the surface were blocked by soaking immobilized aluminum in 100mM ethanolamine
solution for 1hr. Completed SEB immunosensor was thoroughly washed with SDI water,
dried in nitrogen, and stored at -25°C.

Contact angle measurement. Silanized aluminum was placed onto goniometer
(Rame-Hart Contact Angle Goniometer, Rame-Hart, Inc., Netcong, NJ, USA) equipped
with digital camera (Professional, 1.2 Million Pixel Digital Camera System, Pixera, Los
Gatos, CA, USA). Contact angle was measured by analyzing the image of DI water drop on
aluminum surface using an image processing software, Image J (National Institutes of
Health, Bethesda, MD, http://rsb.info.nih.gov/ij).

Fluorescence analysis of immobilized Ab. Activated aluminum was put into
solution containing 10μg/ml of FITC conjugated anti-*E. coli* for 1hr at 37°C then washed
with SDI water. Prepared immunosensors were placed on 24-well plate then the density of
fluorescence was measured by fluorometer (Fluoroskan Ascent FL, Thermo Labsystems,
Helsinki, Finland) using 485nm excitation filter and 538nm emission filter.

3.3.   Results and discussion

APTES comprises methyl chain in its structure and it was assumed that the
deposition of APTES or formation of SAMs would increase contact angle. The formation
of SAMs of APTES could be estimated by contact angle of silanized aluminum.

Contact angle of silanized aluminum was changed as silanization time and APTES concentration, and Figure 3.2 shows the change of contact angle in each APTES concentration as silanization time. A consistent pattern of the changes in contact angle could be observed and contact angle in each APTES concentration was increased until certain time and then decreased. The increase of contact angle might be resulted from the deposition of APTES or formation of SAMs on aluminum due to hydrophobic methyl chain in APTES structure. Apparent increase of contact angle could be observed especially during first 1hr of silanization, and the increase seemed to be proportional to APTES concentration at 1hr. After 1hr of silanization, the increase of contact angle became moderate and it continued until 4hrs for silanization in 1 and 2% APTES, and 6hrs in 0.1, 3, and 4% APTES. However the contact angle from aluminum silanization in 1 or 2% APTES for 4hrs was higher than others.

It is well known that APTES is sensitive to moisture, and APTES tends to be aggregated and can forms lumps on the surface in the presence of moisture [14]. This can be prevented when moisture is strictly controlled during silanization. However, in this study, silanization was conducted using generic incubator without the control of moisture in order for the development of a practical and simple silanization method furthermore Ab immobilization. Therefore APTES aggregates or lumps might cause the decrease of contact angle. Consequently it was concluded that a well arrayed SAMs of APTES would be formed on the surface of aluminum at the time that showed a plateau in contact angle.

From contact angle measurement, we could estimate indirectly the formation of SAMs of APTES on the surface of aluminum. We concluded that silanization of aluminum in 1 and 2% APTES for 4hrs would give better properties of SAMs because of higher
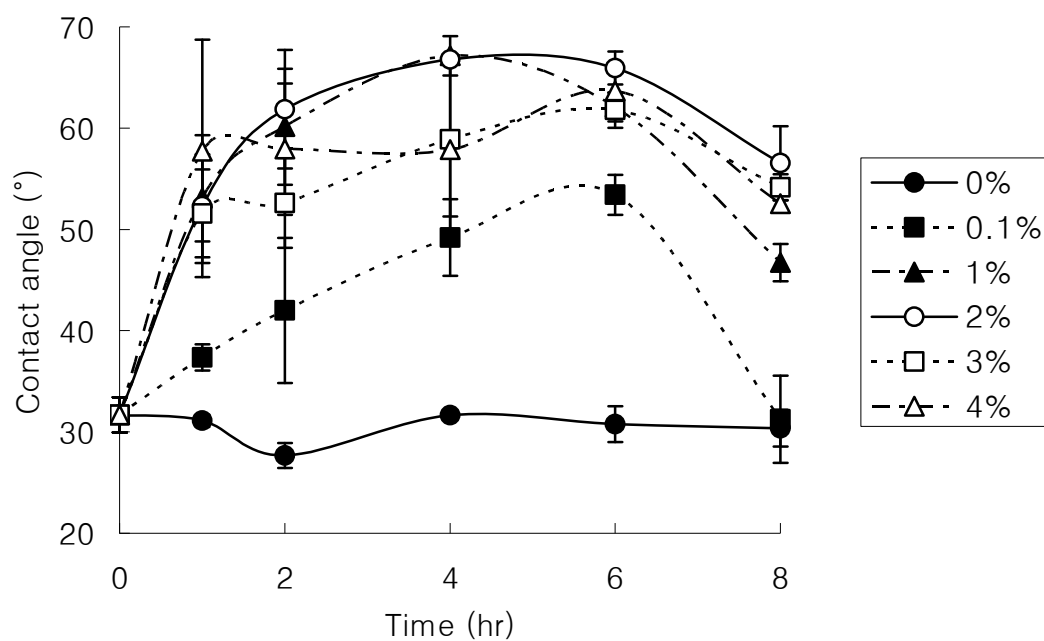
Figure 3.2. Water contact angle of aluminum that is silanized in different concentration of APTES in ethanol as the function of silanization time.

contact angles. However contact angle cannot represent the efficiency for Ab immobilization moreover contact angle from 1 and 2% APTES for 4hrs were very similar thus further investigation for the efficiency of silanized aluminum on Ab immobilization was inevitable.

To investigate the efficiency of silanized aluminum, FITC-Ab was immobilized on silanized aluminum in each APTES concentration for the time that showed a plateau in contact angle (4hrs for 1 and 2% APTES, and 6hrs for 0.1, 3, and 4% APTES). The amount of immobilized Ab on silanized aluminum could be quantified by measuring the intensity of fluorescence from silanized aluminum where FITC-Ab was immobilized (Figure 3.3). More immobilized Ab could be observed from silanized aluminum in 1 or 2% APTES than 0.1, 3, or 4% APTES. This result is well corresponding to result of contact angle. Hence the formation of APTES aggregates or lumps on aluminum might affect not only contact angle but also the efficiency of Ab immobilization. The amount of immobilized Ab on silanized aluminum in 2% APTES was slightly higher than 1% APTES, and 2% APTES gave less variation in the amount of immobilized Ab. Therefore we concluded that silanization of aluminum in 2% APTES for 4hrs might be most appropriate for Ab immobilization.

3.4.   Conclusion

In this study, to develop an efficient method for Ab immobilization on aluminum, the formation of SAMs by APTES as well as the efficiency of Ab immobilization on silanized aluminum in different APTES concentration for different silanization time was investigated. It was found that the formation of SAMs by APTES on aluminum was
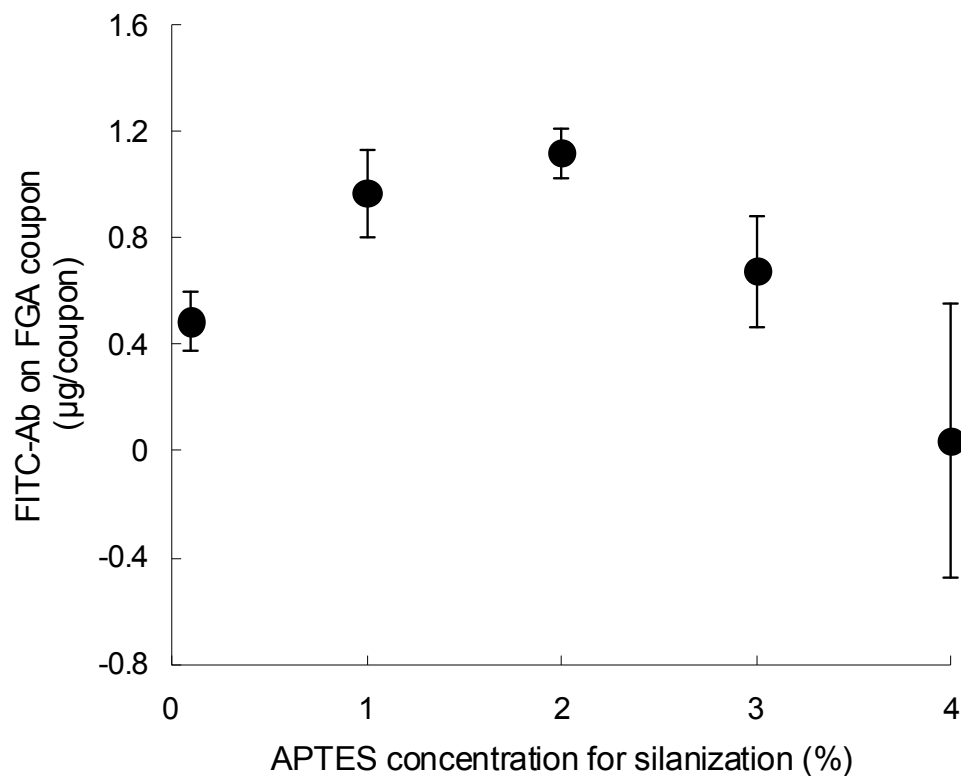
Figure 3.3. The amount of FITC-conjugated anti-*E. coli* that is immobilized on the surface

of silanized aluminum by the addition of glutaraldehyde. Electropolished aluminum was

silanized in 0.1, 1, 2, 3, and 4% APTES for 6, 4, 4, 6, and 6hrs respectively then

FITC-conjugated anti-*E.coli* was immobilized by the addition of 2.5% glutaraldehyde. The

amount of FITC-conjugated anti-*E.coli* was analyzed by measuring the density of

fluorescence.

affected tremendously by APTES concentration and silanization time. Furthermore they influenced the amount of immobilized Ab. As more Ab could be observed from silanized aluminum in 2% APTES for 4hrs than others, we concluded that appropriate APTES concentration and silanization time for an efficient Ab immobilization on aluminum was 2% and 4hrs respectively.

3.5.   References

1. Costa, S. A.; Tzanov, T.; Paar, A.; Gudelj, M.; Gubitz, G. M.; Cavaco-Paulo, A., Immobilization of catalases from *Bacillus* SF on alumina for the treatment of textile bleaching effluents. Enzyme and Microbial Technology 2001, Vol. 28, 815-819.

2. Cullis, A. G.; Canham, L. T.; Calcott, P. D. J., The structural and luminescence properties of porous silicon. Journal of Applied Physics 1997, Vol. 82, 909-965.

3. Dubrowski, A., Adsorption - from theory to practice. Advances in Colloid and Interface Science 2001, Vol. 93, 135-224.

4. Eberhardt, A. M.; Pedroni, V.; Volpe, M.; Ferreira, M. L., Immobilization of catalase from *Aspergillus niger* on inorganic and biopolymeric supports for H_2O_2 decomposition. Applied Catalysis B: Environmental 2004, Vol. 47, 153-163.

5. Grant, S. A.; Pierce, M. E.; Lichlyter, D. J.; Grant, D. A., Effects of immobilization on a FRET immunosensor for the detection of myocardial infarction. Analytical and Bioanalytical Chemistry 2005, Vol. 381, 1012-1018.

6. Ho, M. Y. K.; Rechmitz, G. A., An introduction to biosensors. In; Nakamura, R. M.; Kasahara, Y.; Rechnitz, G. A. (Ed.); Immunochemical Assays and Biosensor Technology for the 1990s, Americal Society for Microbiology: Washington, D.C., USA, 1992; 275-290.

7. Kurth, D. G.; Bein, T., Surface reactions on thin layers of silane coupling agents. Langmuir 1993, Vol. 9, 2965-2973.

8. Lillie, G.; Payneb, P.; Vadgamac, P., Electrochemical impedance spectroscopy as a platform for reagentless bioaffinity sensing. Sensors and Actuators B 2001, Vol. B78, 249-256.

9. Maddox, P. H.; Jenkins, D., 3-Aminopropyltriethoxysilane (APES): a new advance in section adhesion. Journal of Clinical Pathology 1987, Vol. 40, 1256-1257.

10. Mantzila, A. G.; Prodromidis, M. I., Performance of impedimetric biosensors based on anodically formed Ti/TiO_2 electrodes. Electroanalysis 2005, Vol. 17, 1878-1885.

11. Moon, J. H.; Shin, J. W.; Kim, S. Y.; Park, J. W., Formation of uniform aminosilane thin layers: an imine formation to measure relative surface density of the amine group. Langmuir 1996, Vol. 12, 4621-4624.

12. Okahata, Y.; Ebara, Y.; Sato, T., Quantitative detection of protein binding to the membrane surface using a quartz-crystal microbalance. In; Lvov, Y.; Mèohwald, H. (Ed.); Protein Architecture: Interfacing Molecular Assemblies and Immobilization Biotechnology, Marcel-Dekker: New York, USA, 2000; 55-74.

13. Plueddemann, E. P., Silane Coupling Agents. 2nd ed.; Plenum Press: New York, USA, 1991; 253.

14. Popat, K. C.; Johnson, R. W.; Desai, T. A., Characterization of vapor deposited thin silane films on silicon substrates for biomedical microdevices. Surface and Coatings Technology 2002, Vol. 154, 253-261.

15. Sigma-Aldrich, Product information sheet for 3-aminopropyltriethoxysilane. http://www.sigmaaldrich.com/sigma-aldrich/product_information_sheet/a3648pis.pdf (October 3 2007),

16. Tzanov, T.; Costa, S. A.; Gubitz, G. M.; Cavaco-Paulo, A., Hydrogen peroxide generation with immobilized glucose oxidase for textile bleaching. Journal of Biotechnology 2002, Vol. 93, 87-94.

Chapter 4. Homogenous distribution of antibody on nanoporous surface for the application of immunosensor

4.1. Introduction

Immunosensor is a device which combines antibody (Ab) as a molecular recognition element with certain type of signal transducers [2]. In this device Ab is immobilized on planar or porous solid substrate of immunosensor, and recognizes the presence of a target molecule in test sample. The detection is carried out by the conversion of physicochemical changes by antibody-antigen (Ab-Ag) reaction, to analytical signals [2]. The number of immobilized Ab is probably a critical one to determine the sensitivity of immunosensor [1] since the signal output from immunosensor may depends on the formation of Ab-Ag complex. As the higher surface area the more Ab can be immobilized on the surface [8, 11], the use of nanostructured materials having high surface area as substrates of immunosensors allows higher sensitivity, more reliability, and faster analysis than planar immunosensors [4]. In addition to surface area, lateral interactions between Ab molecules or Ab aggregates which occurs during immobilization process are able to affect Ab immobilization, in consequence the number of immobilized Ab on the surface of immunosensor, however their effects have not been emphasized. In nature substance randomly adsorbs or is immobilized on solid substrate, and this produces the formation of clusters or islands [7]. As this phenomenon is very disordered, clusters may be irregular in size and distribution on the surface. Similarly Ab is immobilized on the surface of immunosensor as the formation of Ab cluster during Ab immobilization process. Once Ab

cluster are formed on the surface, they tends to hinder further Ab immobilization near Ab cluster due to lateral-lateral interactions between protein cluster and other proteins [12]. Even lateral interactions between larger protein cluster and protein become stronger because of the thicker adsorption layer at the solid-liquid interface [6], hence homogenous distribution of Ab on the surface of immunosensor may be favorable not only for the number of immobilized Ab but also for the sensitivity of immunosensor.

It is very obvious that the use of nanoporous aluminum as a substrate of immunosensor may improve the sensitivity of immunosensor via increasing the number of immobilized Ab as discussed above. In addition it can be assumed that homogenous distribution of Ab on nanoporous surface leads high efficiency of Ab immobilization further high sensitivity of immunosensor. As different dimension of nanoporous structure affects the formation of Ab clusters or distribution of Ab on the surface of immunosensor due to geometrical difference, the effect of surface area as well as distribution of Ab on nanoporous surface on the number of immobilized Ab are investigated. Particularly, through comparison among the number of immobilized Ab, dimension of nanoporous structure, and surface morphology of immunosensor, the structure of immobilized Ab on planar and nanoporous surface is estimated and illustrated. Then the improvement of sensitivity of immunosensor by the use of nanoporous substrate is presented.

4.2.   Materials and methods

Nanoporous aluminum substrates were prepared by anodization in 0.3M oxalic acid at $5^{o}C$ for 20sec. Nanoporous structure was controlled by applying different

anodization voltage; 10, 20, 30, and 40V. For further control of nanoporous structure,

anodized aluminum substrates at 40V were treated in 5% wt/v phosphoric acid for 1hr at 15

or 25°C. FITC-conjugated Ab (FITC-Ab) or Ab for Staphylococcal enterotoxin B

(anti-SEB) was immobilized on planar or nanoporous aluminum substrate via covalent

linkage between Ab and aluminum surface using 3-aminopropyltriethoxysilane (APTES)

and glutaraldehyde. Ab immobilization regime is as follows; silanization of aluminum

substrates for 4hrs in 2% APTES, surface activation in 2.5% glutaraldehyde for 2hrs, and

Ab immobilization in 10μg/ml of FITC-Ab or anti-SEB at room temperature for 2hrs or

18hrs respectively. The number of immobilized Ab on planar or nanoporous

immunosensor was quantified by measuring fluorescence intensity of prepared

immunosensor. Surface morphology of SEB immunosensor was analyzed via scanning

probe microscope (SPM), and specialized software package, SPIP v.3.3, was used for 3D

image processing, pore diameter analysis. To compare the sensitivity between planar and

nanoporous SEB immunosensor, real part of impedance (Z') from SEB immunosensor in

PBS or 1μg/ml SEB was recorded as a function of time. The signal output was presented as

normalized value of Z' ($Z'_{norm} = Z'_t / Z'_0$). The specific conditions for impedance analysis

were as follows; AC frequency: 56kHz, AC voltage: 10mV, and DC voltage vs. Ag/AgCl

reference electrode: 100mV.

4.3.   Results and discussion

Nanoporous structure was fabricated on aluminum substrate by anodization in

0.3M oxalic acid. Nanoporous structure could be controlled by changing anodization

voltage, and pore diameter was increased as well as nanoporous structure became more significant as the increase of anodization voltage. Figure 4.1. a, b, and c represent a sequence of change of nanoporous structure to anodization voltage (representative SPM images of nanoporous aluminum substrates and SEB immunosensors are presented in Figure 4.1). Nanoporous aluminum substrates fabricated by anodization at higher than 40V (50V and 60V) were excluded from this study because of irregular nanoporous structure. In addition to anodization phosphoric acid treatment allowed further control of fabricated nanoporous structure (Figure 4.1. d), and this widened pore diameter. Pore analysis of SPM images of nanoporous aluminum substrates by SPIP software clarified the morphological observation - the change of nanoporous structure by anodization voltage or phosphoric acid (Figure 4.2). Anodization of aluminum substrate at 10V, 20V, 30V, or 40V produced nanoporous structure on its surface having ~11nm to ~15nm, ~23nm, or ~30nm respectively. Additional phosphoric acid treatment of anodized aluminum substrate at 40V increased pore diameter from ~30nm to ~38nm at 15°C or to ~39nm at 25°C. Well ordered nanoporous structure was observed especially on anodized aluminum substrate at 40V (Figure 4.1 c). The change of pore diameter as anodization voltage, shown in this study, exhibit a good agreement to the previous investigation of pore diameter on anodized aluminum substrate [10].

Ab was successfully immobilized on planar or nanoporous aluminum substrate using APTES and glutaraldehyde. Ab immobilization was confirmed by SPM imaging of SEB immunosensors (Figure 4.1. a-Ab, b-Ab, c-Ab, and d-Ab), moreover immobilized Ab could be quantified by measuring fluorescence intensity on immunosensor where FITC-Ab was immobilized. The amount of immobilized Ab on planar and nanoporous
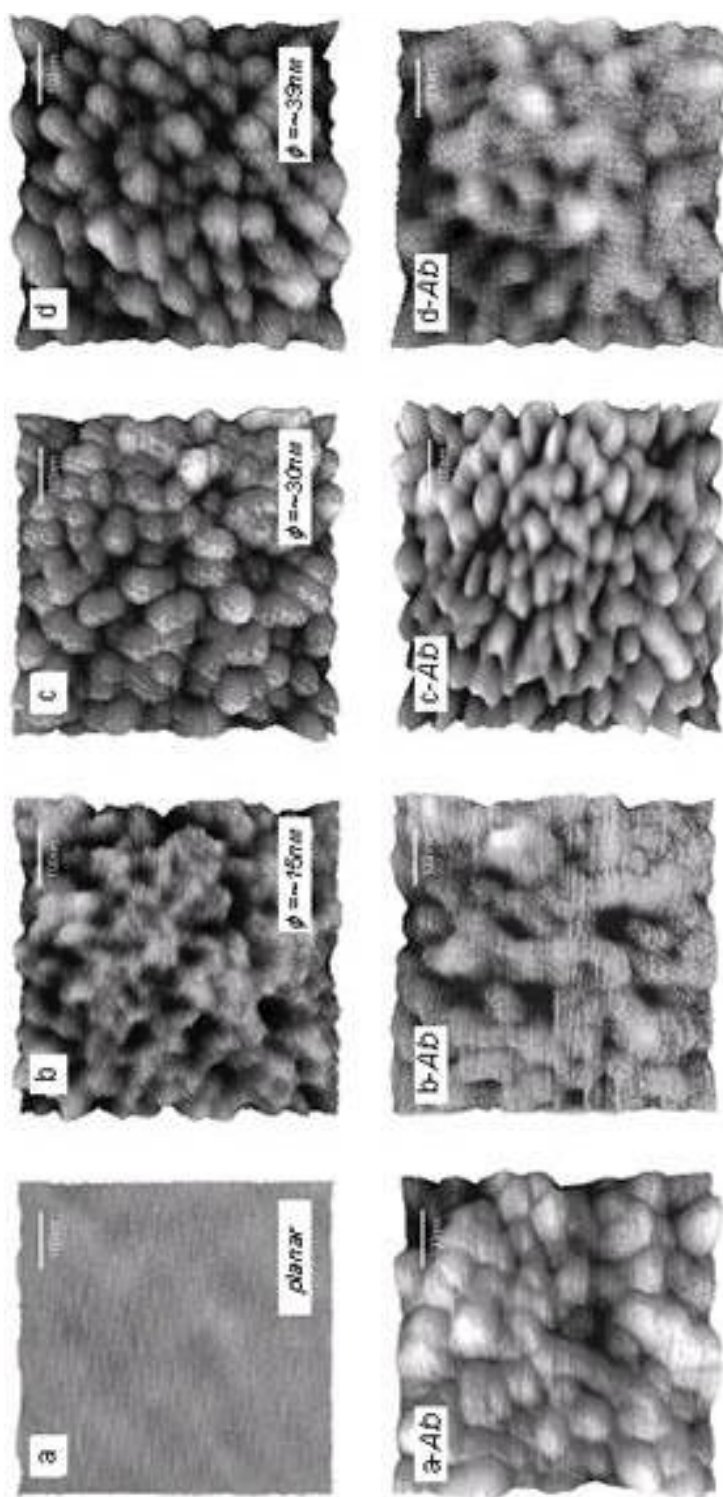
Figure 4.1 SPM images of planar and nanoporous aluminum substrates, and SEB immunosensors
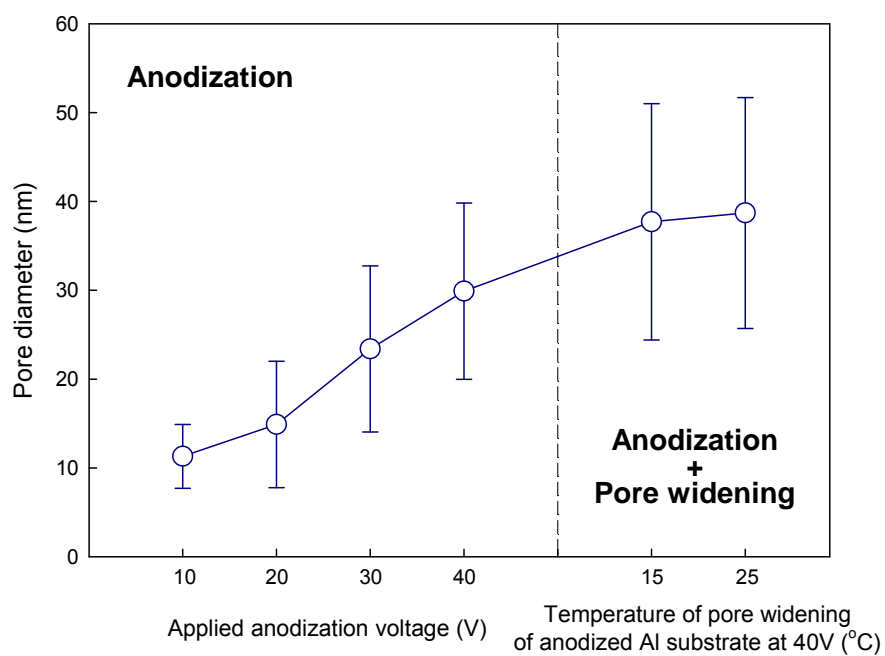
Figure 4.2. Pore diameter of nanoporous aluminum substrate as the voltage of anodization and/or the temperature of pore widening of anodized aluminum at 40V in 5%wt/v phosphoric acid.

immunosensors obtained from the analysis of fluorescence intensity of immunosensors is presented in Figure 4.3. More Ab was observed on nanoporous immunosensor than on planar immunosensor. Among nanoporous immunosensors based on only anodized aluminum substrates the amount of immobilized Ab was increased from ~1.3μg to ~2.1μg, ~2.7μg, and ~3.2μg as pore diameter of nanoporous substrate was increased from ~11nm to ~15nm, ~23nm, and ~30nm. As the dimension of Ab is ~12nm in diameter, ~12nm in height, and ~3nm in thickness [5, 9], the diffusion and immobilization of Ab into nanopores smaller than Ab might be limited. It was assumed that most of immobilized Ab on nanoporous substrates having ~11nm or ~15nm in its pore diameter was located on the top of nanoporous structure rather than in or on nanopores due to the dimensional limit. The assumed structure of immobilized Ab on the top of nanoporous substrate due to the dimensional limit is illustrated in

Figure 4.4. b. More Ab can be diffused into nanopores larger pore diameter is. This might produce the increase of the amount of immobilized Ab on immunosensor by the increase of pore diameter from ~11nm to ~30nm. The importance of dimension of nanoporous structure for the amount of adsorbed protein on porous surface has been mentioned previously, and it has been reported that the specific dimension of nanoporous structure is required for the efficient adsorption of certain protein [11].

It was very notable that there was the increase of the amount of immobilized Ab when pore diameter was increased from planar to ~10nm or ~15nm in pore diameter (Figure 4.3) since it was assumed that surface area for Ab immobilization on nanoporous substrate having ~10nm or ~15nm in its pore diameter was same to or less than on planar
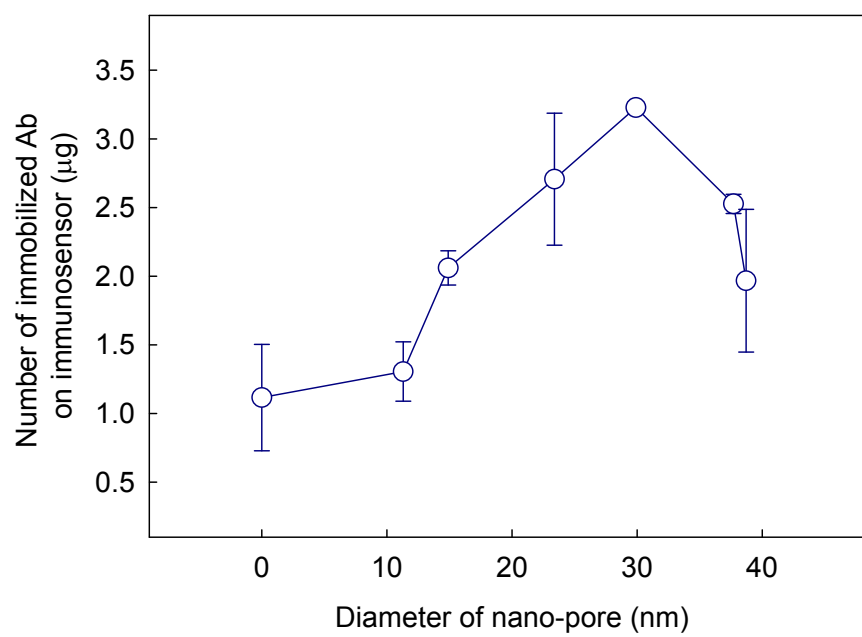
Figure 4.3. The amount of immobilized FITC-conjugated anti-*E. coli* as pore diameter of nanoporous aluminum substrate.
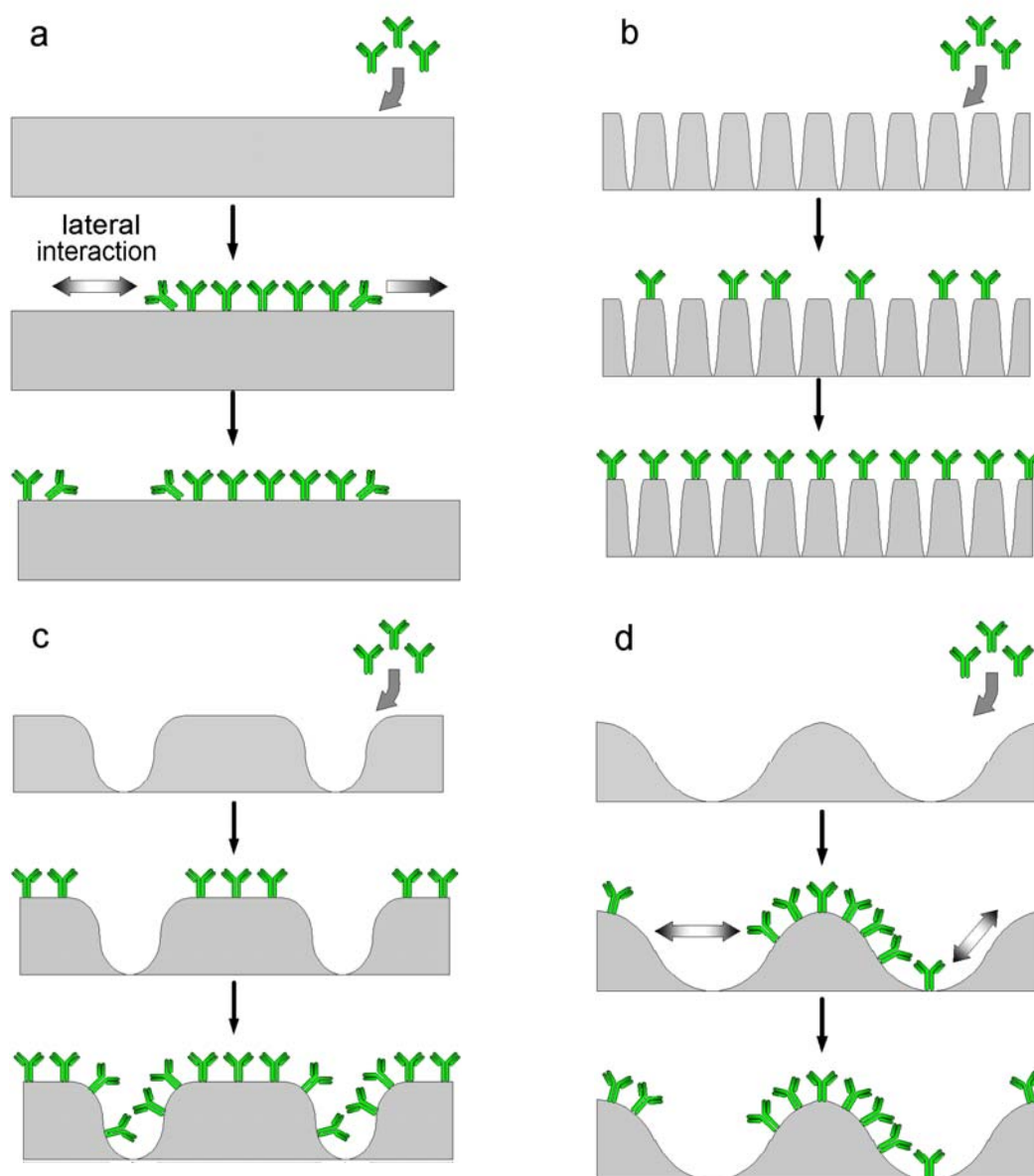
Figure 4.4. Schematic illustration of immobilized Ab on a) planar surface, b) nanoporous surface having pore diameter smaller than the critical diameter, c) nanoporous surface at the critical diameter, and d) nanoporous surface having pore diameter larger than the critical diameter

surface due to the dimensional limit. However it is understandable as the behavior of Ab immobilization on planar surface can differ from nanoporous surface due to lateral-lateral interaction between Ab and Ab cluster. Ab is immobilized as the formation of Ab cluster in nature, and the formation is irregular in the size and distribution [7]. The formation of Ab cluster on planar and nanoporous surface was observed from SPM images (Figure 4.1. a-Ab, b-Ab, c-Ab, d-Ab), and the size of Ab cluster on planar immunosensor was larger than others. It is very probable that lateral interaction occurring on planar surface would be more significant than nanoporous surface furthermore less Ab was immobilized on the surface on planar surface due to strong lateral interaction of large Ab cluster as referred above.

Similarly the decrease of immobilized Ab as the increase of pore diameter from ~30nm to ~38nm or ~39nm in pore diameter can be explained by the effect of lateral interaction on the amount of immobilized Ab. It is quite certain that surface area would be increased as the increase of pore diameter from ~30nm to ~38nm or ~39nm because phosphoric acid treatment influence on pore diameter rather than other dimension of nanoporous structure or number of pores [3, 13]. In addition, pore diameters were large enough for the diffusion and immobilization of Ab into nanopore having ~38nm or ~39nm. However, the size of Ab cluster on those substrates seems to be larger (Figure 4.1. d-Ab), and may have stronger lateral interaction than substrates having ~30nm in pore diameter. This may result in the less immobilized Ab on immunosensor based on nanoporous substrates having larger than ~30nm in their pore diameter.

Dimension of nanoporous structure, surface area, and lateral interaction of Ab cluster may influence the amount of immobilized Ab on nanoporous surface. In order for

the efficient Ab immobilization pore diameter should be enough larger than the dimension of Ab, surface area should be enough for Ab immobilization, and small Ab cluster need to be distributed homogenously to avoid lateral interaction.

We assumed that there may be a critical dimension to accomplish those three factors for the efficient Ab immobilization. In our system, a critical dimension was ~30nm in pore diameter enhanced by anodization of aluminum at 40V in 0.3M oxalic acid for 20sec since homogenous distribution of small Ab cluster could be observed from SPM image (Figure 4.1. c-Ab) as well as more immobilized Ab was found at this dimension (Figure 4.3).

To demonstrate the improvement of the sensitivity of immunosensor, SEB immunosensor based on planar substrate, nanoporous substrates fabricated into a critical dimension (~30nm in pore diameter) and out of a critical dimension (~39nm in pore diameter) were prepared, and subjected to impedance analysis. Planar SEB immunosensor couldn't detect the presence of 1μg/ml of SEB in PBS in 1hr (Figure 4.5. a). But SEB could be detected by nanoporous SEB immunosensor in 1hr (Figure 4.5 b, c). Differentiation between signal output in 1μg/ml of SEB and PBS was observed at 40min for nanoporous SEB immunosensor out of a critical dimension, however at 20min for nanoporous SEB immunosensor at a critical dimension. As a result, the sensitivity of impedimetric immunosensor depends on the amount of immobilized Ab on the surface, and the sensitivity of nanoporous immunosensor is better than planar immunosensor. Especially nanoporous immunosensor at a critical dimension shows higher sensitivity than others.
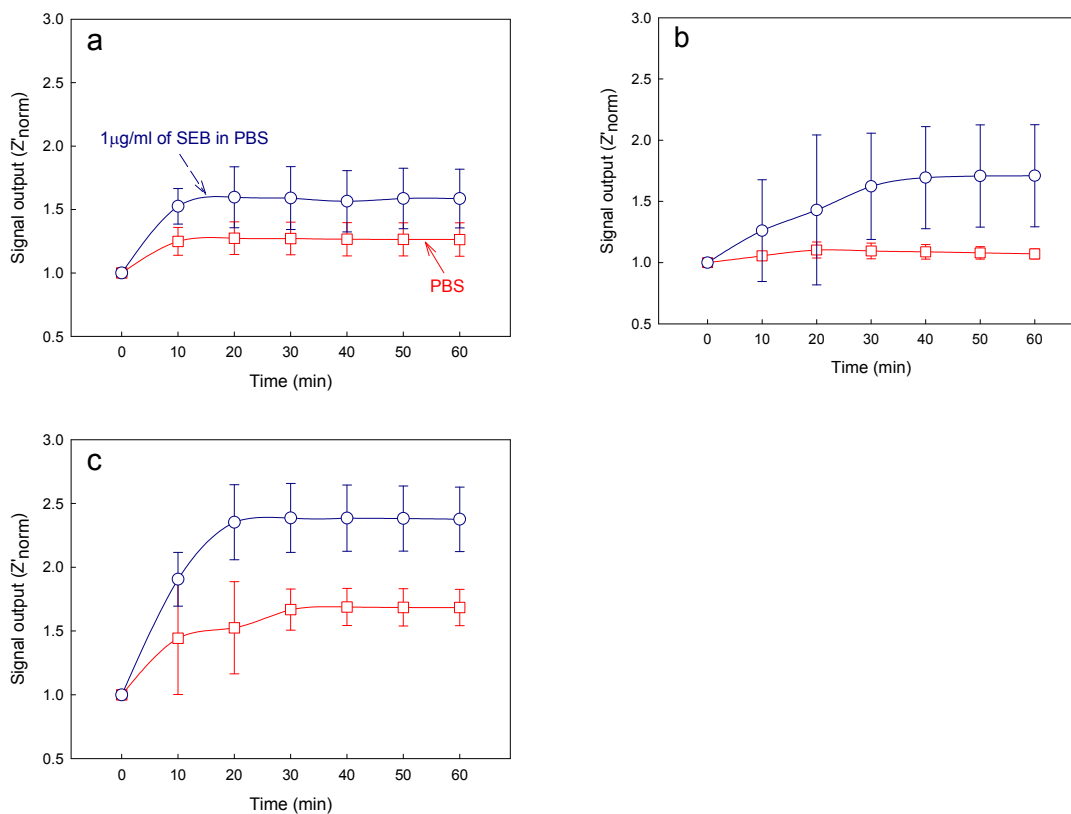
Figure 4.5. Detection of SEB (1μg/ml) in 0.01M phosphate buffer by a) planar SEB immunosensor, b) nanoporous SEB immunosensor out of the critical diameter, and c) nanoporous SEB immunosensor at the critical diameter. □: normalized Z' (Z'norm) from 0.01M phosphate buffer (pH 7.01, NaCl 0.3%), ○: Z'norm from 1μg/ml SEB in 0.01M phosphate buffer

4.4. References

1. Feldkamp, C. S., Evaluation and clinical validation of immunoassays. In; Nakamura, R. M.; Kasahara, Y.; Rechnitz, G. A. (Ed.); Immunochemical Assays and Biosensor Technology for the 1990s, Americal Society for Microbiology: Washington, D.C., USA, 1992; 83-109.

2. Ho, M. Y. K.; Rechmitz, G. A., An introduction to biosensors. In; Nakamura, R. M.; Kasahara, Y.; Rechnitz, G. A. (Ed.); Immunochemical Assays and Biosensor Technology for the 1990s, Americal Society for Microbiology: Washington, D.C., USA, 1992; 275-290.

3. Hwang, S. K.; Jeong, S. H.; Lee, O. J.; Lee, K. H., Fabrication of vacuum tube arrays with a sub-micron dimension using anodic aluminum oxide nano-templates. Microelectronic Engineering 2005, Vol. 77, 2-7.

4. Jianrong, C.; Yuqing, M.; Nongyue, H.; Xiaohua, W.; Sijiao, L., Nanotechnology and biosensors. Biotechnology Advances 2004, Vol. 22, 505-518.

5. Kienberger, F.; Mueller, H.; Pastushenko, V.; Hinterdorfer, P., Following single antibody binding to purple membranes in real time. EMBO Reports 2004, Vol. 5, 579-683.

6. Kondo, A.; Higashitani, K., Adsorption of model proteins with wide variation in molecular properties on colloidal particles. Journal of Colloid and Interface Science 1992, Vol. 150, 344-351.

7. Kopelman, R., Fractal reaction kinetics. Science 1988, Vol. 241, 1620-1626.

8. Mathew, F. P.; Alocilja, E. C., Fabrication of porous silicon-based biosensor, Sensors, 2003. Proceedings of IEEE, 2003; Alocilja, E. C., 2003; 293-298.

9. Muppalla, S.; Brandon, L. D.; Jessica, L. C.; Allen, H. P., Opalescent appearance of an IgG1 antibody at high concentrations and its relationship to noncovalent association. Pharmaceutical Research 2004, Vol. 21, 1087.

10. Ono, S.; Masuko, N., Evaluation of pore diameter of anodic porous films formed on aluminum. Surface and Coatings Technology 2003, Vol. 169-170, 139-142.

11. Suh, C. W.; Kim, M. Y.; Choo, J. B.; Kim, J. K.; Kim, H. K.; Lee, E. K., Analysis of protein adsorption characteristics to nano-pore silica particles by using confocal laser scanning microscopy. Journal of Biotechnology 2004, Vol. 112, 267-277.

12. Tilton, R. D.; Gast, A. P.; Robertson, C. R., Surface diffusion of interacting proteins: effect of concentration on the lateral mobility of adsorbed bovine serum albumin. Biophysical Journal 1990, Vol. 58, 1321-1326.

13. Wang, X.; Han, G. R., Fabrication and characterization of anodic aluminum oxide template. Microelectronic Engineering 2003, Vol. 66, 166-170.

Chapter 5.   Label-free toxin detection by means of time-resolved electrochemical impedance spectroscopy[*]

5.1.   Introduction

The recent advances in electroanalytical chemistry provide a new opportunity for the development of biosensors. These electrochemical devices are relatively inexpensive and well suitable for miniaturization, which is critical for field-deployable applications. Significant progress in the development of electrochemical affinity-based biosensors (immunosensors) has been shown with various electrochemical techniques for the detection of DNA [5, 7] and proteins/toxins [2, 3, 10, 17, 18, 24].

Electrochemical impedance spectroscopy (EIS) is a highly effective analytical method to characterize physico-chemical properties of the electrode/analyte interface [6]. EIS is a sensitive, non-destructive technique suitable for monitoring the dynamics of bound and/or mobile charges near the sensor's surface [11, 13]. If EIS is used in the sensor's signal transducing system, the detection of target molecules can be accomplished directly without labeling [24]. However, the development of reliable EIS-based sensors for the detection of low concentrations of biological toxins remains difficult due to poor understanding of electrochemical processes at the sensor/sample interface. Traditional factors that determine sensor's output signal (*i.e.,* charge transfer resistance and electrical double layer capacitance) can not be interpreted correctly when concentration of antibodies (Ab) is low and surface coverage by the antibody/antigen (Ab/Ag) complexes is far from its maximum value [12].

Staphylococcal enterotoxin B (SEB) is an exotoxin produced by *Staphylococcus aureus*. It causes food poisoning in humans and is classified as a Category B bioterrorism agent. Due to its high virulence and extremely low lethal dose [4], there is a strong need to develop a rapid label-free method for the detection of trace concentrations of the toxin. In the past years, a number of studies had been carried out employing conventional techniques for SEB detection, including chromatography, enzyme-linked immunoassay (ELISA), magnetic microplate chemifluorimmunoassay (MMCIA), and surface plasmon resonance (SPR) [14, 15]. However, these methods are complex, require relatively expensive equipment, materials, and highly trained personnel.

5.2.   Results and Discussion

5.2.1.   Immunosensor fabrication and anti-SEB immobilization

Surface morphology of the sensor's substrate is crucial for the electrochemical immunosensor development since it affects Ab's immobilization, their spatial arrangement and local distribution of the current density at the sensor's surface. To increase surface area and holding capacity of the sensor's substrate, we have applied an electrochemical nanopatterning (anodization) of aluminum - a well-proven technique for surface treatment and improvement of aluminum materials. Before the anodization, an uneven surface of cold-rolled aluminum disk was electropolished to normalize its surface morphology. At the optimal regime (42 V, 40 s, at 4 $^{\circ}$C), the aluminum surface becomes smooth and covered with well-ordered linear patterns of 3-5 nm in depth [26]. Subsequent anodisation of

electropolished aluminum substrate in 0.3M oxalic acid results in the formation of a well-ordered nanoporous surface structure. After the pore widening step (5% w/v H_3PO_4), the diameter of nanopores becomes ~ 60-80 nm.

For the Ab immobilization, a fabricated nanopatterned substrate was modified with the APTES (see Figure 5.1. a) as described in the literature [8]. There are several advantages to use an APTES for the surface activation: it has both a non-hydrolysable hydroxyl group, which is highly reactive to the metal oxides and amine group that presents a reactive moiety, enabling strong interaction with corresponding Ab amino group [16]. Anti-SEB was covalently bonded on the silanized aluminum surface in the presence of glutaraldehyde, which resulted in the formation of well-recognizable surface structures of various Ab aggregates (see Figure 5.1. b). After successful Ab immobilization, the sensor's surface has been treated with 100 mM ethanolamine solution for 1 hr to block remaining vacant sites and fix attached antibodies. Figure 5.1. c clearly indicates changes of the surface morphology due to ethanolamine adsorption. Large gaps between the Ab clusters disappear and the surface becomes smooth and uniform. For the control purpose, developed sensor was exposed to the 0.3% NaCl solution containing 10 μg/ml of SEB for 60 min. SPM image of the sensor's surface shows development of new structures on the surfaces (see Figure 5.1. d). These surface morphology changes are due to the development of Ab/Ag immuno-complexes.

5.2.2.   SEB detection and optimization of measuring parameters

The real-time detection of SEB trace concentrations in the samples with high variability of the sample matrix properties (*e.g.* clinical samples, foodstuff) requires
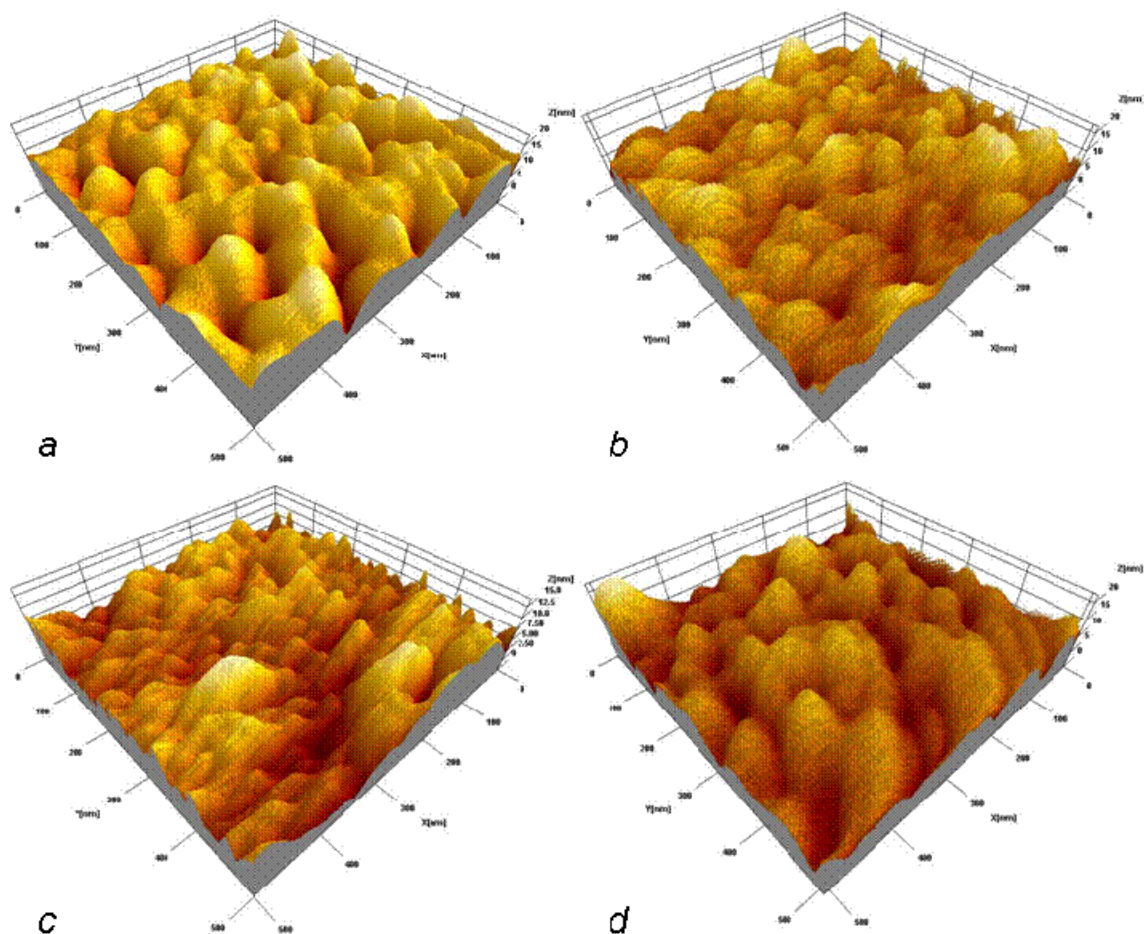
Figure 5.1. SPM images of a nanoporous aluminum surface: silanized with APTES (a);

with anti-SEB immobilized (b); empty sites blocked with ethanolamine (c); morphology

changes due to immunoreaction (d).

significant improvement of the detection methods from those reported in the literature [9]. To develop a highly sensitive and selective detection technique it is necessary to determine the optimal measuring conditions for the sensibilized electrode (i.e. sensor) in three domains: time, frequency and polarization potential. To optimize measuring conditions in order to obtain the best possible performance of a biosensor, a multi-step design approach is required. The steps include:

- To study electrode dynamics associated with the immunoreaction in the presence of excessive amount of highly conductive background electrolyte. The complete electrochemical behavior of a system can be investigated by sweeping the electrode potential with time and recording the resulting current as a function of potential. In that case, cyclic voltammetry is used to identify polarization regime of anti-SEB/SEB reaction and corresponding electrode charge transfer resistance. It allows to determine the optimal detection conditions with the highest sensitivity and stability of immobilized anti-SEB.

- To use time resolved electrochemical impedance spectroscopy (TREIS) to identify the perturbation frequency that corresponds to the specific interaction of probing charge carriers with Ab/Ag complexes. Measuring the sensor's impedance at this optimal frequency provides the best signal-to-noise ratio and stability of an output signal.

- To determine the dynamic characteristics of detector and to identify the minimal detection time of the sensor by recording sensor's complex impedance at the optimal single frequency as a function of time.

5.2.3.   Cyclic voltammetry of the SEB immunosensor

CV is a powerful technique to characterize the chemical composition and surface

morphology of an electrode surface that widely used to investigate the surface-associated

electrode processes [21]. CV responds sensitively to deposition of organic substances on the

electrode surface as well as to the changes due to development of new organic structures as

a result of Ab/Ag reaction [10, 22, 23, 25]. Cyclic voltammetry data provide crucial information

for the correct interpretation of observed changes in surface properties. It allows to

distinguish the changes induced by an Ab/Ag reaction form the changes due to a

non-specific interaction of the background electrolyte with the sensor surface. We perform

all measurements in two parallel experiments in two different media: one in the pH 6.0

0.3% NaCl with pre-determined concentrations of SEB (10 µg/ml), and the other in the

same medium with no SEB added.

 Figure 5.2 depicts the resulting plots of cyclic voltammetry study of SEB sensors in the

solution containing 10 µg/ml of SEB and corresponding control solution with no toxin

added. Due to the significant difference in the scale, cathodic and anodic branches of the

voltammogramm are shown separately.

As one can observe, the change of charge transfer resistance of the positively

polarized electrode (Figure 5.2. c) is much higher than that of the negatively polarized one

(Figure 5.2. a). The resulting shift in the anodic current is about 50 µA (Figure 5.2. a), and

only ~20 µA for the cathodic current (Figure 5.2 c). Addition of SEB into the solution does

not produce significant changes in the shape of the cyclic voltammogramms (Figure 5.2. b,

d). There are very small differences in the observed currents in both solutions. However,
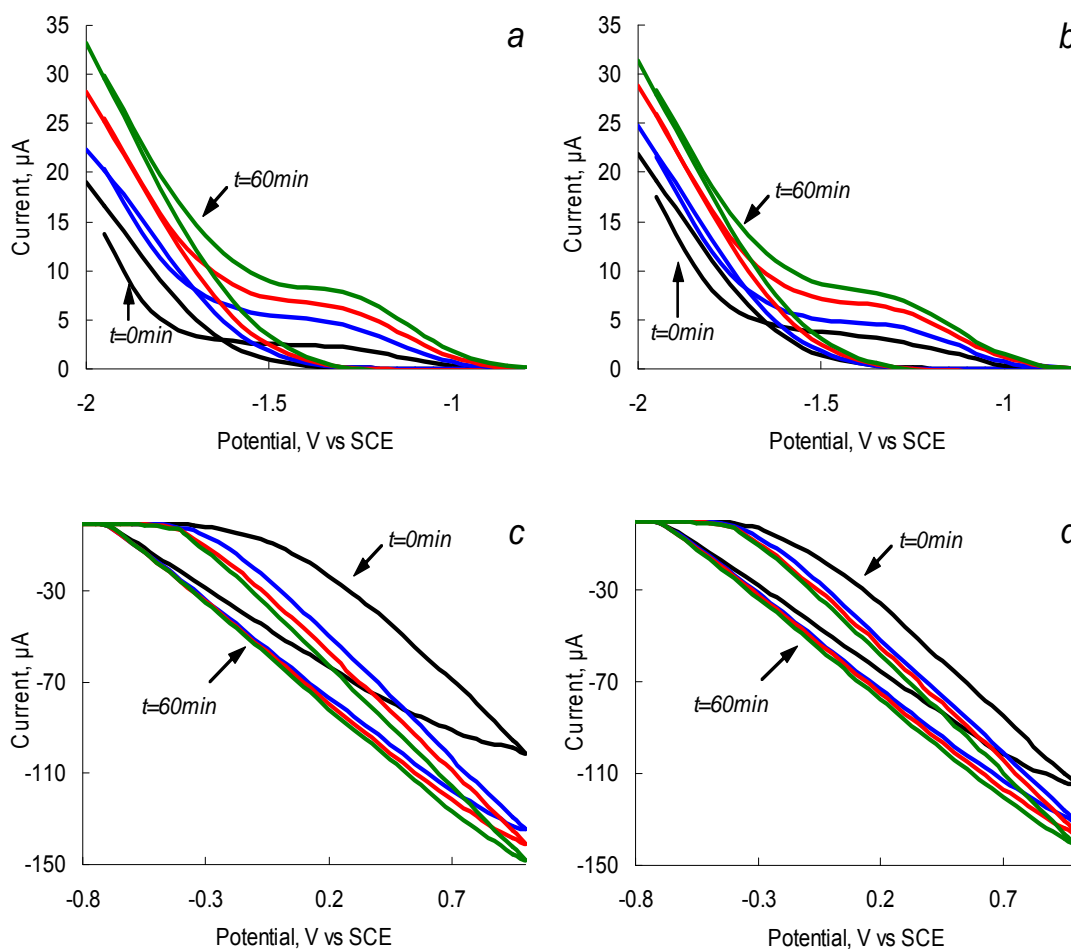
Figure 5.2. Cyclic voltammogramms of SEB immunosensors in 0.3% NaCl solution without toxin (a,c) and with addition of 10 μg/ml SEB (b,d) as a function of time (0 min, 10 min, 30 min, and 60 min).

time dependence of CVA in SEB solution is profoundly different. The slope of the anodic branch does not change gradually (Figure 5.2. d) as in pure NaCl solution (Figure 5.2. c). Rapid changes during the first 20 min slow down at longer exposure times (Figure 5.2. c, d). This behavior is in a good agreement with the reaction kinetics and characteristic times for diffusion-controlled immunoreactions [20]. Observed CVA shapes are typical for the diffusion-controlled processes, with no profound peaks commonly existing in red/ox reactions. It is important to note that the value of hysteresis between the ascending and descending parts of CV scan remains the same during the experiment. One can assume that all current is carried out by the background electrolyte ions, and redistribution of the target analyte (*i.e.* Ag) in the solution is not impacted by electromigration of the current carriers.

It seems that the optimal value of polarizing potential at the sensing surface, which allows to reveal the formation of Ab/Ag complexes, is ~1 V. However, the results of performed chronopotentiometry experiments with a sensor polarized at 1V and consequent SPM imaging of the surface (data not shown) indicate that the high values of positive polarization potential cause detachment of immobilized Ab from the sensor's surface. This may happen due to replacement of Ab by the negatively charged ions from the solution. We have found experimentally that the optimal polarization voltage, which allows the precise detection of the immunoreaction but does not cause Ab detachment, is 0.1 V vs. Ag/AgCl electrode. It is noticeable that in both solutions the point of zero charge (isoelectric point) of the sensor's surface is -0.765 V, which corresponds to the isoelectric point of pure aluminum [1]. Thus, one can conclude that the ions of a background electrolyte penetrate through the immobilized Ab layer and determine the equilibrium potential of the sensor's surface.

5.2.4.   Time-resolved electrochemical impedance spectroscopy

Based on the results of CV experiments, we can quantify the conditions for EIS

detection schemes. The use of a non-polarized electrode is very attractive for future field

applications, since the schematics is very simple. Additionally, a 2-electrode measuring

scheme provides fewer disturbances to the surface composition of the sensor by probing

surface impedance near the equilibrium potential. On the other hand, the polarization of a

working electrode allows to achieve better sensitivity of the sensor due to optimization of

the charge transfer at the sensor's interface.

The measuring parameter in TREIS is impedance $\dot{Z}(t,\omega)$, a complex resistance

that can be represented as:

$$\dot{Z}(t,\omega) = \frac{U(t,\omega)}{I(t,\omega)} = Z_0(t)e^{j\theta} = Z'(t,\omega) + jZ''(t,\omega) \qquad (1)$$

To compare output signals obtained from different sensors in various experimental

conditions, we use normalized values of the real and imaginary parts of a complex

impedance: $Z_{norm}(t,\omega) = \dfrac{Z(t,\omega)}{Z(0,\omega)}$. The normalization of obtained data allows discovering

the detection patterns that would be undetectable with the standard data representation. EIS

experiments were designed in the same manner as cyclic voltammetry studies. Two sets of

measurements – one in a pure background electrolyte, and the other with SEB added to the

medium – were performed.

5.2.4.1. TREIS analysis of non-polarized SEB immunosensor

Typical impedance spectra obtained with the non-polarized SEB sensor are depicted in Figure 5.3. Observed changes in the impedance value and phase angle are associated with two major effects: adsorption of solute ions onto the electrode surface and protein layer and formation of the Ab/Ag complexes (immunoreaction). The most significant changes of both impedance and phase angle are observed at low (< 1 kHz) frequencies. It is clear that the impedance of the sensor drops tremendously as probing frequency increases. Recognizable deviations in the impedance value are observed in the high frequency region.

Normalized values of real and imaginary parts of the complex EI spectra are depicted in Figure 5.4. It is not surprising that the most significant relative changes in phase angle values are observed at the low frequencies (< 10 Hz). Electric field-enforced ionic transport directly interferes with the Ab adsorption-desorption process at the surface. Additionally, the characteristic rate constant of the immunoreaction is $\sim 1.0 \times 10^{-9}$ M^{-1} [19], which gives us characteristic frequency values in the same range. The phase angle spectra of the sensors exposed to the pure NaCl and SEB-containing solutions are similar in shape, although the maximum on the phase angle curve for SEB-containing medium is shifted towards the high frequency region (see Figure 5.4. d). This frequency shift is quite small and is unlikely to be used for the detection purposes. The real parts of impedance spectra of pure NaCl and SEB-containing solutions that are depicted in Figure 5.4. a and b have significantly different patterns in time and frequency domains. An increase in low frequency resistance of the sensor surface in pure NaCl solution is followed by its decrease
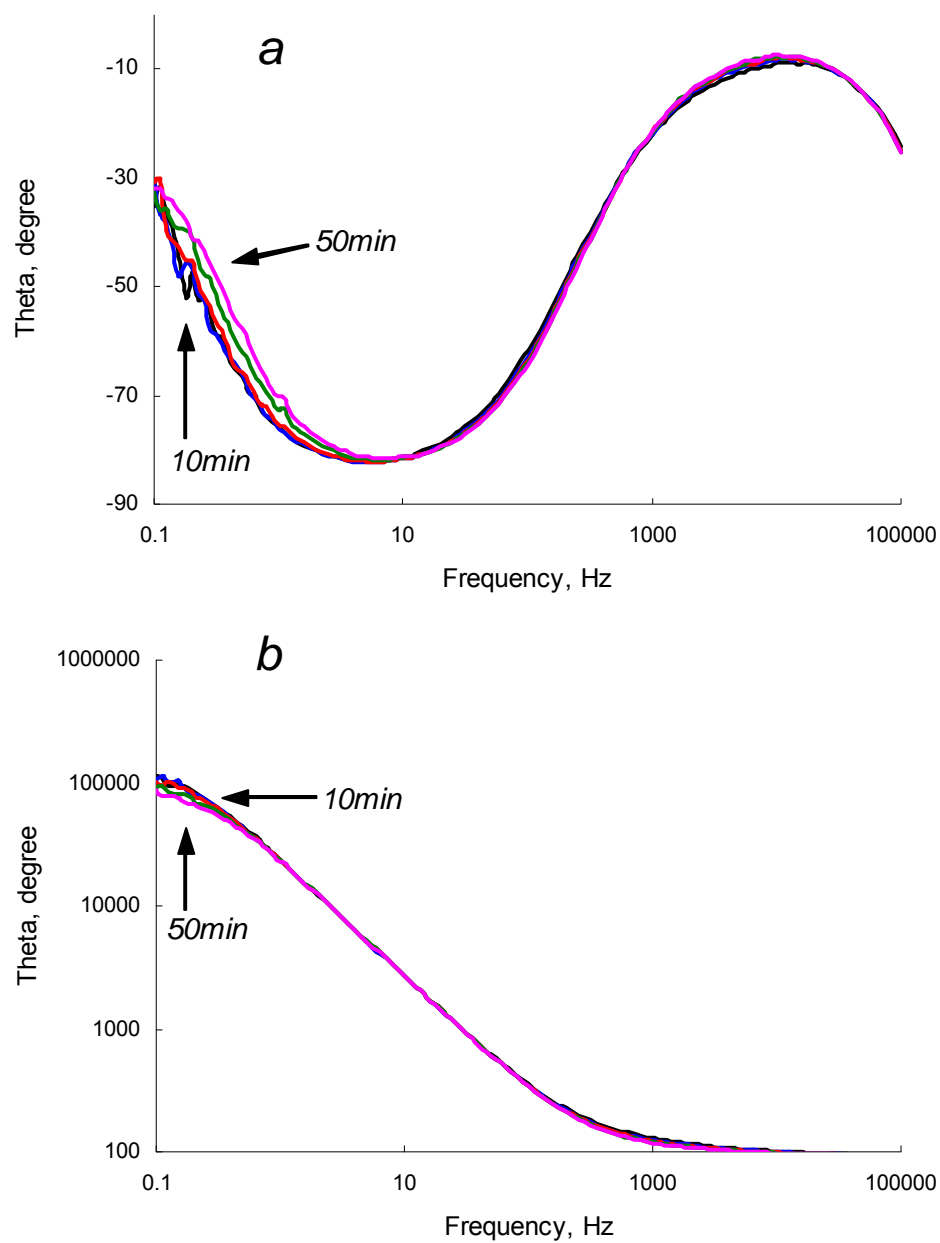
Figure 5.3. Phase angle (*a*) and impedance spectrum (*b*) of a non-polarized (φ_{eq} = -0.765 V

vs. Ag/AgC) SEB immunosensor in 10 µg/ml of SEB in 0.3% NaCl solution.
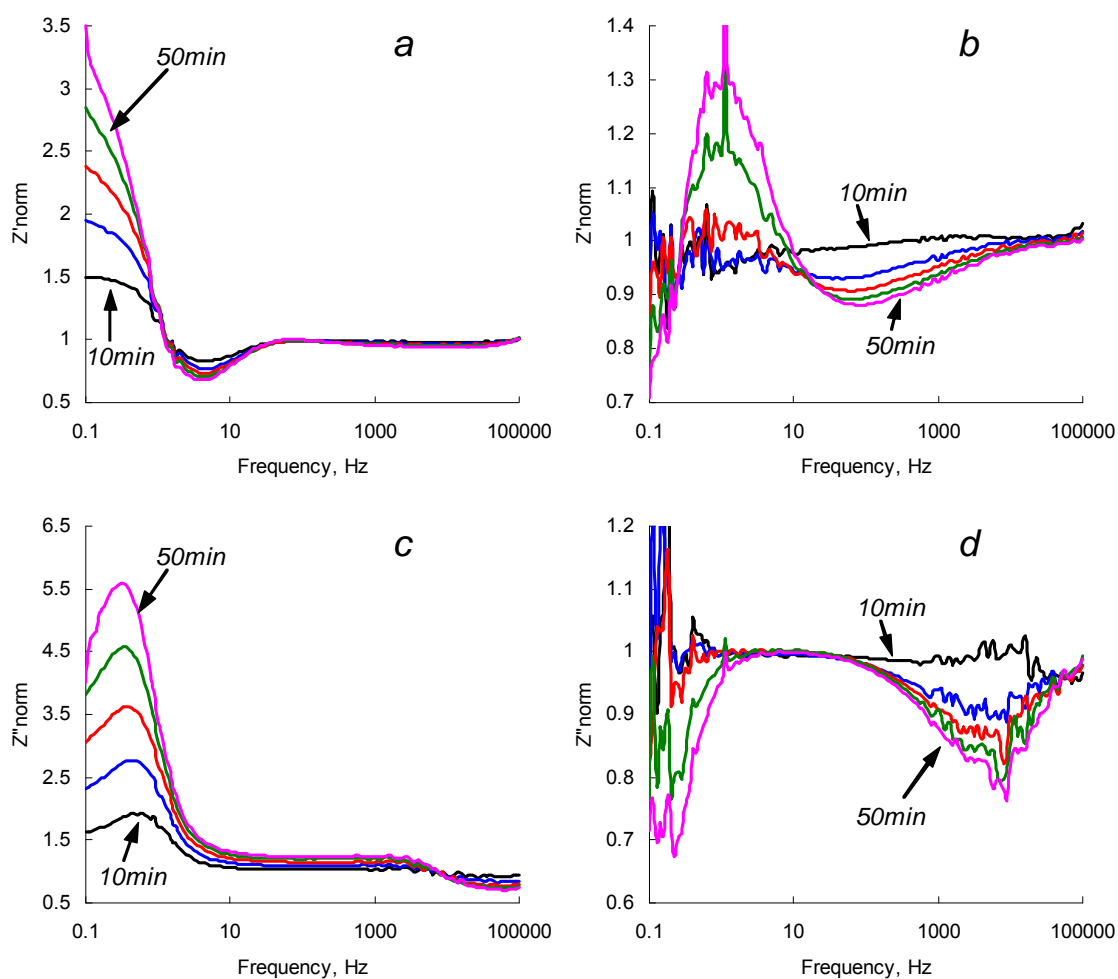
Figure 5.4. Normalized values of Z' (a,b) and Z'' (c,d) parts of electrochemical impedance spectra of a non-polarized (φ = -0.765 V vs. Ag/AgCl) SEB immunosensor in 0.3% NaCl (a, c) and 0.3% NaCl + 10 µg/ml (b, d) as a function of time (10 min, 20 min, 30 min, 40 min, and 50 min).

at high frequencies (Figure 5.4. a). These two regions, therefore correspond to the surface layers that differ in spatial arrangement and transport properties. Addition of SEB toxin causes dramatic changes in the surface response (Figure 5.4. b). A drop in low frequency resistance and appearance of characteristic peaks at 30-50 kHz are the results of immunoreaction. These patterns are distinct and reveal the unique signature of a target analyte. However, due to the extremely low impedance values, signal-to-noise ratio of the sensor in this frequency range is far from desirable, which limits application of the non-polarized sensor electrodes for relatively high concentrations of the toxin (~0.5 μg/ml).

5.2.4.2.   TREIS analysis of polarized SEB immunosensor

To enhance the sensor's sensitivity one should choose the measuring conditions so that a small perturbation would cause the most significant changes in the charge transfer at the sensor interface. This regime is characterized by the highest values of the hysteresis of the CVA curves. Based on the results from CV analysis, immunosensibilized electrode was polarized at + 0.1 V vs Ag/AgCl. This regime provides the maximum difference between polarization and depolarization electron transfer rate, at the sensor's interface. As shown in Figure 5.5, polarization of the sensing element results in dramatic improvements of the sensor's response over the frequency domain,. Time-dependent changes in phase angle and impedance are much more pronounced than those of a non-polarized electrode. The shapes of the spectra change significantly. The impedance value decreases as perturbation signal changes from low to high frequency, similar to the non-polarized electrode.

Significant changes in the impedance and phase angle are observed at low (< 1 kHz) frequencies. A decrease of impedance in the low frequency region is found in TREI spectra of 0.3% NaCl solution and SEB contaminated medium. Significant changes in the impedance in the low frequency domain are dominated by the adsorption/desorption interactions of a background electrolyte with the immobilized Ab layer and sensor's substrate.

Normalized real and imaginary parts of immunosensor's response in the described experiments are depicted in Figure 5.6. The behavior of polarized immunosensors in a low frequency region is very similar in both media. At the frequencies that correspond to the characteristic reaction time (< 10 Hz), the spectrum loses its monotonicity and exibits irregular peaks due to an overlap of the characteristic times of perturbation signal and immunoreaction (see Figure 5.6. c, d).

The major difference between the sensor's responses in SEB contaminated and control samples is observed in the medium frequency region (~ 10 kHz). This finding is quite reasonable since an additional surface layer existing due to the formation of Ab/Ag complexes, is very thin, and can only impact migration of ions at high frequencies, where the characteristic migration time corresponds to the relaxation time in the newly formed SEB Ab/Ag layer. The optimal frequency range has to be determined between 10 ~ 50 kHz, where the effect of supporting electrolyte is negligible, but the changes of impedance with time (following diffusion-controlled kinetics of immunoreaction) by Ab/Ag layer are significant. Additional criteria are also important in choosing the optimal detection frequency: low signal-to-noise ratio, signal stability, and reproducibility of the detection results. We used a multi-variable optimization (data not shown) to identify the best
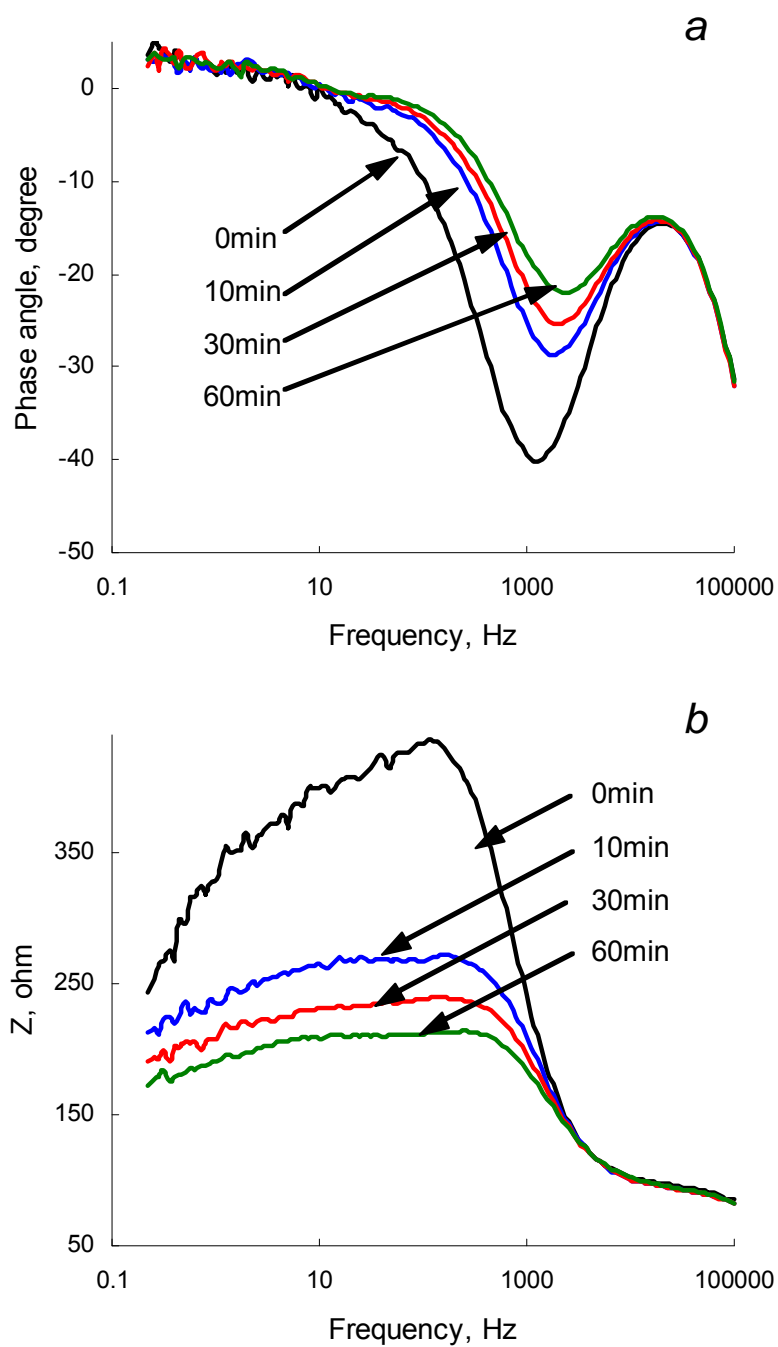
Figure 5.5. Phase angle and impedance spectrum of polarized ($\Delta\varphi = +0.1$ V vs. Ag/AgCl)

SEB immunosensor in 10 μg/ml of SEB in 0.3% NaCl solution
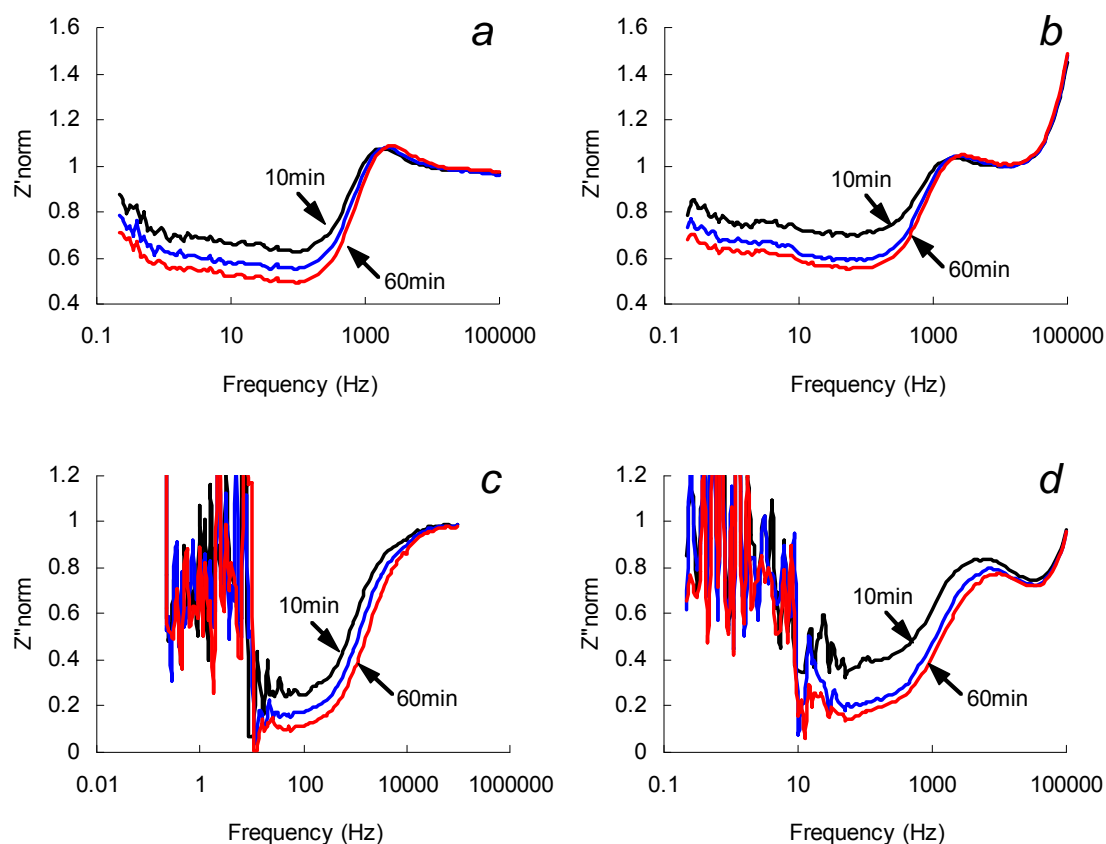
Figure 5.6. Normalized values of Z' (a,b) and Z'' (c,d) parts of the electrochemical impedance spectrum of a SEB immunosensor polarized at $\Delta\varphi$ = +0.1 V vs. Ag/AgCl in 0.3% NaCl (a, c) and 0.3% NaCl +10 g/ml SEB (b, d) media as a function of time (10 min, 30 min and 60 min).

possible detection frequency for high-performance immunosensors, and if has been determined to be 31 kHz.

5.2.5.   Detection of ultra-low SEB concentrations with polarized immunosensor

The optimal parameters for toxin detection have been identified from the cyclic voltammetry experiments and time-resolved EIS data as follows: the detection frequency of 31 kHz and polarizing potential of +0.1 V vs Ag/AgCl. The real part of SEB biosensor impedance was analyzed at the identified optimal conditions. The normalized values of the real part of impedance in 0.3% NaCl solution containing 10 pg·ml^{-1} are depicted in Figure 5.7 and compared with the values obtained for the control (no SEB added) system.

Performed 3-D parametric optimization of the detection method (polarization value, frequency domain and detection time) expands the detection limit of the developed biosensor up to picogram quantities of the toxin. A statistically recognizable difference in the sensor's output appear after 10 min of exposure then reaches the saturation level after 15 min of contact with the tested sample. The output signal is stable and there is no overlap between SEB-contaminated and control media.

5.3.   Conclusion

In this work, the design of impedimetric immunosensor for rapid and label-free detection of trace concentrations of *Staphylococcus* enterotoxin B is presented. Developed biosensor combines antibody as a molecular recognition element sensing the specific
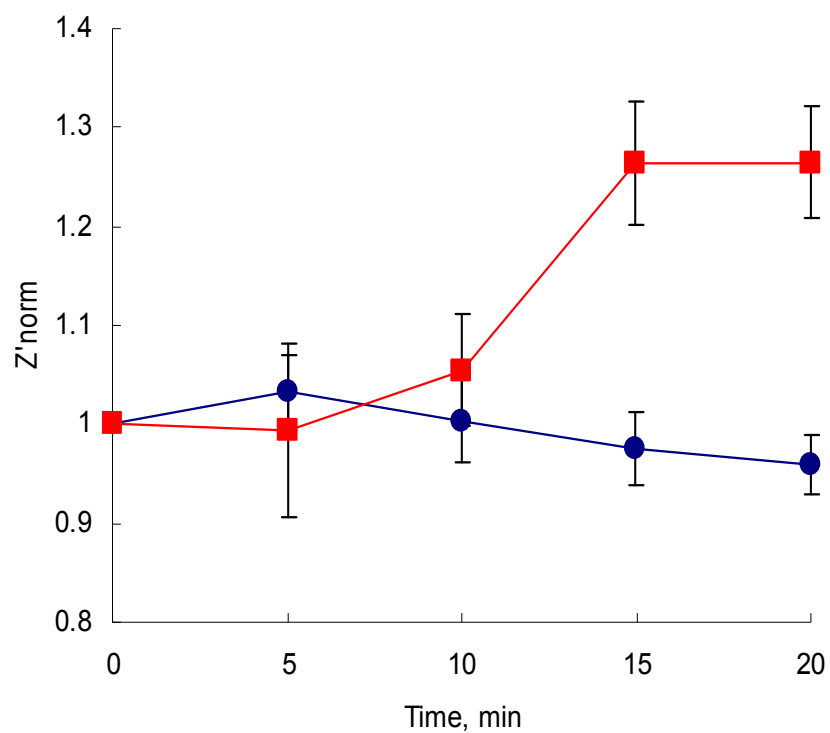
Figure 5.7. Normalized value of Z'_{norm} at a single frequency (31 kHz) electrochemical impedance of a polarized SEB immunosensor in 0.3% NaCl (●) and 0.3% NaCl+10 pg/ml SEB (■) media as a function of time.

antigen-antibody binding reaction with a signal transduction system. The presence of a biological toxin is determined through the conversion of physico-chemical changes driven by an antibody-antigen (Ab/Ag) reaction in to analytical signals by TREIS technique. An application of novel nanostructured material for the sensor's substrate has significantly improved its binding capacity, hence, sensor's output. Performed electrochemical detection with non-polarized and polarized sensing electrodes allowed to determine the optimal parameters for the SEB toxin detection. The developed measuring method is capable to selectively separate the specific response in the real part of impedance to Ab/Ag reaction from the background effect of electrolytes as well as to distinguish the test sample, containing an extremely low concentration of SEB. Using the developed immobilization method and optimized detection regime, it is possible to determine in real time the presence of biological toxins in concentrations less than 10 pg ml^{-1}.

5.4.   Experimental Section

5.4.1.   Materials

Oxalic acid, anhydrous 98% and phosphoric acid, 85% water solutions were purchased from Acros Organics (NJ, USA). Ethanol, HPLC grade and acetone, HPLC grade were obtained from Fisher Scientific (Fair Lawn, NJ, USA). Perchloric acid, 60% and 2-butoxyethanol $CH_3(CH_2)_3OCH_2CH_2OH$ were obtained from Alfa Aesar (Ward Hill, MA, USA) and J. T. Baker (Phillipsburg, NJ, USA). 3-Aminopropyltriethoxysilane (APTES) 98% was purchased from Strem Chemicals (Newburyport, MA, USA).

Glutaraldehyde 70% v/v (Grade I), ethanolamine 98%, and sodium chloride 99% were

purchased from Sigma Aldrich (St. Louis, MO, USA). Electropolishing solution was

prepared by mixing 70.0 vol.% of ethanol, 13.8 vol.% of distilled water, 10.0 vol.% of

2-butoxyethanol, and 6.2 vol.% of perchloric acid.

Monoclonal anti-*Staphylococcus aureus* enterotoxin B (anti-SEB) and

Staphylococcus aureus enterotoxin B were purchased from Biodesign International (Saco,

ME, USA) and Toxin Technology, Inc. (Sarasota, FL, USA), respectively. Sterilized

deionized (SDI) water was used to prepare the reagents. Anti-SEB was dissolved with

sterilized 0.01M phosphate buffer saline (NaCl 0.08%) and stock solution was stored at

-25°C. SEB solution was prepared by diluting dissolving SEB and diluting with sterilized

0.3% NaCl solution (pH 6.0).

Commercial food-grade aluminum foil (alloy 1100, thickness 0.25 mm), PTFE,

polycarbonate, and stainless steel 316 were purchased from McMaster-Carr (Dayton, NJ,

USA). To prepare sensor substrate blanks, aluminum foil was cleaned with acetone and cut

into 12.8-mm discs.

5.4.2.   Methods

Nanopatterning of biosensor's substrate: *electropolishing and anodization.*

Nanoporous aluminum substrate for the biosensor was fabricated following a three-steps

procedure: annealing at 500°C to homogenize surface structure via re-crystallization,

electropolishing, and anodization. Electropolishing was performed as described elsewhere

[26]. Aluminum discs were placed into the specimen holder and polished at 5°C in

electropolishing solution for 40 sec with vigorous stirring, under an applied voltage of

42V, supplied by PC-controlled DC power supply, 1787A (BK Precision Corp.,Yorba

Linda, CA, USA). Electrochemical nanopatterning of the aluminum surface was

performed by its anodization in 0.3M oxalic acid solution. The overall process

performance was monitored with multifunctional data acquisition system InstruNet 100

(InstruNet, Somerville, MA, USA). To obtain a well-ordered nanoporous surface structure

the anodization was carried out at the temperature below $5^{o}C$, controlled by the 3016

Isotemp refrigerating circulator (Fisher Scientific, Pittsburgh, PA, USA). After the

processing, aluminum discs were rinsed with deionized water and placed into 5 wt%

phosphoric acid for 1 hr. Processed nanoporous aluminum discs were then washed with

sterilized distilled (SDI) water and dried in nitrogen atmosphere. To prevent accidental

surface contamination, prepared discs were stored in a sterilized vacuumed desiccator.

Sensibilization of nanoporous aluminum: silanization and anti-SEB

immobilization. To immobilize antibodies, electrochemically processed aluminum discs

were placed into a 2.5% v/v solution of APTES in ethanol for 4 hrs. Silanized aluminum

surface was activated in the glutaraldehyde solution for 2 hrs. Then, activated aluminum

discs were placed into the solution containing 40 $\mu g \cdot ml^{-1}$ of anti-SEB for 1 hr at 37 ^{o}C and,

further, for 12 hrs at $4^{o}C$. Remaining vacant sites on the sensor's surface were blocked by

soaking the discs in 100 mM ethanolamine solution for 1 hr. Completed anti-SEB sensing

elements were thoroughly washed with SDI water, dried in nitrogen atmosphere, and

stored at $-25^{o}C$.

Surface morphology control: The morphological changes of the aluminum surface

due to electrochemical processing, APTES condensation, anti-SEB immobilization, and

SEB conjugation were analyzed by scanning probe microscope (SPM) Q-Scope 350

(Quesant Inst. Corp., Agoura Hills, CA, USA) in tapping mode with NSC-16 cantilevers. A specialized software package, SPIP 3.3 (NanoScience, Phoenix, AZ, USA) was used for image processing and analysis of nanoscale patterns on aluminum surface.

Electrochemical measurements: Cyclic voltammogramms (CVA) and impedance spectra (IS) of anti-SEB immunosensor were collected with PC-controlled electrochemical workstation DHC2, equipped with PC4 (750)/DC105 potentiostat (Gamry Instruments, Warminster, PA, USA). Double junction Ag/AgCl reference electrode PHE 3211 (Omega Engineering, Inc., Stamford, CT, USA) was used for CV and EIS in the three-electrode setups. 0.3% NaCl stock solution, used in all experiments, was conditioned by purging high-pure nitrogen prior to the electrochemical measurements. CV scans were performed in the voltage range of -2.0...+1.0 V vs. Ag/AgCl reference electrode at the scan rate of 100 mVs^{-1}. The impedance spectra were collected in the frequency range of 0.25 Hz …100 kHz with the excitation voltage of 10 mV. In the experiments with polarized working electrode, the sensor was polarized with $\Delta\varphi = +0.1$ V vs. Ag/AgCl electrode. All presented experiments were triplicated. The error bars are placed on the plots where appropriate.

A custom-made electrochemical cell with two- and three- electrode configuration was used for all measurements. The cell contains a disk-shaped stainless steel counter electrode (CE), conductive support for the working electrode (sensor) embedded into the polycarbonate body with appropriate channels for filing and drainage of the testing solutions, and a placeholder for the reference electrode. This design allows to avoid interconnects on the sensor's surface minimizing time and cost of the sensor fabrication and replacement. An internal compartment of the chamber is conically-shaped. Thus a

counter electrode with larger surface area than that of a working electrode ($S_{CE}/S_{WE} \sim 10$)

can be used. This eliminates the effect of CE polarization on the sensor's output.

5.5. References

1. Bockris, J. O. M.; Reddy, A. K. N., Modern Electrochemistry 1: Ionics. 2nd ed.; Plenum: New York, USA, 1998; 828.

2. Cui, X.; Pei, R.; Wang, Z.; Yang, F.; Ma, Y.; Dong, S.; Yang, X., Layer-by-layer assembly of multilayer films composed of avidin and biotin-labeled antibody for immunosensing. Biosensors and Bioelectronics 2003, Vol. 18, 59-67.

3. DeSilva, M. S.; Zhang, Y.; Hesketh, P. J.; Maclay, G. J.; Gendel, S. M.; Stetter, J. R., Impedance based sensing of the specific binding reaction between *Staphylococcus* enterotoxin B and its antibody on an ultra-thin platinum film. 1995, Vol. 10, 675-682.

4. Evenson, M. L.; Ward Hinds, M.; Bernstein, R. S.; Bergdoll, M. S., Estimation of human dose of staphylococcal enterotoxin A from a large outbreak of staphylococcal food poisoning involving chocolate milk. International Journal of Food Microbiology 1988, Vol. 7, 311-316.

5. Farace, G.; Lillie, G.; Hianik, T.; Payne, P.; Vadgama, P., Reagentless biosensing using electrochemical impedance spectroscopy. Bioelectrochemistry 2002, Vol. 55, 1-3.

6. Gabrielli, C., Electrochemical impedance spectroscopy: principles, instrumentation, and applications. In; Rubinstein, I. (Ed.); Physical Electrochemistry, Principles, Methods, and Applications, Marcel-Dekker: New York, USA, 1995; 243-292.

7. Gheorghe, M.; Guiseppi-Elie, A., Electrical frequency dependent characterization of DNA hybridization. Biosensors and Bioelectronics 2003, Vol. 19, 95-102.

8. Horner, M. R.; Boerio, F. J.; Clearfield, H. M., An XPS investigation of the adsorption of aminosilanes onto metal substrates. In; Mittal, K. L. (Ed.); Silanes and Other Coupling Agents, VSP: Utrecht, Netherlands, 1992; 305 − 321.

9. Ivnitski, D.; Abdel-Hamid, I.; Atanasov, P.; Wilkins, E., Biosensors for detection of pathogenic bacteria. Biosensors and Bioelectronics 1999, Vol. 14, 599-624.

10. Jie, M.; Ming, C. Y.; Jing, D.; Cheng, L. S.; Huai na, L.; Jun, F.; Xiang, C. Y., An electrochemical impedance immunoanalytical method for detecting immunological interaction of human mammary tumor associated glycoprotein and its monoclonal antibody. Electrochemistry Communications 1999, Vol. 1, 425-428.

11. Jonscher, A. K., Dielectric relaxation in solids. Journal of Physics D: Applied Physics 1999, Vol. 32, R57-R70.

12. Katz, E.; Willner, I., Probing biomolecular interactions at conductive and semiconductive surfaces by impedance spectroscopy: routes to impedimetric immunosensors, DNA-sensors, and enzyme biosensors. Electroanalysis 2003, Vol. 15, 913-947.

13. Macdonald, J. R., Impedance Spectroscopy-Emphasizing Solid Materials and Systems. Wiley-Interscience: New York, USA, 1987; 346.

14. Medina, M. B., Detection of staphylococcal enterotoxin B (SEB) with surface plasmon resonance biosensor. Journal of Rapid Methods and Automation in Microbiology 2003, Vol. 11, 225-243.

15. Naimushin, A. N.; Soelberg, S. D.; Nguyen, D. K.; Dunlap, L.; Bartholomew, D.; Elkind, J.; Melendez, J.; Furlong, C. E., Detection of *Staphylococcus aureus* enterotoxin B at femtomolar levels with a miniature integrated two-channel surface plasmon resonance (SPR) sensor. Biosensors and Bioelectronics 2002, Vol. 17, 573-584.

16. Nashat, A. H.; Moronne, M.; Ferrari, M., Detection of functional groups and antibodies on microfabricated surfaces by confocal microscopy. Biotechnology and Bioengineering 1998, Vol. 60, 137-146.

17. Naumann, R.; Schmidt, E. K.; Jonczyk, A.; Fendler, K.; Kadenbach, B.; Liebermann, T.; Offenhausser, A.; Knoll, W., The peptide-tethered lipid membrane as a biomimetic system to incorporate cytochrome C oxidase in a functionally active form. Biosensors and Bioelectronics 1999, Vol. 14, 651-662.

18. Ouerghi, O.; Touhami, A.; Jaffrezic-Renault, N.; Martelet, C.; Ouada, H. B.; Cosnier, S., Impedimetric immunosensor using avidin-biotin for antibody immobilization. Bioelectrochemistry 2002, Vol. 56, 131-133.

19. Rucker, V. C.; Havenstrite, K. L.; Herr, A. E., Antibody microarrays for native toxin detection. Analytical Biochemistry 2005, Vol. 339, 262-270.

20. Sadana, A.; Alarie, J. P.; Vo-Dinh, T., Antigen-antibody diffusion-limited binding kinetics for biosensors: A fractal analysis. Sensors and Actuators B: Chemical 1996, Vol. 32, 195-201.

21. Schmickler, W.; Leiva, E., A note on the surface stress and tension of solid metal electrodes. Journal of Electroanalytical Chemistry 1998, Vol. 453, 61-67.

22. Snejdarkova, M.; Csaderova, L.; Reh, M.; Hianik, T., Amperometric immunosensor for direct detection of human IgG. Electroanalysis 2000, Vol. 12, 940-945.

23. Tang, D.; Yuan, R.; Chai, Y.; Dai, J.; Zhong, X.; Liu, Y., A novel immunosensor based on immobilization of hepatitis B surface antibody on platinum electrode modified colloidal gold and polyvinyl butyral as matrices via electrochemical impedance spectroscopy. Bioelectrochemistry 2004, Vol. 65, 15-22.

24. Vagin, M. Y.; Karyakina, E. E.; Hianik, T.; Karyakin, A. A., Electrochemical transducers based on surfactant bilayers for the direct detection of affinity interactions. Biosensors and Bioelectronics 2003, Vol. 18, 1031-1037.

25. Wang, X.; Han, G. R., Fabrication and characterization of anodic aluminum oxide template. Microelectronic Engineering 2003, Vol. 66, 166-170.

26. Yuzhakov, V. V.; Takhistov, P. V.; Miller, A. E.; Chang, H.-C., Pattern selection during electropolishing due to double-layer effects. Chaos: An Interdisciplinary Journal of Nonlinear Science 1999, Vol. 9, 62-77.

Chapter 6.   Applicability of EIS immunosensor to foods including acidic foods

6.1.   Introduction

Detection of biological toxins in foods is on the practical front line to keep food safety from bioterrorism [4]. As concern of the efficient food safety, the detection method has to be sensitive and rapid moreover applicable to diverse foods. However it is a challenge to develop an immunosensor for the detection of biological toxins in diverse foods since food constituents can affect the performance of immunosensors [3]. For example, metal ions, salts, acids, and etc composing foods can hinder immunoreaction. Among food constituents, acids may be the most critical one to be considered for the development of an immunosensor for the detection of biological toxins in foods since immunoreaction is a biological reaction that is dependent on pH. Generally optimal pH of immunoreaction is in neutral pH, and the rate of immunoreaction may be low or extremely low in acidic environments (Table 6.1). However most of biological toxins can maintain their structures in acidic environments, and exhibit their toxicities in acidic foods. Additionally there still exist potentials of foodborne illness from acidic foods, hence Food and Drug Administration of United States (FDA) regulates acidic foods strictly by classifying foods into neutral foods ($\sim$ pH 7.0), low acid foods (pH 4.6 <) and acid foods (< pH 4.6) [1,2]. Accordingly traditional immunosensors such as ELISA (enzyme-linked immunosorbent assay), RIA (radioimmunoassay), and electrophoretic immunoassay frequently include a step of pH adjustment prior to the analysis of target toxins in order to avoid the hindrance

Classification of foods by pH [1]	pH	Food examples	Immunoreaction
Neutral foods	7.0	Milk, soy bean milk, chicken broth, beef broth	Occur without hindrance
Low acid foods	4.6 <	Vegetable soups	Low or extremely low
Acid foods	< 4.6	Fruit juices	Extremely low

Table 6.1. Classification of foods by pH [1] and assumed immunoreaction in each food class.

acidic environments.

of immunoreaction by acids, thus they are hardly applied to in-line detection or direct detection of target toxins.

As a direct method for the detection of biological toxins in acidic foods, electrochemical impedimetric spectroscopy (EIS) immunosensor is more advantageous over traditional immunosensors [5]. EIS immunosensor can detect target toxins without a labeling step that is frequently included in traditional immunosensors hence EIS immunosensor has less chance to be influenced by acids than traditional immunosensors. Moreover we found a potential of EIS immunosensor to be applied to foods out of neutral pH. EIS immunosensor showed high sensitivity under the polarization of immunosensor especially when immunosensor was polarized by maintaining DC potential between immunosensor and reference electrode. It was quite certain that pH near the surface of immunosensor might be shifted by the polarization therefore it was assumed that EIS immunosensor might be applicable to acidic foods.

This chapter is to investigate the potential of EIS immunosensor as a direct method for the detection of biological toxins in acidic foods. EIS immunosensor for the detection of ricin that is one of the most potent biological toxins for bioterrorism was developed based on nanoporous aluminum substrate. The effects of acids and immunoreaction on impedimetric signal outputs were studied through EIS analysis of ricin immunosensor. Then the applicability of EIS ricin immunosensor to neural food, low acid food, and acid food was discussed and additionally the performance of EIS immunosensor for ricin detection was compared to a standard method that is based on ELISA.

6.2. Materials and methods

Development of EIS immunosensor for the detection of ricin. Nanoporous aluminum was fabricated by anodization of alloy 1100 at 40V as described in chapter 2 and 4. Then EIS immunosensor for the detection of ricin was developed by immobilizing anti-ricin (Toxin technology Inc., Sarasota, FL, USA) on nanoporous aluminum through a practical method of Ab immobilization as described in chapter 3.

Impedance analysis. Impedance spectra (IS) from ricin immunosensor over wide range of applied frequency (0.25Hz ~ 100kHz) were collected as described in previous chapters. The details of impedance analysis were AC frequency: 56kHz, AC voltage: 10mV, and DC voltage vs. Ag/AgCl reference electrode: 100mV. To investigate the effect of immunoreaction on impedimetric signal outputs, EIS from ricin immunosensor in 0.3% salt solution with or without 1μg/ml of ricin (Toxin technology Inc., Sarasota, FL, USA) were collected and compared. From EIS comparison, a frequency that is specific to immunoreaction between anti-ricin and ricin was decided. The time functional changes of impedimetric signal outputs were monitored in 0.3% salt solution with or without ricin by single frequency EIS at the specific frequency. The regime for single frequency EIS was carried out in a same manner as described above. The applicability of EIS ricin immunosensor was investigated by single frequency EIS of ricin immunosensor in real foods with or without ricin. Food samples were milk, vegetable soup, and tomato juice that could represent neutral foods, low acid foods, acid foods and they were purchased from a local supermarket.

Ricin analysis by a standard ELISA method. The analysis of ricin by a standard

ELISA kit (Tetracore Inc., Rockville, MD, USA) was carried out in food samples

containing 500ng/ml of ricin. To compare the sensitivity in low pH foods between

developed our ricin immunosensor and a standard method, food samples were directly

applied to a standard method without pH adjustment although the manufacturer

recommended pH adjustment of samples in the manual.

6.3. Results

6.3.1. EIS analysis of ricin immunosensor

Z_0 and θ, or Z' and Z'' were obtained from EIS analysis of ricin immunosensors.

We assumed that immunoreaction would influence on a specific impedimetric signal

output (Z_0, θ, Z', or Z''), and it was found that the immunoreaction between anti-ricin

and ricin on the surface of immunosensor influences on Z' rather than others regardless of

pH by comparing the time-functional changes of impedimetric signal outputs from ricin

immunosensor in salt solutions and ricin solutions (1μg/ml) at different pH (data not

shown). Accordingly the immunoreaction between immobilized anti-ricin and ricin may

change inductive characteristics of immunosensor rather than the capacitive characteristics

because Z' is an impedimetric signal output that is dependent on inductive characteristics.

Therefore we conclude that Z' is appropriate to represent the performance of EIS ricin

immunosensor. In this paper, normalized Z' (Z'_{norm}) is used in order to compare Z' from

each ricin immunosensor in different conditions.

To investigate the effects of electrolytes and immunoreaction on Z'_{norm}, Z'_{norm} spectra from ricin immunosensors in pH 7.0, 5.0, and 3.0 salt solutions, and pH 7.0, 5.0, and 3.0 ricin solutions (1μg/ml) were collected every 20min for 60min (Figure 6.1). The effects of electrolytes and immunoreaction on Z'_{norm} could be elucidated by comparing Z'_{norm} at the frequency higher than 10Hz since huge noise was observed below 10Hz. In pH 7.0 salt solution, Z'_{norm} was decreased gradually and the decrease was obvious at the frequency from 10Hz to 1kHz (Figure 6.1. a). Such decrease of Z'_{norm} in pH 7.0 salt solution is regarded as the effect of electrolytes on Z'_{norm} since it is very certain that electrolytes including acids may be diffused from the bulk solution and adsorb on the surface of ricin immunosensor until the equilibrium when ricin immunosensor is put into salt solutions. However Z'_{norm} spectra in pH 7.0 ricin solution were higher than Z'_{norm} spectra in pH 7.0 salt solution (Figure 6.1. a'). Because the adsorption of electrolytes occurs regardless of the immunoreaction, the differences between Z'_{norm} spectra in pH 7.0 salt solution and Z'_{norm} spectra in pH 7.0 ricin solution is regarded as the effect of immunoreaction on Z'_{norm}. Therefore we conclude that the adsorption of electrolytes on the surface of ricin immunosensor results in the decrease of Z'_{norm} and the immunoreaction between anti-ricin and ricin hampers the decrease of Z'_{norm}. Furthermore, as Z'_{norm} at the frequency from 1kHz to 100kHz was increased in pH 7.0 ricin solution despite of the adsorption of electrolytes, 1kHz to 100kHz is regarded as the specific frequency region to the immunoreaction between anti-ricin and ricin (Figure 6.1. a').

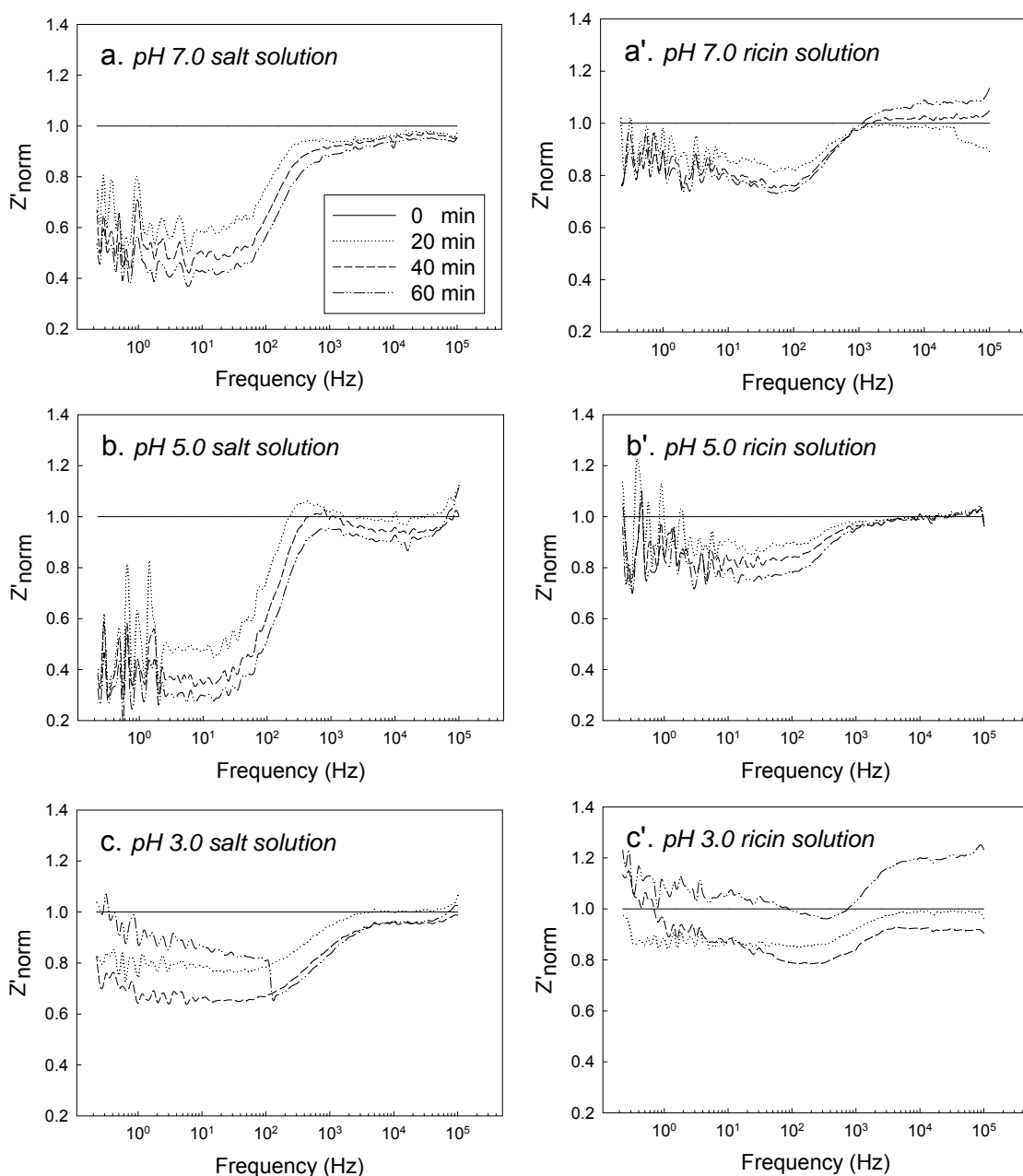Figure 6.1. Time-functional changes of Z'_{norm} spectra betained from ricin immunosensors in a) pH 7.0 salt solution, a') pH 7.0 ricin solution, b) pH 5.0 salt solution, b') pH 5.0 ricin solution, c) pH 3.0 salt solution, and c') pH 3.0 ricin solution, The concentration of ricin in ricin solution at different pH was 1μg/ml. Z'_{norm} spectrum was collected every 20min for 60min in sample solution.

The decrease of Z'_{norm} by electrolytes and the hampering of the decrease by immunoreaction were also observed in pH 5.0 salt solution and pH 5.0 ricin solution respectively (Figure 6.1. b and b'). However the increase of Z'_{norm} from 1kHz to 100kHz that was observed in pH 7.0 ricin solution could not be found in pH 5.0 ricin solution (Figure 6.1. b'), and this may be due to the effect of acids on immunoreaction. In pH 5.0 ricin solution, acids diffused from the bulk solution may adsorb on the surface of ricin immunosensor then they probably hinder the immunoreaction between anti-ricin and ricin. Hence the number of antibody-antigen (Ab-Ag) complexes resulted from the immunoreaction in pH 5.0 ricin solution might not be enough to give the increase of Z'_{norm} from 1kHz to 100kHz. The effect by acids on Z'_{norm} became more significant in pH 3.0 salt solution and pH 3.0 ricin solution (Figure 6.1. c and c'). Z'_{norm} were shifted even during EIS analysis when ricin immunosensor was exposed to pH 3.0 for 60min (Figure 6.1. c). Since it can be assumed considerable amount of acids was adsorbed on the surface of ricin immunosensor especially when ricin immunosensor was exposed to pH 3.0 for 60min, immobilized anti-ricin might be denatured by acids. Electrochemical properties of ricin immunosensor would be changed tremendously by the denaturation of immobilized anti-ricin, and this might result in the shift in Z'_{norm} spectra. Moreover the fact that whole Z'_{norm} spectrum in pH 3.0 ricin solution at 60min was shifted completely (Figure 6.1. c') assures the denaturation of immobilized anti-ricin by the exposure to pH 3.0 for 60min because denatured protein tends to aggregate nonspecifically with foreign proteins. However Z'_{norm} in pH 5.0 ricin solution and pH 3.0 ricin solution at 20min and 40min were

higher than pH 5.0 salt solution and pH 3.0 salt solution at 20min and 40min respectively (Figure 6.1. b' and c').

6.3.2.   Single frequency EIS of ricin immunosensor in acidic environments

The sensitivity of EIS immunosensor in different pH environments was investigated by comparing the time-functional changes of Z'_{norm} obtained from single frequency EIS of ricin immunosensor in pH 7.0, 5.0, and 3.0 salt solutions, and in pH 7.0, 5.0, and 3.0 ricin solutions (500ng/ml). 10kHz was chosen as a frequency for single frequency EIS since 10kHz was on the middle of log scale of the frequency region (1kHz - 100kHz) that is specific to the immunoreaction between immobilized anti-ricin and ricin (Figure 6.1. a'). Single frequency EIS of ricin immunosensor were triplicated and the results is presented in Figure 6.2.

In pH 7.0 salt solution and pH 7.0 ricin solution, the adsorption of electrolytes decreased Z'_{norm} and the immunoreaction increased Z'_{norm} (Figure 6.2. a). Furthermore the difference of Z'_{norm} between pH 7.0 salt solution and pH 7.0 ricin solution became significant because the more electrolytes and ricin were diffused, the more electrolytes might adsorb and the more immunoreaction might occur. The decrease of Z'_{norm} by electrolytes and the increase of Z'_{norm} by the immunoreaction also could be found on 20min in pH 5.0 and 3.0 salt solutions, and pH 5.0 and 3.0 ricin solutions (Figure 6.2. b and c). However, after 20min, Z'_{norm} was unpredictable at pH 5.0 and 3.0. Since the variation of Z'_{norm} became significant as the exposure to acidic environments was extended as well
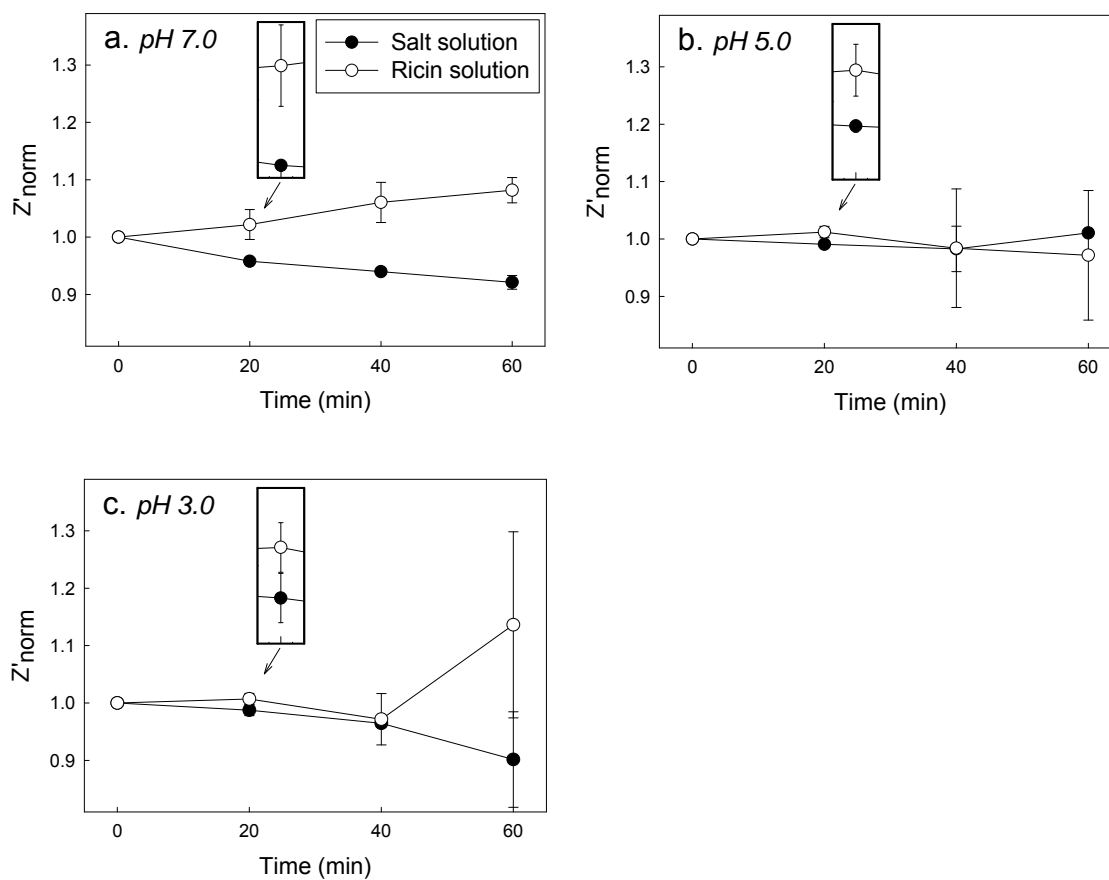
Figure 6.2. Time-functional changes of Z'_{norm} obtained from single frequency EIS (10kHz) of ricin immunosensor in a) pH 7.0 salt solution and ricin solution, b) pH 5.0 salt solution and ricin solution, and c) pH 3.0 salt solution and ricin solution. The concentration of ricin in ricin solution at different pH was 500ng/ml.

as pH of sample solution was lower, unpredictable changes of Z'_{norm} at pH 5.0 and 3.0

might be due to the denaturation of immobilized anti-ricin by acids (Figure 6.2. b and c).

Despite of the effect of acids on the immunoreaction and the structure of

immobilized anti-ricin, EIS ricin immunosensor could detect the presence of ricin in acidic

environments in 20min (Figure 6.2. b and c). This indicates indirectly that not only

immobilized anti-ricin was not denaturated fully in 20min but also EIS ricin immunosensor

was sensitive enough to recognize small number of Ab-Ag complexes.

6.3.3. Applicability of EIS immunosensor for ricin detection to acidic foods

The applicability of EIS ricin immunosensor to acidic foods was investigated by

single frequency EIS of ricin immunosensor in milk, vegetable juice, and tomato juice that

could represent neutral food, low acid food, and acid food respectively. The concentration

of ricin in food samples was 500ng and the frequency was at 10kHz. We regarded that the

presence of ricin in foods was detected by EIS ricin immunosensor if Z'_{norm} at the presence

of ricin was higher than that at the absence of ricin. Especially the window for detection

period was limited to 20min as EIS ricin immunosensor was able to detect the presence of

ricin in salt solution in 20min (Figure 6.1).

In milk, vegetable soup, and tomato juice, the immunoreaction increased Z'_{norm}

gradually and the adsorption of electrolytes decreased Z'_{norm} gradually (Figure 6.3).

Therefore we conclude that EIS ricin immunosensor is applicable to neutral food, low acid

food, and acid food. One can note that the increase of Z'_{norm} by the immunoreaction that

was observed in pH 7.0 ricin solution (Figure 6.2. a) can not be found in milk (Figure 6.3.

a). This may due to the interference of milk constituents on the performance of EIS ricin
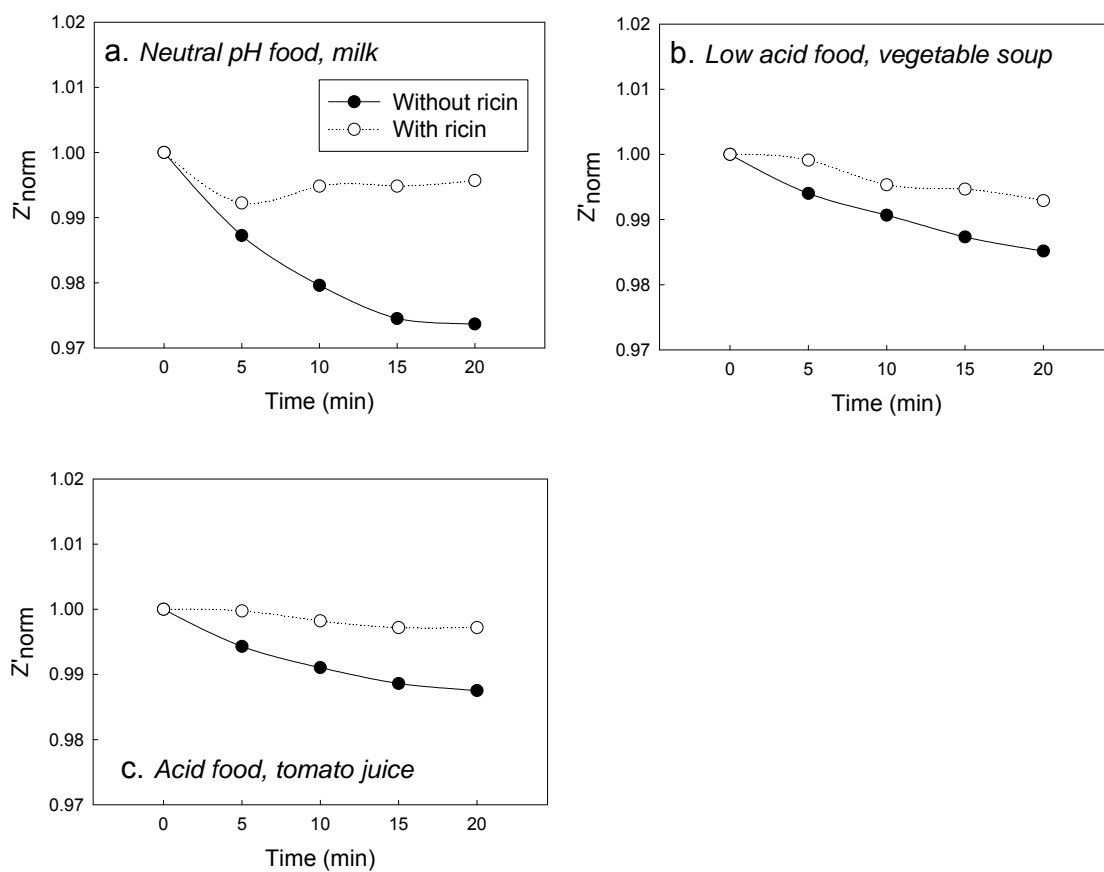
Figure 6.3. Time-functional changes of Z'_{norm} obtained from single frequency EIS

(10kHz) of ricin immunosensor in a) milk (neutral food), b) vegetable soup (low acid food),

and c) tomato juice (acid food) with or without ricin (500ng/ml). Z'_{norm} at 10kHz was

collected every 5min for 20min.

immunosensor although the reason could not be identified.

6.4.   Discussion

The performance of EIS immunosensor in acidic foods was compared to that of a standard immunosensor based on ELISA. For the direct comparison between two different methods, the analysis of ricin in real foods including neutral (milk), low acid (vegetable soup), and acid foods (tomato juice) using a standard method was conducted without pH adjustment of sample foods. Table 6.2 shows the actual amount of ricin and analyzed quantity of ricin obtained from the analysis of ricin in food samples by a standard immunosensor. The presence of ricin in acidic foods was not detectable by a standard immunosensor since there were huge differences between actual amount and analyzed quantity especially in tomato juice.

It is probably impossible to avoid the effect of acids while immunosensor was used for the detection of target toxins in acidic foods since immunosensor should be exposed to acidic environments for the recognition and detection of target toxins. Acids in acidic foods might affect on the structure of immobilized anti-ricin presented on a standard immunosensor hence resulted in insensitivity in acidic foods. Especially the denaturation of immobilized anti-ricin on a standard immunosensor might be significant since a standard immunosensor requires a step for immunoreaction in food sample for 1hr. However EIS immunosensor developed in this thesis was able to detect target toxins in 20min before the full denaturation of immobilized anti-ricin although the effect of acids on the structure of immobilized anti-ricin was unavoidable.

Category [1]	Foods	pH	Actual amount of ricin	Analyzed quantity of ricin from a standard immunosensor	
				1st trial	2nd trial
Neutral food (~pH 7.0)	Milk	6.5	500ng/ml	920ng/ml	1020ng/ml
Low acid food (pH 4.6 <)	Vegetable soup	4.8	500ng/ml	3020ng/ml	-3080ng/ml
Acid food (< pH 4.6)	Tomato juice	3.9	500ng/ml	-2580ng/ml	-2880ng/ml

Table 6.2. The analysis of ricin (500ng/ml) in neutral (milk), low acid (vegetable soup), and acid foods (tomato juice) using a standard immunosensor (Ricin ELISA kit, Tetracore Inc.).

6.5.   Conclusion

A method to keep food safety from bioterrorism has to be sensitive and rapid moreover applicable to diverse foods. In this study, we demonstrated a highly sensitive and rapid impedimetric immunosensor that is applicable to low acid and acid foods. Our ricin immunosensor was sensitive enough to detect the presence of 500ng/ml of ricin in low acid and acid foods in 20min before the denaturation of immobilized anti-ricin by acids. Additionally the immunosensor seems to be more appropriate for field application or in-line detection of target toxin since it can detect target toxin directly without sample treatments such as pH adjustment or additional labeling steps. Moreover EIS immunosensor may be more amenable for the economization and miniaturization therefore it is highly expected that the development of immunosensor for the application to real world out of laboratory such as industrial fields, school lunch, field military, etc.

6.6.   References

1. FDA, Acidified Foods. Department of Health and Humans Services. 2002, 21 CFR Part 108.25.

2. FDA, Thermally Processed Low-Acid Foods Packaged in Hermetically Sealed Containers. Department of Health and Humans Services. 2004, 21 CFR Part 113.

3. Huang, J.-C.; Yang, J.-W.; La, i. W.-D.; Song, M.-D.; Deng, F.; Lin, J.-Y., Impedance method for rapid detection of total counts of bacteria and fungi in bottled purified water. Journal of AOAC International 2003, Vol. 86, 719-721.

4. Sullivan, B. M., Bioterrorism detection: the smoke and the canary. Technology Review Journal 2003, Vol. 11, 135-141.

5. Vagin, M. Y.; Karyakina, E. E.; Hianik, T.; Karyakin, A. A., Electrochemical transducers based on surfactant bilayers for the direct detection of affinity interactions. Biosensors and Bioelectronics 2003, Vol. 18, 1031-1037.

Chapter 7.   Conclusion

A sensitive, rapid, direct, and field applicable EIS immunosensor is presented and its applicability to real foods is demonstrated in this thesis. Practical methods to improve the sensitivity of EIS immunosensor were established through the systematic studies including aluminum anodization, APTES silanization, and designing of EIS immunosensor. EIS immunosensor built on nanoporous aluminum by Ab immobilization using APTES showed a good sensitivity, moreover EIS immunosensor was as sensitive as to detect the presence of 10pg/ml of target toxin in 20min especially if the potential between reference electrode and immunosensor was maintained at 100mV. EIS immunosensor developed in this thesis was applicable to real foods including acidic foods.

Food grade aluminum was used for the development of EIS immunosensor. Because of its cost efficiency in raw material and processes for nanofabrication, EIS immunosensor based on nanoporous aluminum may be more cost effective in the manufacturing productivity than traditional immunosensors based on silicon or gold. Furthermore since EIS is an electrochemical technique that is more amenable for miniaturization and economization, it is expected that a field applicable EIS immunosensor will be commercialized in a near future. Particularly the development of electronics allows the development of "On-Air" immunosensing systems that is able to transmit automatically the safety of foods from fields to government or department for food safety. Illustrates an ideal immunosensing system to achieve the efficient food safety or food protection from bioterrorism.

Figure 7.1. Schematic presentation of "On-Air" immunosensing system

Appendix

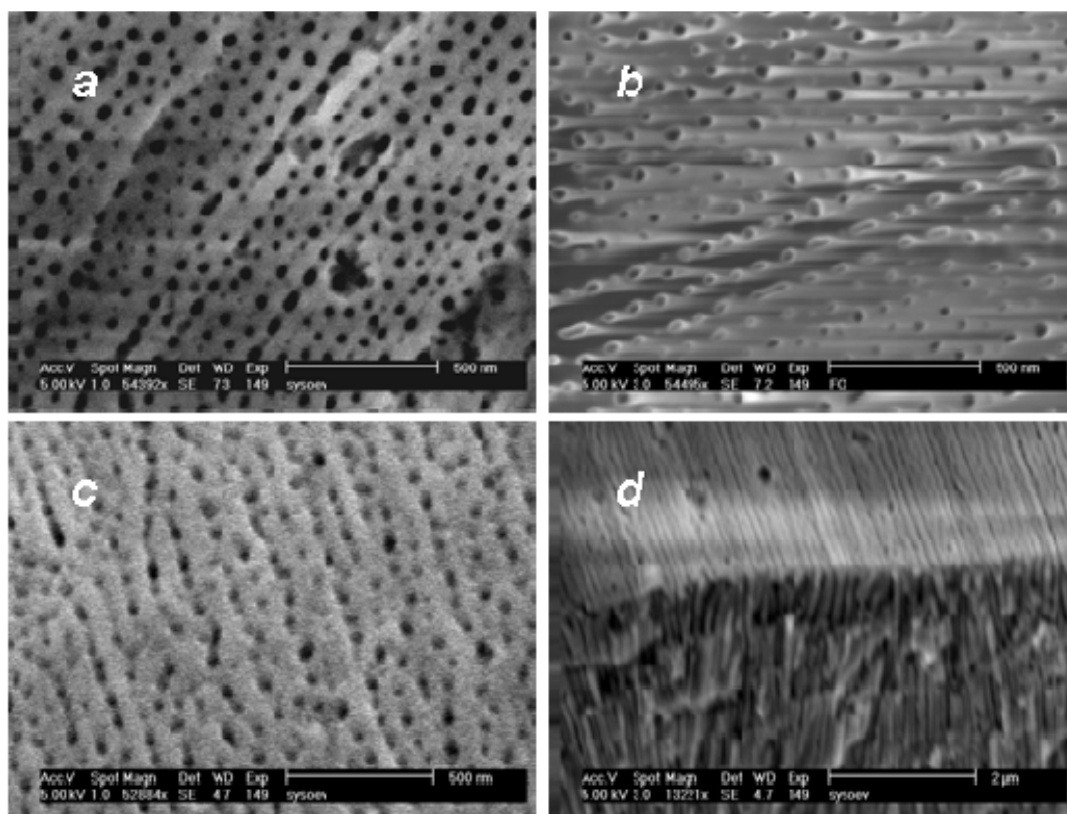## A.1.   Surface morphology of anodized aluminum

Figure A.1. Scanning electron microscopic (SEM) images of a), b), and c) surface and d) cross-section of anodized aluminum at a) at 40V, b) 50V, c), d) 60V in 0.3M oxalic acid.

A.2. Comparison of Ab immobilization as the different polysiloxanes
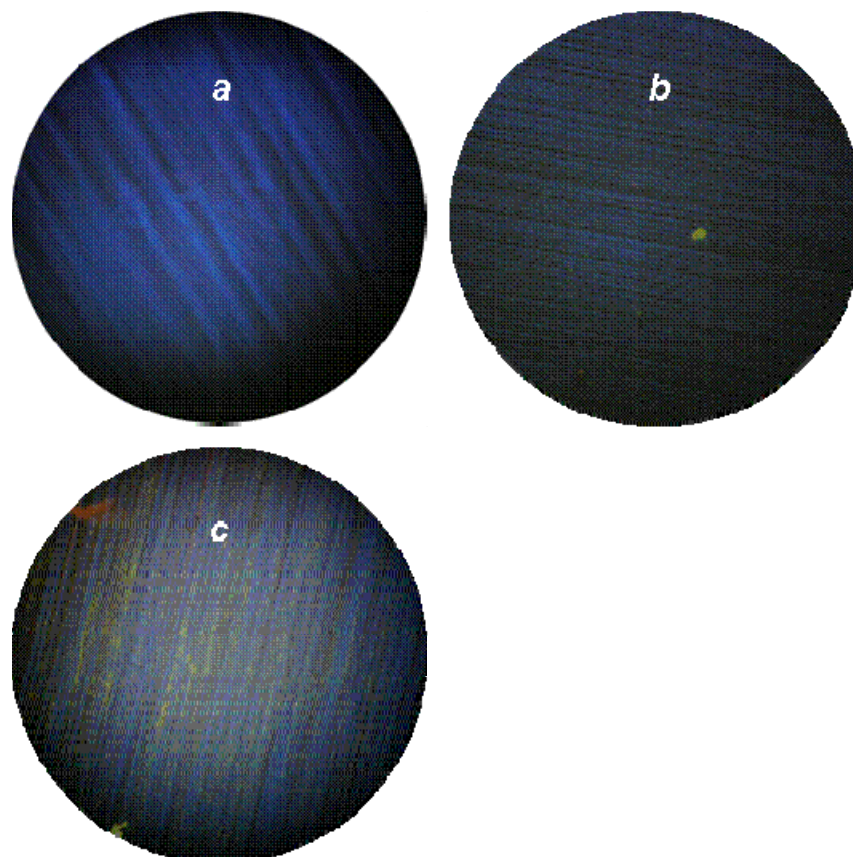
Figure A.2. Fluorescence images of a) bare aluminum and FITC-conjugated anti-*E. coli* immobilized aluminum using b) 3-cyanopropyldimethylchlorosilane (CPDES) and c) 3-aminopropyltriethoxysilane (APTES). Aluminum was silanized in CPDES or APTES as reported by Falipou [1] or described in previous chapter in this thesis. Then images were obtained using a microscope (Labophot-2, Nikon, Japan) equipped with 100 watt mercury illuminator and two filter sets (Nikon, Japan).

---

[1] Falipou, S. et al. *Bioconjugate Chemistry* **1999**, *10*, 346-353.

A.3.   Standard curve for the quantification of immobilized Ab on

immunosensor

$y = 0.0315x - 0.0024$

$R^2 = 0.995$

Fluorescence density
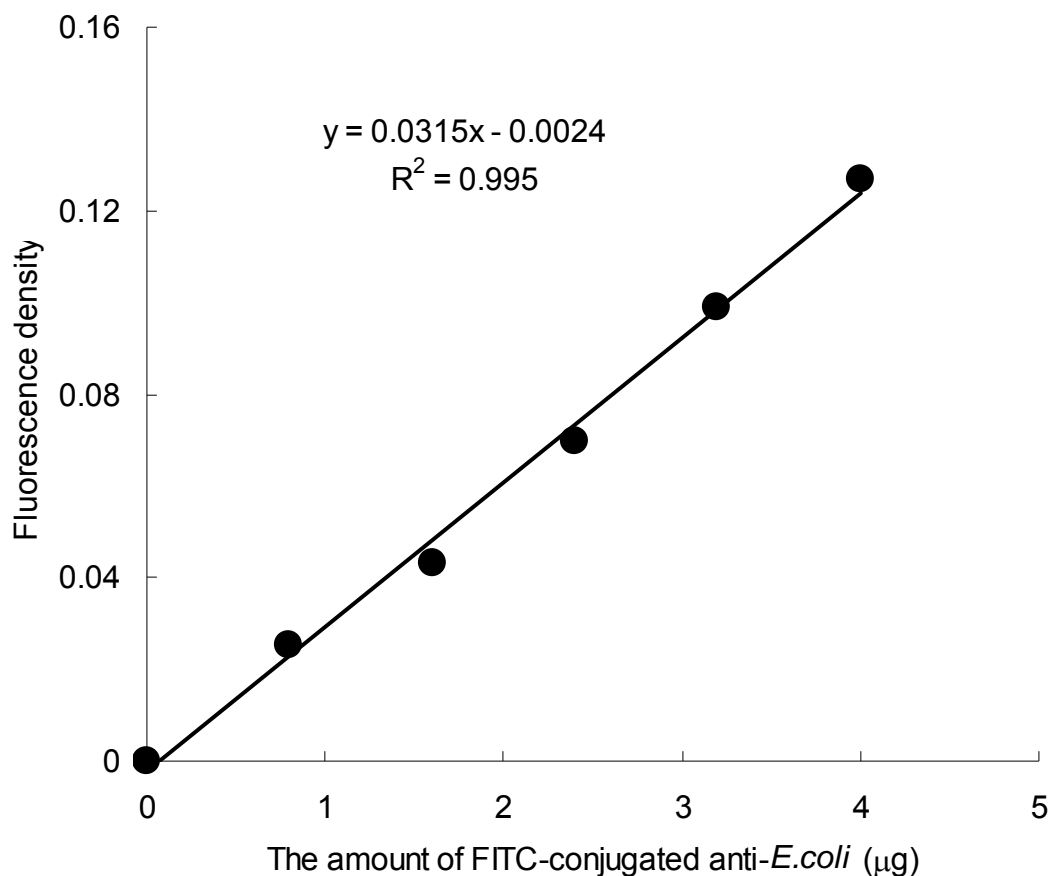
The amount of FITC-conjugated anti-*E.coli* (μg)

Figure A.3. Standard curve for the quantification of FITC-conjugated anti-*E. coli* (FITC-Ab) that is immobilized on immunosensor. The intensity of fluorescence from standard curve should be comparable to that from immunosensor where FITC-Ab is immobilized. However standard curve is obtained by measuring the intensity of fluorescence in liquid phase but FITC-Ab on immunosensor is on solid phase. To make them comparable, standard curve was obtained from FITC-Ab solution prepared not by the concentration but by the total amount of FITC-Ab. Therefore the amount of immobilized Ab could be calculated by the equation obtained from the standard curve.

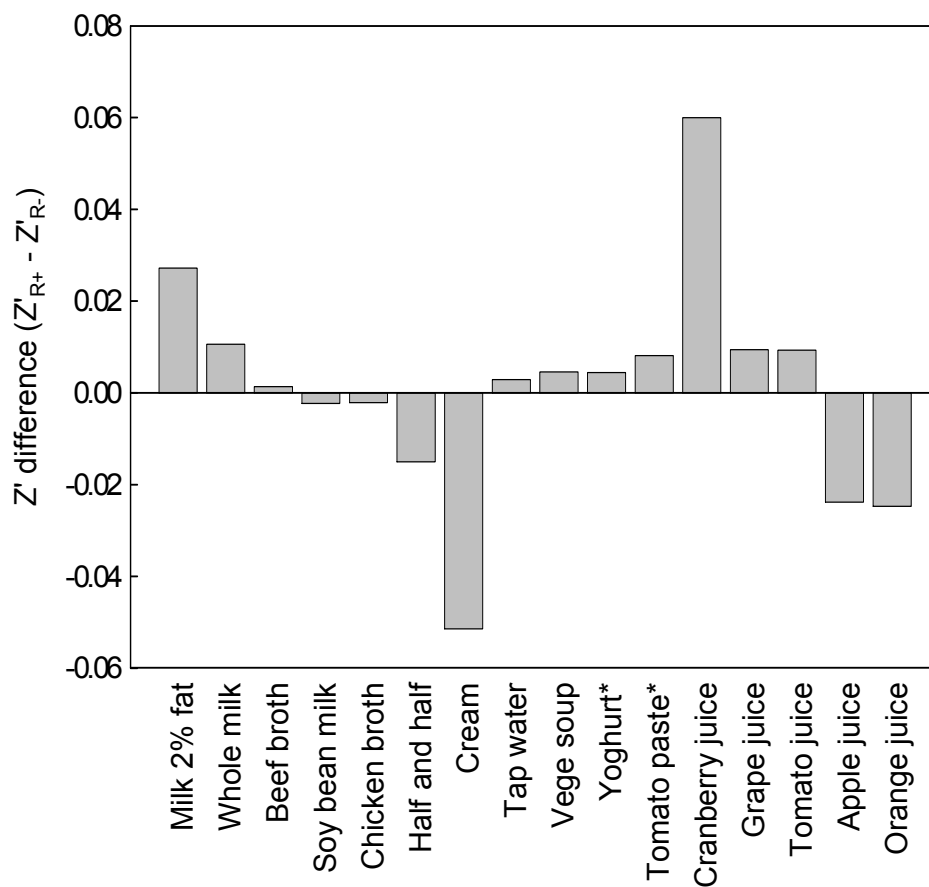A.4.   Detection of ricin in foods by EIS immunosensor

Figure A.4. Real part of impedance (Z') of EIS immunosensor for ricin detection was collected in food samples (Z'_{R-}) and in food samples containing 500ng/ml of ricin (Z'_{R+}) at 20min then the differences between Z'_{R+} and Z'_{R-} are presented. * Yoghurt and tomato pulp was diluted 2 times with distilled water due to their viscosity.

A.5. Performance of EIS immunosensors based on polyclonal or monoclan Ab in toxin mixture

Ab are proteins belonging to a family of related structural glycoproteins called immunoglobulins [2]. They are synthesized and secreted from plasma cells derived from B lymphocytes of animal cells [3]. Traditionally they have been obtained from blood serums of immunized mammals. Ab produced in this process are called polyclonal antibodies since they are products of many different populations of Ab-producing plasma cells. The process for polyclonal Ab is inexpensive, and large quantities of an Ab can be isolated from a single extraction. Therefore polyclonal Ab are widely used to develop various types of immunosensors including optical [4], electrochemical[5,6], QCM (quartz crystal microbalance) [7], and SPM (surface plasmon resonance) immunosensors [8]. However polyclonal Ab differ in their precise specificity and affinity for their target Ag, that is, polyclonal Ab can form Ab-Ag complex with various analogues of target toxins since many different populations of plasma cells take part in the production of Ab [3]. Modern biotechnology enables to isolate and proliferate Ab-producing plasma cells of a single clone. Monoclonal Ab, synthesized from a single clone, are homogenous and very specific to target Ag and hence the use of monoclonal Ab for immunosensor allows the development of highly sensitive and specific immunosensor. In addition, it has been well

[2] Nakamura, R. M. *et al. Immunochemical Assays and Biosensor Technology for the 1990.* American society for microbiology: Washington, D.C., USA, 1992, p 57-82.
[3] Stryer, L. In *Biochemistry*; 4th ed.; Stryer, L., Ed.; W.H. Freeman: New York, 1995, p 361-390.
[4] Fodey, T.*et al. Analytica Chimica Acta* 2007, *592*, 51-57.
[5] Berney, H. C.*et al. Journal of Molecular Recognition* 1998, *11*, 175-177.
[6] Moore, E.*et al. Analytica Chimica Acta* 2003, *484*, 15-24.
[7] Ayela, C.*et al. Biosensors and Bioelectronics* 2007, *22*, 3113-3119.

known that monoclonal Ab are generally more sensitive to target Ag than polyclonal Ab [9].

However it is difficult and expensive to establish a single clone producing Ab therefore

limited number of monoclonal Ab are commercially available. For example, polyclonal

anti-ricin used in this study was $305 per 1mg but monoclonal anti-SEB used in this study

was $820 per 1mg. This study is to investigate the sensitivity of EIS immunosensors as

different types of Ab (monoclonal and polyclonal Ab) as well as to investigate the

specificity of EIS immunosensors to their target toxins.

EIS immunosensors for SEB and ricin were prepared by immobilizing monoclonal

anti-SEB and polyclonal anti-ricin as described in chapter 4 and 5. Six different sample

solutions were prepared to investigate the sensitivity and specificity of EIS

immunosensors: *sample solution 1*: PBS buffer (pH 7.0, 0.3% NaCl), *sample solution 2*:

500ng ricin in PBS buffer for negative control for SEB immunosensor, *sample solution 2'*:

500ng SEB in PBS buffer for negative control for ricin immunosensor, sample solution 3:

500ng SEB in PBS buffer for positive control for SEB sensors, *sample solution 3'*: 500ng

ricin in PBS buffer for positive control for ricin sensors, and *mixture solution*: mixture of

500ng SEB and 500ng ricin in PBS.

To investigate the sensitivity and specificity of EIS immunosensor, the effect of

Ab-Ag reaction on impedimetric signal outputs had to be studied first. The changes of

Z'_{norm} of immunosensors in PBS buffer were regarded as the effect by ion adsorption on

signal outputs since it is very general that ions migrate and adsorb from bulk solution on

metal surface when metal is put into buffer solution. Z'_{norm}, specific to Ab-Ag reaction,

---

[8] Bokken, G. C. A. M.*et al. FEMS Microbiology Letters* 2003, *222*, 75-82.
[9] Fuller, A. O.*et al. Journal of Virology* 1985, *55*, 475-482.

were investigated through comparison between Z'_{norm} from PBS buffer and positive

control (sample solution 3 or sample solution 3'). Then the changes of Z'_{norm} from PBS

buffer or positive control were compared to those from negative control (sample solution 2

or sample solution 2') or mixture of target Ab in order to investigate the specificity of

developed immunosensors.

The specific changes induced by ion adsorption and Ab-Ag reaction could be

observed in Z'. However, in this study, impedance was analyzed under nonpolarized

condition. The behaviors of Z'_{norm} from EIS immunosensor responding to ion adsorption

and Ab-Ag reaction were different from Z'_{norm} obtained by polarized condition. Gradual

increase of Z'_{norm} was observed in PBS buffer but Ab-Ag reaction hindered the increase of

Z'_{norm} by ion adsorption. Specific changes in Z' by ion adsorption and Ab-Ag reaction

could be found especially at 100Hz. Therefore Z' of EIS immunosensor at 100Hz in

sample solutions was collected every 5min for 30min and Z'_{norm} was presented for the

comparison of the selectivity and sensitivity (Figure A.5). Applied AC voltage for

impedance analysis was 10mV.

Z'_{norm} of SEB immunosensor ($Z'_{norm}{}^{SEB}$) at 100Hz was increased gradually in PBS

buffer. As the changes in Z'_{norm} in PBS buffer might be by the effect of ion adsorption, the

increase of $Z'_{norm}{}^{SEB}$ at 100Hz might be driven by ion adsorption from bulk solution to the

surface of SEB sensor. The increase of $Z'_{norm}{}^{SEB}$ was relatively fast for first 5min and

continued to the end of EIS analysis (30min). Thus ion adsorption might not be reached to

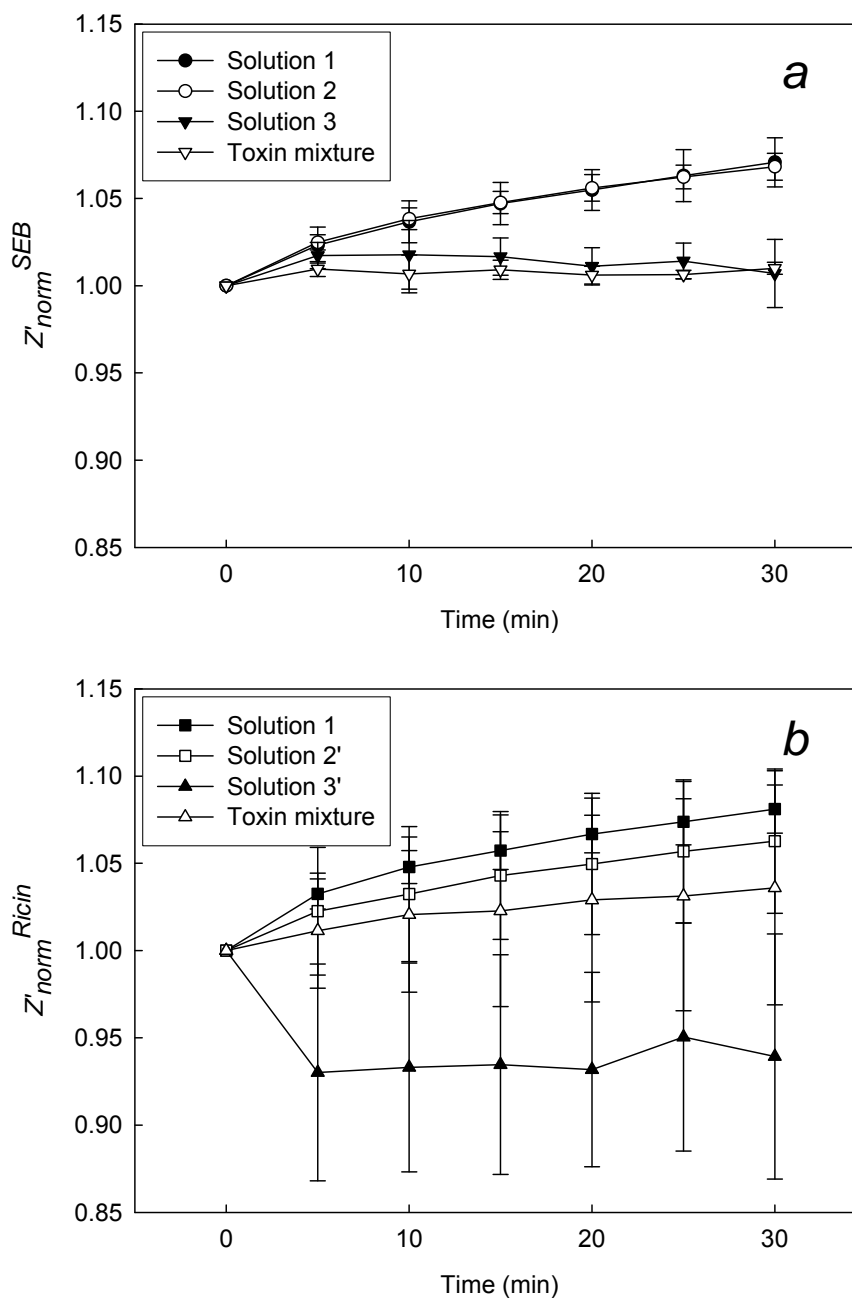equilibrium in 30min. In sample solution 3, $Z'_{norm}{}^{SEB}$ at 100Hz was not increased and

Figure A.5. Normalized real part of impedance from a) SEB immunosensor ($Z'_{norm}{}^{SEB}$) and b) ricin immunosensor ($Z'_{norm}{}^{Ricin}$) in sample solutions.

$Z'_{norm}{}^{SEB}$ in sample solution 3 was significantly lower than $Z'_{norm}{}^{SEB}$ in PBS buffer.

It would be very certain that ion adsorbed on the surface of SEB sensors regardless of

Ab-Ag reaction. Therefore the difference between $Z'_{norm}{}^{SEB}$ at 100Hz in PBS and sample

solution 3 might be caused by Ab-Ag reaction, and we concluded that ion adsorption

resulted in the increase of $Z'_{norm}{}^{SEB}$ at 100Hz but Ab-Ag reaction hindered the increase.

Particularly the behavior of $Z'_{norm}{}^{SEB}$ at 100Hz in PBS or in sample solution 3 was very

corresponding to those in sample solution 2 or in mixture solution. Hence SEB

immunosensor might react with SEB without non-specific reaction with other proteins.

As seen in SEB immunosensor, the increase of Z'_{norm} at 100Hz by ion adsorption

and significantly lower $Z'_{norm}{}^{Ricin}$ in sample solution 3' than in PBS buffer could be

observed from ricin sensors. Lower $Z'_{norm}{}^{Ricin}$ in sample solution 3' than in PBS buffer

might also be caused by Ab-Ag reaction. However the behavior of $Z'_{norm}{}^{Ricin}$ at 100Hz in

PBS buffer or in sample solution 3' and those in sample solution 2' or in mixture solution

were not corresponding as much as seen from SEB immunosensors. In addition the

variation of $Z'_{norm}{}^{Ricin}$ at 100Hz was higher than that of $Z'_{norm}{}^{SEB}$ at 100Hz. Those results

from ricin sensor were very understandable because ricin sensor was based on polyclonal

Ab. The lower $Z'_{norm}{}^{Ricin}$ at 100Hz in sample solution 2' than in PBS buffer and the higher

$Z'_{norm}{}^{Ricin}$ at 100Hz in mixture solution than in sample solution 3' might be caused by the

non-specific adsorption of foreign protein (SEB) to polyclonal anti-ricin. Consequently the

specificity and sensitivity of immunosensor based on monoclonal Ab are better than those

of immunosensor based on polyclonal Ab. Despite of interference by nonspecific reaction

between foreign protein and anti-ricin, ricin immunosensor was able to detect the presence of 500ng ricin in 30min.

The sensitivity and specificity of EIS immunosensor could be altered by the use of different types of Ab. The use of monoclonal Ab enabled to develop a highly sensitive and selective EIS immunosensor that is highly specific to target Ag. As expected, the nonspecific reaction between foreign protein and Ab seemed to occur on the surface of EIS immunosensor based on polyclonal Ab. Despite of the interference by the nonspecific adsorption of foreign protein onto immunosensor, EIS immunosensor based on polyclonal Ab could detect the presence of target Ag in nanolevel in critically short time (30min).

It seems that the development of EIS immunosensor can be controlled according to the demanded purposes. Polyclonal Ab may be applied to immunosensor if the cost efficiency of immunosensor is demanded rather than sensitivity. Additionally monoclonal Ab may be used for immunosensor if a highly sensitive immunosensor is demanded. Briefly it can be assumed that immunosensor based on polyclonal Ab may be appropriate for the application to food chain system, and immunosensor based on monoclonal Ab may be more appropriate for the use of medical purpose.

Curriculum Vitae

Changhoon Chai

February 1999	**B.S., Animal Science** Korea University, Seoul, Korea
March 1999 ~ December 2000	Teaching assistant Korea University, Seoul, Korea
February 2001	**M.S., Animal Science** Korea University, Seoul, Korea
December 2000 ~ January 2002	Research Scientist Pulmuone R&D Center, Seoul, Korea
February 2002 ~ June 2002	Consultant Victorian Government of Australia business office, Seoul, Korea
2003	S.J. Kim, Y.H. Cho, W.S. Park, D.S. Han, **C.H. Chai** and J.Y. Imm. Solubilization of water-soluble anthocyanins in apolar medium using reverse micelle. J. of Agri. Food Chem. 51:7805-7809 (2003)
2006	3rd place award of poster competition Annual meeting of New York Institute of Food Technologists, NJ
October 2008	**Ph.D., Food Science** Rutgers, The State University of New Jersey, NJ
2008	**C. Chai** and P. Takhistov, Label-free toxin detection by means of time-resolved electrochemical impedance spectroscopy, *Sensors Journal, in press*